INTRA-, INTER- AND EXTRAMUSCULAR MYOFASCIAL FORCE TRANSMISSION

A COMBINED FINITE ELEMENT MODELING AND EXPERIMENTAL APPROACH

Can. A. Yücesoy

Graduation Committee:

Chairman and Secretary:	
Prof. dr. C. Hoede	Universiteit Twente
Promotors:	
Prof. dr. P.A.J.B.M. Huijing	Vrije Universiteit / Universiteit Twente
Prof. dr. ir. H.J. Grootenboer	Universiteit Twente
Assistant Promotor:	
Dr. ir. H.F.J.M. Koopman	Universiteit Twente
Members:	
Prof. dr. A. de Boer	Universiteit Twente
Prof. dr. ir. P.H. Veltink	Universiteit Twente
Prof. dr. J.H. van Dieën	Vrije Universiteit
Prof. dr. F.C.T. van der Helm	Technische Universiteit Delft / Universiteit Twente
Dr. ir. J.M.R.J. Huyghe	Technische Universiteit Delft / Universiteit Maastricht

Cover design: Ecem Ecevit Pogge and Eda Ünlü Yücesoy

ISBN: 90-365-1933-0

Printed by DPP-Utrecht B.V., Utrecht, The Netherlands

INTRA-, INTER- AND EXTRAMUSCULAR MYOFASCIAL FORCE TRANSMISSION

A COMBINED FINITE ELEMENT MODELING AND EXPERIMENTAL APPROACH

PROEFSCHRIFT

ter verkrijging van
de graad van doctor aan de Universiteit Twente,
op gezag van de rector magnificus,
prof. dr. F.A. van Vught,
volgens besluit van het College voor Promoties
in het openbaar te verdedigen
op vrijdag 27 juni 2003 te 15:00 uur

door

Can Ali Yücesoy

geboren op 13 juli 1970

te Ankara, Turkije.

Promotors:
Prof. dr. P.A.J.B.M. Huijing
Prof. dr. ir. H.J. Grootenboer
Assistant Promotor:
Dr. ir. H.F.J.M. Koopman

The following parts of this thesis have been published or submitted for publication

Yucesoy, C. A., Koopman, H. J. F. M., Huijing, P. A. and Grootenboer, H. J., 2002. Three-dimensional finite element modeling of skeletal muscle using a two-domain approach: Linked fiber-matrix mesh model. Journal of Biomechanics 35, 1253-1262.

Yucesoy, C. A., Koopman, H. J. F. M., Huijing, P. A. and Grootenboer, H. J., 2001. Finite element modeling of intermuscular interactions and myofascial force transmission. Proceedings of the 23rd Annual International Conference of the IEEE Engineering in Medicine and Biology Society, Istanbul, Turkey.

Yucesoy, C. A., Koopman, H. J. F. M., Guus, C. B., Grootenboer, H. J. and Huijing, P. A., 2003. Extramuscular myofascial force transmission: Experiments and finite element modeling. Archives of Physiology and Biochemistry, in revision.

Yucesoy, C. A., Koopman, H. J. F. M., Guus, C. B., Grootenboer, H. J. and Huijing, P. A., 2003. Effects of inter- and extramuscular myofascial force transmission on adjacent synergistic muscles: Assessment by experiments and finite element modeling. Journal of Biomechanics, in press.

Yucesoy, C. A., Maas, H., Koopman, H. J. F. M., Grootenboer, H. J. and Huijing, P. A., 2003. Finite element modeling of relative position of a muscle: Effects of extramuscular myofascial force transmission. International Journal of Mechanics in Medicine and Biology, in press.

Contents

Acknowledgements

This research was carried out at the Biomechanical Engineering research group of the Mechanical Engineering Department, Universiteit Twente, Enschede. The experimental studies were conducted at the Myology Laboratory of the Institute of Human Movement Sciences, Vrije Universiteit, Amsterdam. I would like to gratefully acknowledge these institutions.

This work involves a multidiscipline study in which physiological questions were addressed employing principles of solid mechanics. Therefore, this thesis is a result of a wonderful teamwork and it would have never been completed otherwise.

In the first place, I would like to express my gratitude to Peter Huijing for his excellent supervision, for making me affiliated with the physiological aspects of the research, and for helping me gain the skills of interpreting the results of mechanical analyses leading to physiological conclusions. His never-ending enthusiasm for the research was most inspiring and encouraging. I would also like to thank him very much for his support and concern in several situations, which made my experience in the Netherlands more pleasant and comfortable.

Henk Grootenboer is “the” role model; a mechanical engineer doing research in the field of biomechanics would want to be. I am grateful for his exceptional supervision.

I would like to thank my assistant promotor, Bart Koopman for the very valuable weekly discussions and for helping me resolve several issues. It was most pleasurable to work with him.

Guus Baan, with his infinite energy, was the person who made the physiological experiments possible. I learned so much from him and had great long days working in the lab with him. Thanks very much Guus.

Huub Maas, my inspiring colleague in Vrije Universiteit, Amsterdam. It was a real pleasure to cooperate with him.

I feel honored to have worked with them.

I would like to thank my colleagues Arthur, Arturo, Miguel, Hendrik-Jan, Bart, Herman, Edsko, Stella, Theo, Ray, Marian, Freek, Jan, Edwin, Ralf, Jasper, Yvonne, Nikolai, Johan, Willem, and Richard for their helps, ideas and support.

Two of my colleagues, Laurens Kamman and Anton Sanders strongly deserve a distinguished acknowledgement. From helping me find my ways in the first days to supporting me as my *paranimfen* in the last day, they were a special part of my experience in the Netherlands.

Special thanks to

Murat, Tolga, Sinan, Ayse, and Atila for their everlasting support and friendship,

Tuna, Herman, and Gabriela for their inspiration and helps,

Hüseyin, Belgin, Marieke, Karin, Caner, Evren, Sıtkı and Sonia for their supports and friendship in the Netherlands,

Trudi van Rooijen for the great times in the Netherlands and in Turkey,

and my former colleagues Alptekin, and Senih for their encouragement and for fruitful scientific discussions.

I would like to express my gratitude for my parents who had done every sacrifice necessary to give me a good future.

Finally, I would especially like to thank my wife Eda. Bızbızım tesekkürler.

Can A. Yücesoy
June, 2003

Summary

Exertion of force onto the bony skeleton is the fundamental requirement for animals to move their limbs in order to accomplish several tasks. Muscle is the motor for generation of the necessary force. Yet, exertion of force involves not only generation of force but also transmission of it. Conceivably due to its highly specialized morphology, the myotendinous junction (the junction between the ends of muscle fibers and the aponeurosis) has been very widely accepted to be the exclusive site for transmission of force from muscle fibers where the force is generated. From this assumption, it follows that commonly individual skeletal muscles are considered as independent functional units having unique muscle length-force characteristics.

However, muscle fibers and the extracellular matrix are connected not only at the myotendinous junctions, but also along the remainder of the full perimeter surface of the muscle fibers. Experiments have shown that these connections play a significant role in force transmission. Moreover, neighboring muscles are connected to each other as well as to the boundaries of the compartments within which they operate. This implicates that transmission of muscle force is not limited to the myotendinous junction exclusively, but it also involves a complex network of pathways provided by the myofascial apparatus.

One of the goals of this study was to study, quantitatively, the importance of effects of myofascial force transmission on muscle length-force characteristics and on distributions of lengths of sarcomeres. In addition, the hypothesis was tested that, if force is transmitted between muscles as well as from muscles to nonmuscular structures via myofascial pathways, individual muscles should not be viewed as fully independent functional units. These hypotheses were tested using a combined finite element modeling and experimental approach. Both approaches include methods that were designed specifically to study myofascial force transmission.

The model is equipped with two elastically linked meshes within the same space to represent the muscle fibers and its extracellular matrix. The experiments were performed with connective tissues intact as much as possible or manipulated for specific effects.

As a first application, a model of isolated medial gastrocnemius muscle of the rat was used to study transmission of force between the muscle fibers and the extracellular matrix via the transsarcolemmal connections (Chapter 2). The stiffness of links at selected locations within the muscle was manipulated, i.e. certain links were made much more compliant than the highly stiff links at other locations within the modeled muscle. Note that such altered connections between the muscle fibers and their extracellular matrix are found in diseases such as muscular dystrophies. Within the high length range, this model study showed drops in muscle force following small increases of isometric length. Analysis of stress and strain

distributions in the fiber direction showed that the force drop is caused by an overall decrease in the total stress in the fiber mesh. This is due to a combination of very high positive or negative strains found near the compliant links. The high local strains found in the fiber mesh (not in the matrix mesh) were caused by geometrical changes in the muscle model dominated by the shear between the fiber and cross-fiber directions. It is concluded that the extracellular matrix as well as the trans-sarcolemmal connections between the two domains play a major role in force transmission and are essential for the muscle fibers to preserve a physiological state.

Exclusive effects of intermuscular myofascial force transmission on muscle force on muscle properties were studied (Chapter 3). The results of a model representing a rat extensor digitorum longus muscle (EDL) connected intermuscularly to a model of an adjacent muscle were compared to model results for an EDL muscle fully isolated from its surrounding muscular and nonmuscular structures. In both models EDL muscle was lengthened distally. For the model with intermuscular connections, the adjacent muscle was restrained at low length. This comparison indicates that myofascial force transmission does occur intermuscularly: active force generated within one muscle may be exerted at the tendon of another muscle. In addition, substantial differences for the fiber mesh of modeled EDL in the two conditions were found: Both distributions of the fiber direction stress and strain were affected by myofascial force transmission. The model of EDL with intermuscular connections shows sizable strain distribution. In contrast, the model representing isolated EDL shows a more uniform strain indicating limited differences of the lengths of sarcomeres arranged in series.

The exclusive effects of extramuscular myofascial force transmission on muscle length-force characteristics were investigated (Chapter 4) with experiments on EDL muscle. The muscle's extramuscular connective tissues were left intact and EDL isometric forces were measured simultaneously at the distal and proximal tendons. After distal lengthening, significant differences were found between proximal and distal muscle isometric forces ($F_{dist} > F_{prox}$, ΔF approximates maximally 40 % of the proximal force). Making use of the model results, the length dependent increasing proximo-distal force difference in favor of distal muscle force was explained to be a consequence of a proximally directed extramuscular force, which increases as EDL is lengthened distally. The model results also indicate that extramuscular myofascial force transmission leads to a substantial serial distribution of lengths of sarcomeres. Experiments on EDL muscle with minimal extramuscular connections (leaving only part of the extramuscular connective tissues intact that is absolutely essential to keep the muscle in physiological conditions) showed that the proximo-distal force difference remains. Note that this is a common condition in physiological experiments in situ after dissection from other muscles and connective tissues.

Therefore, it was concluded that a truly isolated muscle should be distinguished from a muscle studied in situ.

The integrated effects of inter- and extramuscular myofascial force transmission on muscle length-force characteristics were also investigated (Chapter 5). For the experimental work, the connective tissues at bellies of EDL, m. tibialis anterior (TA) and m. extensor hallucis longus (EHL) were left intact. EDL muscle was lengthened distally, but TA and EHL muscles were kept at constant muscle-tendon complex length. Proximal and distal EDL forces, as well as distal forces of TA and EHL muscles were measured simultaneously. Substantial differences were found in EDL isometric force measured at the proximal and distal tendons (maximally 46 % of the proximal force). A significant decrease (approximately 17% of the initial force) in TA+EHL complex distal force was measured at higher EDL lengths. In addition, the specific effects of intermuscular myofascial force transmission were assessed by comparing the results of these experiments with the results of the experiments presented in Chapter 4. This comparison showed that for EDL with inter- and extramuscular connections length range between active slack and optimum length was increased as muscle optimum length was shifted to higher length by more than 2 mm. In addition, EDL distal optimum force was higher. Finite element modeling showed that combined inter- and extramuscular myofascial force transmission leads to serial distribution of lengths of sarcomeres within muscle fibers. Moreover, an increased heterogeneity of fiber mean sarcomere lengths among the fibers of EDL modeled with inter- and extramuscular connections was found compared to EDL modeled with extramuscular connections exclusively. It is concluded that the enhanced distributions of sarcomere length explain the higher length range of force exertion. Distribution of fiber direction stress within the fiber mesh suggests that due to myofascial force transmission, the muscle fiber cannot be considered as a unit exerting equal forces at both ends. It is concluded that inter- and extramuscular myofascial force transmission has major effects on muscle length-force characteristics and muscle properties.

The studies presented in Chapters 3 to 5 involved changes in EDL length. Changes in muscle length also involve changes in relative position of (parts of) a muscle with respect to neighboring tissues (i.e. neighboring muscles and/or nonmuscular structures such as bone and compartmental boundaries). The significant effects of myofascial force transmission on muscle length-force characteristics do suggest that the relative position of a muscle is a co-determinant of muscle force in addition to muscle length. This hypothesis was tested in Chapter 6. In an experiment, muscle length was kept constant but relative position of EDL muscle with extramuscular connections was manipulated. The results show proximo-distal force differences varying both in sign and in magnitude as a function of muscle relative position, confirming the role of muscle relative position as a co-determinant of muscle force. Modeled altered muscle relative position, showed sizeable serial distributions of sarcomere

lengths at higher muscle lengths. In contrast, at lower muscle lengths the effects of muscle relative position on such distributions were relatively limited. The length dependent effects were explained by the role of the extracellular matrix in force transmission, which was concluded to be a major determinant of proximo-distal muscle force as well as muscle properties.

In conclusion, the results of this thesis indicate that within the context of surrounding tissues (as in vivo), muscle is not a fully independent functional unit exerting equal force at both tendons and that muscles are not comprised of muscle fibers, which function independent of their neighboring muscle fibers. Due to the integrated effects of intra- inter- and extramuscular myofascial force transmission variables of muscle length-force characteristics, such as muscle optimum length and optimal force are not specific properties of individual muscles. Instead, actual muscle length-force characteristics also depend on relative position of muscle with respect to its neighboring muscles and nonmuscular connective tissue structures. Therefore, the results of this thesis suggest that rather than individual muscles, groups of neighboring synergistic muscles may form functional units.

Chapter 1

Introduction

The primary condition for obtaining movement of limbs is exertion of force onto the bony skeleton, which requires transmission of the force generated within the muscle fibers. The widely accepted site for such transmission is the junction between the ends of muscle fibers and the aponeurosis, which is referred to as myotendinous junction. Often myotendinous force transmission is implicitly assumed to be the exclusive means of force transmission. In addition, in accordance with morphological knowledge, individual muscles have been distinguished anatomically. Conceivably that has contributed to most physiological experiments having been conducted on isolated muscle (i.e., dissected from the surrounding structures). It is likely that these aspects shaped the classical point of view, in which individual skeletal muscles are considered as independent functional units. However, the highly complex structure of skeletal muscle tissue includes not only the activatable muscle fibers but also several levels of organization of connective tissue that house them. Moreover, muscle fibers and the connective tissue structures are interconnected not only at the myotendinous junctions, but also along the full perimeter surface of the muscle fibers. This causes neighboring muscle fibers as well as neighboring muscles to be connected to each other. In addition this complex of muscles is connected to the compartmental boundaries. Therefore, the mechanism of transmission of muscle force is likely to be more complex, i.e. if stiff enough, the fascial apparatus will provide additional paths for force transmission. Conceivably, this has significant functional implications.

Intracellular Space

Contractile apparatus

The activatable single cells of skeletal muscle are the *muscle fibers*. Muscle fibers and surrounding connective tissues are arranged in bundles that are referred to as fascicles. Each muscle fiber is elongated, and in many muscles may, or may not span the full length of the fascicle (i.e., attached at both ends to either aponeuroses or bone) even having a length of over 30 cm in long human muscles. Non-spanning muscle fibers span only part of the length of a fascicle (i.e., have no junction with aponeurosis, bone or tendon at least at one end).

Most of the cytoplasm of a muscle fiber is packed with myofibrils, each of which consists of numerous thick (myosin) and thin (actin) filaments. The thick and thin filaments are arranged in a repeating pattern along the length of each myofibril. One unit of this repeating pattern is known as a sarcomere, which is the basic force-producing unit within a muscle fiber. The space between the overlapping thick and thin filaments is bridged by *cross bridges*, which comprise the force-generating sites in a muscle fiber. Sarcomere force depends on the overlap of the myofilaments (Fig.1) according to the sliding filament theory (Huxley, 1957). The sliding filament theory explains how force is generated, by the movements of the thick and thin filaments, without undergoing any length changes, propelled by the movements of the cross bridges.

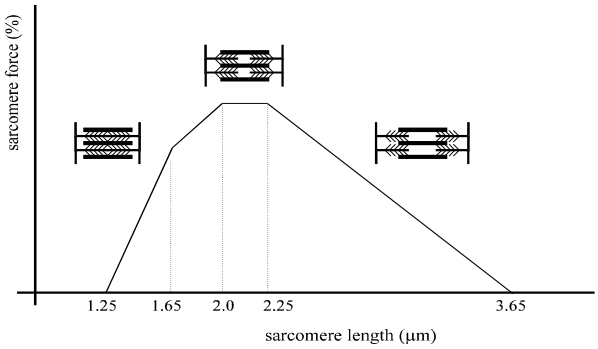

Fig.1 Sarcomere length-force characteristics.

Intrasarcomeric cytoskeleton

Within the intracellular space, in addition to the contractile proteins actin and myosin, several others such as titin, nebulin, α-actinin, skelemin, troponin and tropomyosin are found (e.g. Berthier and Blaineau, 1997). These proteins form an intrasarcomeric cytoskeleton responsible from anchoring of the myofilaments and regulation of their respective displacements. For example, troponin and tropomyosin which are located on the thin filaments prevent interaction of the cross bridges with actin, in a resting muscle fiber. However, the very large structural protein titin (Trinick, 1991), that connects thick filaments

end to end, is the main source of intrasarcomeric passive tension (Maruyama, 1994; Trombitas et al., 1995) and therefore, receives attention in the present thesis. In addition to passively supporting the sarcomere, titin stabilizes the sarcomere against high muscle forces, and helps to protect the orderly array. If titin is destroyed selectively, normal muscle contraction causes significant myofibrilar disruption (Horowits and Podolsky, 1987). One end of each titin filament is connected to a network of proteins known as the Z disc. Thin filaments from two adjacent sarcomeres are connected to the two sides of each Z disc therefore, two successive Z lines define the lateral boundaries of one sarcomere. Z disc protein MLP (muscle specific LIM protein) provides connection of the intrasarcomeric cytoskeleton to the molecules of the extrasarcomeric cytoskeleton.

Extracellular Space

Extracellular matrix

Like any tissue, muscle tissue is not composed solely of cells i.e., muscle fibers. A substantial part of its volume is extracellular space, which is largely filled by macromolecules constituting the extracellular matrix. The macromolecules assemble in a network consisting primarily of fibrous proteins embedded in a hydrated polysaccharide gel (Huijing, 1999a). The major protein found in the extracellular matrix in the form of fibrils is collagen. However, collagen fibrils are not isolated structures. Instead, they form complex interaction between collageneous and non-collagenous components of the extracellular matrix (Huijing, 1999a).

Basal lamina

The basal lamina is a specialized component of extracellular matrix that surrounds individual muscle cells and separates the muscle cells from the underlying or surrounding connective tissue. It is composed mainly of the non-fibril-forming type IV collagen, proteoglycans and laminin. The basal lamina is largely synthesized by the cells that rest on it and is responsible for several complex functions. As seen in the electron microscope after conventional fixation and staining, the basal lamina consists of two distinct layers: an electron-lucent layer (lamina lucida) which is located adjacent to the cell membrane, *sarcolemma* and an electron-dense layer (lamina densa). The lamina densa is connected to lamina lucida mainly by the presence of laminin and on the opposite side fibronectin helps to bind to the matrix macromolecules and connective tissue cells (Alberts et al., 1989).

Intramuscular connective tissue

Muscular connective tissue can be described as a fiber network composed of collagen in which collagen fibers run in several directions. Three levels of intramuscular connective

tissue organization are distinguished (e.g. Borg and Caulfield, 1980): (1) endomysium surrounding each muscle fiber, (2) perimysium surrounding fascicles of muscle fibers and (3) epimysium surrounding the whole muscle. It should be noted that perimysium is connected to the epimysium and endomysium is connected to the perimysium suggesting continuity within intramuscular connective tissues. A multiple functional role is ascribed to the fascial apparatus of the muscle, including providing a pathway for the intramuscular nerves and blood vessels, media for exchange of ions and metabolites etc. However, such roles ascribed to this continuous structure do not usually include transmission of force. Using scanning electron microscopy, Trotter and Purslow (1992) generated images of muscle from which muscle fibers were removed (Fig.2). This picture allows consideration of muscle as an extensive 3D set of organized endomysial tunnels or tubes within which muscle fibers operate. Such an organization indicates the role of the intramuscular myofascial apparatus in transmission of force provided that the intracellular space and the extracellular space are linked mechanically by transsarcolemmal connections along the perimeter surface of the muscle fibers.

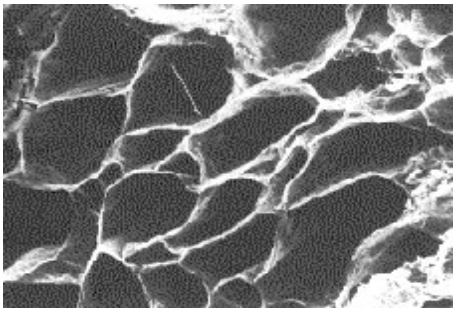

Fig.2 Scanning electron micrograph of the transversely cut surface of the bovine sternomandibularis muscle showing the endomysial tubes (Trotter and Purslow, 1992).

Trans-sarcolemmal Connections Between the Two Domains

To fulfill their functions, muscle fibers strongly depend not only on being repetitively active but also being effectively attached to their extracellular matrix (e.g. Berthier and Blaineau, 1997). This attachment is provided by a highly specialized cytoskeleton, which can be characterized by three parts: (1) the subsarcolemmal part of the extrasarcomeric cytoskeleton, (2) the trans-sarcolemmal molecules (e.g. integrins and dystrophin-associated glycoproteins) and (3) their connection to the extracellular matrix. Several different proteins are involved in this multimolecular complex system (see for a review Patel and Lieber, 1997). Fig.3 shows a schematic representation of such connections.

Berthier and Blaineau (1997) describe that the contractile sarcomeric cytoskeleton (composed of actin and myosin filaments) as well as the intrasarcomeric cytoskeleton are connected to (1) peri-sarcomeric and inter myofibrilar cytoskeletons which are essentially comprised of desmin-containing intermediate filaments that provide linkage between adjacent myofibrils and (2) the subsarcolemmal cytoskeleton, which is thought to provide the peripheral myofibrils a linkage to the sarcolemma and an indirect connection to the extracellular matrix.

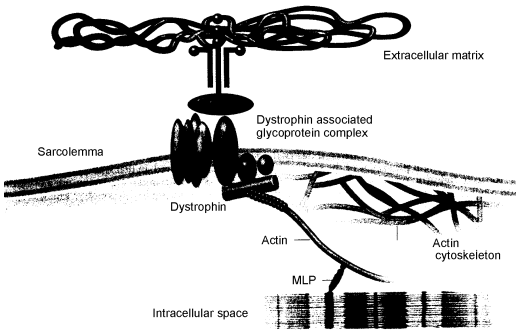

Fig.3 Schematic representation of connections from within the intracellular space to the extracellular matrix. Modified from Leiden (1997).

All along the sarcolemma, vinculin rich repetitive subsarcolemmal cytoskeletal units are found which are referred to as costameres (Pardo et al., 1983a; Pardo et al., 1983b). Craig and Pardo (1983) and Shear and Bloch (1985) proposed that costameres could play a role in anchoring the perisarcomeric cytoskeleton of the most peripheral myofibrils to the membrane and link it to the extracellular matrix. Danowski and co-workers (1992) were among the few researchers to propose that costameres and their attachment to the extracellular matrix transmit both active and resting tension of muscle fibers to the sarcolemma and subsequently to the extracellular matrix.

Dystrophin is a subsarcolemmal protein that links F-actin to a group of transsarcolemmal glycoproteins, which are anchored to merosine, a compound of the extracellular matrix. The role of dystrophin based membrane cytoskeleton is not fully understood. Generally the major role that is attributed to dystrophin and associated proteins is the maintenance of sarcolemmal integrity (Menke and Jockusch, 1991; Petrof et al., 1993; Menke and Jockusch, 1995; Pasternak et al., 1995). However, decreased or lacking capability to synthesize dystrophin is known to lead to serious muscular diseases such as Duchenne muscular dystrophy (e.g. Campbell 1995; Worton 1995; Ohlendieck 1996). The consequences of such diseases include severe difficulties for the patients to keep their

muscles morphologically and functionally intact. This is a direct indication of the functional significance of this molecule conceivably in force transmission. It should be noted that missing links in the multimolecular system of trans-sarcolemmal connections will lead to different types of muscular dystrophy.

Transmission of Muscle Force

Myotendinous Force Transmission

The myotendinous junction is localized at the interface between the ends of muscle fibers and the aponeurosis. The ends of muscle fibers have a highly specialized morphology featuring a substantial decrease in their diameter towards their tendinous origin or insertion (e.g. Loeb et al., 1987; Tidball, 1991). On the other hand, at the same locations the sarcolemma folds extensively in the muscle fibers' longitudinal direction to form invaginations of the plasma membrane into the myofiber, and finger-like processes protruding from the myofiber. Collagen fibers are located within the invaginations and force is expected to be transmitted from the intracellular space through the finger like structures onto the collagen fibers (Huijing, 1999a). The invaginations effectively increase the surface area available for force transmission and allow shear stress to be the predominant mechanism over tensile stress (e.g. Tidball, 1991), which is explained to be an essential determinant of the breaking strength of the connection (e.g. Tidball, 1983). It is conceivable that owing to this specialized morphology, the myotendinous junction is very widely accepted to be the exclusive site of force transmission.

Myofascial Force Transmission

Intramuscular myofascial force transmission

Despite the predominant ascription of force transmission to myotendinous junction, the idea of non-myotendinous force transmission was conceptualized much earlier:

(1) Based on the continuity of the endomysium to the endotenon of tendons together with assumed collagenous connections to the intracellular domain (e.g. Lindhard, 1931). (2) After measuring extensibility in partially skinned pieces of frog myofibers, Podolsky (1964) concluded that the sarcolemma is linked to the enclosed myofibers by structures capable of transmitting force. (3) Bartels and co-workers (1979) suggested that transmission of active tension by connective tissue around extremely stretched fiber fractions occurs in mammalian muscle.

(4) Experiments on muscle fibers that have damaged sarcomeric contractile protein morphology allowed very important observations regarding transmission of force (Ramsey and Street, 1940; Street and Ramsey, 1965). The preparations tested were muscle fibers injured at one end so that the sarcolemmal tube (empty of contractile proteins) remained as

the only connection between the still functioning myoplasm and the tension recorder (Fig.4a). Isometric tension measured showed only a little decrease compared to the force measured before the muscle fiber was damaged. (5) Street (1983) later described the concept as lateral transmission of tension from the myofilaments to the interfiber connective tissue across the sarcolemma covering the body of the fiber or conversely, from the connective tissue to the myofilaments. In that work she showed strong evidence on such transmission studying the behavior of a single myofiber in relation to the surrounding myofibers of a small bundle (Fig.4b and c, see the legend for detailed information on these experiments).

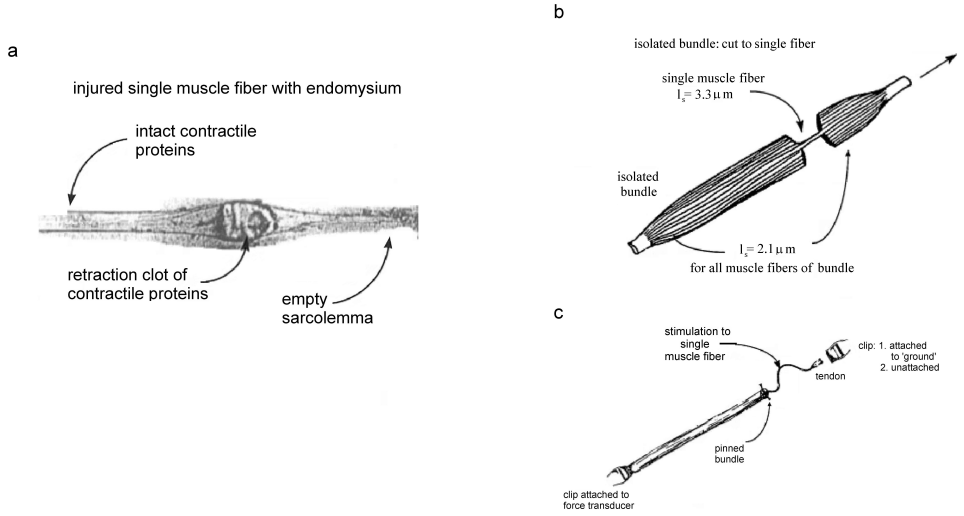

Fig.4 Classical experiments showing evidence of lateral force transmission from myofibers.
(a) A damaged single muscle fiber with an empty sarcolemma on the right side and intact contractile proteins on the left was tested (Ramsey and Street, 1940; Street and Ramsey, 1965). (b) The passive interaction between a single muscle fiber and its neighboring tissues was studied using a preparation of a small bundle (Street, 1983). The middle of the fascicle was dissected to leave a single muscle fiber intact and isolated. In contrast, at other locations along its length, the target muscle fiber was surrounded by its neighboring muscle fibers. After imposing stretch on the passive fascicle, sarcomere lengths in all muscle fibers remained at approximately 2.1 µm, except for the bare part of the target muscle fiber in the middle. Sarcomere lengths reaching 3.3 µm in the bare part of the target myofiber, indicated that the passive force becomes large enough to cause redistribution of lengths of sarcomeres in series with in the target muscle fiber (c) In a second type of preparation, the interaction between an active single muscle fiber and its neighboring passive muscular tissues was studied (Street, 1983). The target muscle fiber was isolated at one of its ends, but surrounded by endomysium and its neighboring muscle fibers at the other end. The cut ends of neighboring muscle fibers and their connective tissue were restrained by a pin. Regardless of its bare end being attached or unattached to the ground, active force exerted by the target muscle fiber was similar. This indicates that the surrounded part of the target muscle fiber did not shorten to its active slack length. Instead, the force exerted by the restrained parts of the fascicle onto the surrounded part of the target muscle allowed that part to remain at a length at which it can exert force. Modified from Huijing (1999a).

With their work on non-spanning myofibered muscles Trotter and his colleagues (Trotter, 1990; Trotter, 1991; Trotter and Purslow, 1992; Purslow and Trotter, 1994) made very important contributions to identification of force transmission laterally. In this kind of muscle, a large amount of muscle fibers (or all of them) span only part of the length of a muscle hence they have no direct myotendinous junction at least at one end. Therefore, force must necessarily be transmitted onto the endomysial network and beyond (Trotter and Purslow, 1992; Trotter, 1993). These authors studied the functional implications of the tapering ends of muscle fibers and suggested that the surface area of the tapered muscle fiber is constant at all sarcomere lengths (Trotter, 1991). Also argued was the likelihood of constant endomysial thickness and unlikelihood of the endomysial shear properties being affected by the in-plane properties of the collagen fibers at physiologically relevant sarcomere lengths. Noting that the tensile properties of the endomysium are unsuitable for transmission of contractile force, they concluded that such force has to be transmitted between neighboring muscle fibers by shear through the endomysium rather than by in-plane tension (Purslow and Trotter, 1994).

In addition to introducing the terminology of "myofascial force transmission" (Huijing, 1999b), Huijing and co-workers provided major experimental evidence through a series of experiments on gastrocnemius medialis (GM) and extensor digitorium longus (EDL) muscles of the rat. The particular anatomy of EDL muscle (discussed in detail in a later section in this chapter) makes it very suitable for studying intramuscular myofascial force transmission: the muscle has a single proximal tendon however, distally four separate heads of it have separate aponeuroses and tendons connected to the digits II to V of the foot. The experiments included incisions of intramuscular connective tissues which creates conditions that avoids myotendinous force transmission within a part of the muscle belly. Three groups of incisions can be distinguished in the performed experiments:

(1) *Tenotomy:* The distal tendons of selected heads were cut to prevent direct myotendinous force transmission within these heads (Huijing et al., 1998). If myotendinous force transmission were the only mechanism of force transmission, than the force exerted by the muscle would be expected to decrease. However, EDL force was shown to remain at high levels after acute tenotomy. Cutting of tendons of the two most proximal heads (II and III) did not alter muscle length-force characteristics significantly. Cutting also the tendon of head IV (i.e., leaving only the most distal head in its original condition) introduced a significant change in length-force characteristics however, muscle optimum force was maintained at 84% of that of the intact muscle.

(2) *Fasciotomy:* With the same experimental group of animals, the effect of interference between the two most distal heads (i.e., heads IV and V) was studied after cumulative tenotomy (Huijing et al., 1998). This was done by dissecting first approximately 30% and later approximately 70% of the fascial interface between the two heads. As a result of

progressive fasciatomy the force dropped to much lower levels, with muscle optimum force being decreased by up to 50% of that of the intact muscle. It was concluded that fascicle connective tissue sheets are important force transmitting structures.

(3) *Aponeurotomy:* Clinically, this surgery is performed in spastic young patients having relatively short muscles with the ultimate goal of restoring more normal patterns of gait. The intervention involves the sectioning of muscles' aponeurosis approximately at right angles to its longitudinal direction. An acute effect of aponeurotomy is a tearing of the active muscle if brought to high lengths. The proximal aponeurotomy experiments on GM of healthy rat acutely yielded a gap that opened further at higher muscle lengths due to progressive tearing of the muscle (Huijing, 1999a; Jaspers et al., 1999). This tearing resembles that of the fasciotomy experiment, but is not caused *directly* by the experimental intervention, as the muscle tears itself apart. It should be noted that such intervention prevents myotendinous force transmission for the distal half of GM. The relationship of the length of the most proximal and most distal fascicle to muscle length showed that no significant length changes occurred for the most proximal fascicle (the muscle fibers of which were still capable of myotendinous force transmission). In contrast, distal muscle fibers, prevented from myotendinous force transmission, showed a severely decreased capability to attain higher lengths as the muscle was brought to higher lengths. Such behavior of muscle fibers was concluded to indicate diminishing but not eliminated intramuscular myofascial force transmission in aponeurotomized GM muscle.

Inter- and extramuscular myofascial force transmission

Major connective tissue components are formed by structures that encapsulate extramuscular main nerves and blood vessels (Huijing and Baan, 2001b). Such connective tissues are referred to as neurovascular tracts and are continuous with the extra- and intramuscular connective tissues. In rat, the neurovascular tract to the muscles of the anterior crural compartment pass through a fenestration within the anterior intermuscular septum that separates the anterior crural and peronei compartments and reach the target muscles being embedded in structures of connective tissue. These structures not only provide the muscles with the necessary conditions to maintain their physiological state but also constitute an anatomical path of force transmission out off the muscle. Therefore, transmission of force from the extracellular matrix of a muscle to surrounding non-muscular elements of a compartment and bone is referred to as *extramuscular myofascial force transmission*. On the other hand, the muscles within a compartment that are located adjacent to each other in a very close proximity have short, direct connections between their epimysia. Consequently, the intramuscular connective tissues of such muscles have continuity. Transmission of force from the extracellular matrix of a muscle to the extracellular matrix of an adjacent muscle

through the direct connections between the muscles is referred to as *intermuscular myofascial force transmission*.

The effects of inter- and extramuscular myofascial force transmission on muscle length-force characteristics have been shown in certain experiments. A study investigating the effects of blunt dissection and compartmental fasciotomy (Huijing and Baan, 2001b) showed that a systematic manipulation of the extra and inter-muscular connective tissue structures altered the muscle length-force characteristics. In recent experiments in which connective tissues at muscle bellies were left intact to maintain physiological relations of intra-, inter- and extramuscular connections, significant proximo-distal force differences were found for EDL muscle of the rat after proximal lengthening (Huijing, 1999b; Huijing, 2000; Huijing and Baan, 2001a; Maas et al., 2001). Such experiments indicated intramuscular myofascial force transmission between adjacent muscles (Huijing and Baan, 2001a; Maas et al., 2001) as well as the role of the relative position of a muscle with respect to adjacent muscles and nonmuscular structures in inter- and extramuscular myofascial force transmission (Huijing and Baan, 2003). In addition to these experiments, some other studies not focused exclusively on myofascial force transmission show results that can be interpreted as effects of such transmission. For example a study on unintended force exertion in human showed that exertion of isometric force with one, two, or three fingers causes the other fingers of the hand also to exert a certain force (Li et al., 2000). It is likely that, in addition to inter-tendinous connections in human, myofascial pathways may also be responsible for such results. Experiments to verify effects of distal tendon transfer of the rectus femoris muscle, which is believed to provide conversion of it from a knee extensor to a knee flexor showed that rectus femoris still generated a knee extension moment (Riewald and Delp, 1997). Besides, using cine phase-contrast magnetic resonance imaging, joint movement was shown to change the relative position of muscle bellies in vivo in a study on human rectus femoris and vastus intermedius muscles (Asakawa et al., 2002).

Finite element modeling

Modeling of mechanics of skeletal muscle using finite element method (FEM) allows consideration of muscle tissue as a continuum and accounting for material and geometric nonlinearities. Moreover, such modeling makes it possible to study various conditions that can be used to support experimental results as well as extrapolation of them to address questions for which no direct measurements were made. This approach has been used successfully in earlier work.

A 3-D finite element mesh was mapped on a reconstructed geometry of a GM muscle of rat (Donkelaar et al., 1996) and the mechanical behavior of blood perfused muscle tissue was studied assigning blood perfused linear elastic muscle material behavior to this mesh (Vankan et al., 1996). Subsequently Vankan and coworkers (1998) developed a finite

element model of blood perfused muscle tissue and performed FE simulation of blood flow through a contracting rat calf muscle. This model includes a transversely isotropic, non-linearly elastic description of deforming muscle tissue and the local contraction stress was prescribed as a function of time. The same group also performed FEM modeling of heart muscle tissue (e.g. Huyghe et al., 1991b). Huyghe and coworkers (1991b) studied the mechanics of the passive left ventricle by considering the muscle tissue as a two-component mixture i.e., a solid component and a liquid component in their model in which changing fiber orientation was accounted for. Representing the myocardial tissue in the same way, Huyghe and coworkers (1991a) formulated a triaxial constitutive law that describes myocardial stress with two components: an elastic stress resulting from volume change and a viscoelastic stress resulting from shape change. The later component includes a strain energy function representing the anisotropic elastic response of the material described in the local coordinate system, which incorporates the fiber direction. This function is also employed in the present model to represent the non-linear and anisotropic material properties of extracellular matrix.

Using a continuum mechanics approach, Gielen (1998) developed a FEM model of skeletal muscle in which the contraction mechanism was described with a Huxley type model. That study aimed at determining detailed information about the stress and strain distributions within the muscle and applying the model for the study of damage and adaptation of muscle tissue.

Van der Linden (1998) developed a two-dimensional muscle element in which the integrated properties of muscle fibers and connective tissue were represented. The local coordinate system used, allowed assessment of stress and strain distributions in the fiber direction. This model was used to study the effects of intramuscular interventions such as tenotomy, myotomy (van der Linden, 1998) and aponeurotomy (van der Linden, 1998; Rekveldt, 1999) on muscular mechanics. The same model was also applied to study intramuscular pressure during isometric contraction of skeletal muscle (Jenkyn et al., 2002). Using similar methods to those of van der Linden (1998), Johansson and coworkers (2000) developed a 3D-muscle element.

In earlier applications of FEM in modeling of mechanics of skeletal muscle, both active and passive properties of muscle tissue were lumped in one finite element (e.g. van der Linden, 1998; Johansson et al., 2000; Jenkyn et al., 2002). In contrast, for the FEM model developed in the present thesis, a two-domain approach is employed specifically to study the effects of myofascial force transmission. This approach incorporates explicitly the two separate domains of skeletal muscle and their connections: (1) the intracellular domain and (2) the extracellular matrix domain. The two domains are represented as two separate meshes (referred to as *fiber mesh* and *matrix mesh)*. (3) trans-sarcolemmal connections are accounted for by linking the two meshes elastically. The two-domain approach allows

accounting for myofascial force transmission mechanism explicitly and addressing specific questions regarding the mechanical roles of the two domains and the links between them. Moreover, it allows elastic linking of the matrix mesh of a modeled muscle to that of an adjacent modeled muscle, as well as to mechanical ground (or to a modeled nonmuscular elastic structure) in order to represent the intermuscular and extramuscular myofascial pathways respectively.

Experimental muscles of the anterior crural compartment of the rat

For the present thesis, the experimental work was performed in the anterior crural compartment of the rat. This compartment encloses m. tibialis anterior (TA), m. extensor hallucis longus (EHL) and m. extensor digitorum longus (EDL). EDL is a unipennate muscle with rather small angles of pennation (e.g. Huijing et al., 1994). The muscle fibers do span the lengths of the fascicles in EDL. Proximally EDL has a single aponeurosis from which all of its muscle fibers originate. In contrast, distally the insertions of these muscle fibers are divided over four separate aponeuroses forming four muscle heads. The tendons of these heads span a long distance before they attach to the four digits of the foot (e.g. Balice-Gordon and Thompson, 1988; Chleboun et al., 1997). EDL extends the toes and is also a dorsal flexor of the ankle. In the rat, the proximal EDL tendon also crosses the knee joint and hence it functions as a knee extensor as well. The presence of proximal and distal tendons, extending beyond the anterior crural compartment, allows simultaneous measurement of proximal and distal muscle forces without opening the anterior crural compartment. Moreover, the positions of both proximal and distal EDL tendons can be altered conveniently, which allows imposition of different experimental conditions in terms of muscle length and relative positions of the muscles with respect to each other. TA has a very complex architecture. Its muscle fibers originate both from bony origins and from a proximal aponeurosis and some from the intermuscular septum and they insert on a distal tendon. It completely covers EDL and EHL and functions as an ankle dorsal flexor. All muscle fibers of EHL originate from anterior intermuscular septum and insert on a distal aponeurosis. The distal tendon of EHL is connected to the big toe. Owing to the unique anatomy of EDL, as well as to the short intermuscular connective tissues which connect EDL, TA and EHL muscles to each other and to the compartmental boundaries, the anterior crural compartment of the rat provides distinct advantages for studying intramuscular myofascial force transmission (Huijing et al., 1998; Huijing, 1999a) as well as inter- and extramuscular myofascial force transmission.

Goals and outline of the present study

This thesis is focused exclusively on myofascial force transmission. The available background regarding myofascial force transmission suggests that:

(1) The extracellular matrix as well as the trans-sarcolemmal connections between the muscle fibers and the extracellular matrix are likely to play a functional role in transmission of force intramuscularly.
(2) Intramuscular connective tissues are continuous with extramuscular connective tissues and the direct connections between adjacent muscles therefore, myofascial force transmission is also conceivable to occur inter- and extramuscularly.

Therefore, reconsideration of muscle functioning accounting for the integrated effects of intra-, inter- and extramuscular myofascial force transmission yields the following hypotheses:
(1) Myofascial force transmission will have important effects on muscle length-force characteristics

- If muscle force is transmitted via pathways other than the tendons, unequal forces will be exerted at proximal and distal tendons of a muscle.
- The relationship between isometric muscle force and muscle length may depend on the conditions in which muscle is functioning, i.e., determinants of muscle length-force characteristics such as muscle optimum force and length may not be unique properties of individual muscles

(2) Muscle properties such as distributions of lengths of sarcomeres may be altered as a result of myofascial force transmission.
(3) The classical role ascribed to individual muscles, as independent functional units may be representing an over simplified point of view, i.e., if force is transmitted between muscles, groups of muscles may be functional units.

The goal of this study is to test these hypotheses in a systematical approach using:
(A) Experimental results: to investigate and quantify the effects of inter- and extramuscular myofascial force transmission on muscle length-force characteristics
(B) FEM modeling: (1) to identify the roles of the two domains and the links between them in force transmission. (2) To investigate the effects of myofascial force transmission on muscular properties by studying local strain and stress distributions. (3) To correlate the global effects on muscle length-force characteristics to muscular properties and therefore to make use of FEM modeling in interpreting experimental results.

These goals were addressed in a systematic sequence of studies that are presented in the following chapters of this thesis.
Chapter 2: The FEM model developed is introduced. In addition, using a model of isolated GM muscle of the rat, a study exclusively on intramuscular myofascial force transmission is performed: the significance of transmission of force between the two domains via the transsarcolemmal connections is assessed.

Chapter 3: To be used in the successive studies on inter- and extramuscular myofascial force transmission a model of EDL muscle of the rat is built. To carry out a theoretical study of intermuscular myofascial force transmission exclusively, two modeled muscles are connected: the corresponding nodes of the matrix meshes of the two models were linked elastically. The results of this model are compared to the results of a model of isolated EDL in order to identify the effects of intermuscular myofascial force transmission on muscular properties as well as on muscle length-force characteristics such as transmission of force from one muscle to the neighboring muscle.

Chapter 4: The effects of extramuscular myofascial force transmission on muscle length-force characteristics are investigated with experiments on EDL muscle leaving the muscles' extramuscular connective tissues intact. Using the FEM model, the effects of such transmission on muscular properties are investigated with emphasis on monitoring distributions of lengths of sarcomeres arranged in series within muscle fibers. In this chapter as well as in Chapters 5 and 6 studying the stress distributions within the fiber mesh i.e., comparing the stress values at proximal and distal fiber ends, the consideration of muscle fibers as independent force producing units that exert identical forces at both ends (which should be true if myotendinous force transmission is the exclusive means of force transmission) is tested.

Chapter 5: The integrated effects of inter- and extramuscular myofascial force transmission on muscle length- force characteristics are investigated with experiments on the muscles of the anterior crural compartment of the rat by leaving the connective tissues at bellies of EDL, TA and EHL muscles intact. Also the specific effects of intermuscular myofascial force transmission are assessed by comparing the results of this experiment with the results of the experiments presented in Chapter 4. The results of this comparison suggesting that the determinants of muscle length-force characteristics, such as muscle optimum length and muscle optimum force are affected by such force transmission generates hypotheses regarding distributions of lengths of sarcomeres. The correlation between altered length range of active force exertion and such distributions is tested using the FEM model.

Chapter 6: Effects of changing relative position of a muscle with respect to the surrounding nonmuscular connective tissue structures are assessed with experiments on EDL muscle (Maas et al., 2002) and using the FEM model presented in Chapter 4. In this study the muscle length is kept constant whereas the relative position of the muscle belly is altered. The hypothesis suggesting that that the relative position of a muscle with respect to its surrounding connective tissues is a co-determinant of muscle force in addition to muscle length is tested. Moreover, the FEM model is used to investigate the integrated effects of intra- and extramuscular myofascial force transmission on muscular mechanics. The contribution of intracellular domain and the extracellular matrix domain to total muscle force is assessed for different fascicles within the muscle belly.

References

Alberts, B., Bray, D., Lewis, J., Faff, M., Roberts, K. and Watson, J. D. (1989). Molecular biology of the cell. New York, Garland Publishing.

Asakawa, D. S., Blemker, S. S., Gold, G. E. and Delp, S. L., 2002. In vivo motion of the rectus femoris muscle after tendon transfer surgery. Journal of Biomecanics 35, 1029-1037.

Balice-Gordon, R. J. and Thompson, W. J., 1988. The organization and development of compartmentalized innervation in rat extensor digitorum longus muscle. Journal of Physiology 398, 211-231.

Bartels, E. M., Skydsgaard, J. M. and Sten-Knudsen, O., 1979. The time course of the latency relaxation as a function of the sarcomere length in frog and mammalian muscle. Acta Physiologica Scandinavica 106, 129-137.

Berthier, C. and Blaineau, S., 1997. Supramolecular organization of the subsarcolemmal cytoskeleton of adult skeletal muscle fibers. A review. Biology of the Cell 89, 413-434.

Borg, T. K. and Caulfield, J. B., 1980. Morphology of connective tissue in skeletal muscle. Tissue Cell 12, 197-207.

Campbell, K. P., 1995. Three muscular dystrophies: loss of cytoskeleton-extracellular matrix linkage. Cell 80, 675-679.

Chleboun, G. S., Patel, T. J. and Lieber, R. L., 1997. Skeletal muscle architecture and fiber-type distribution with the multiple bellies of the mouse extensor digitorum longus muscle. Acta Anatomica 159, 147-155.

Craig, S. W. and Pardo, J. V., 1983. Gamma actin, spectrin, and intermediate filament proteins colocalize with vinculin at costameres, myofibril-to-sarcolemma attachment sites. Cell Motil 3, 449-462.

Danowski, B. A., Imanaka-Yoshida, K., Sanger, J. M. and Sanger, J. W., 1992. Costameres are sites of force transmission to the substratum in adult rat cardiomyocytes. The Journal of Cell Biology 118, 1411-1420.

Donkelaar, C. C. v., Drost, M. R., Mameren, H. v., Tuinenburg, C. F., Janssen, J. D. and Huson, A., 1996. Three-Dimensional reconstruction of the rat triceps surae muscle and finite element mesh generation of the gastrocnemius medialis muscle. European Journal of Morphology 34, 31-37.

Gielen, S., A continuum approach to the mechanics of contracting skeletal muscle (PhD thesis). Eindhoven, The Netherlands: Eindhoven University of Technology, 1998.

Horowits, R. and Podolsky, R. J., 1987. The positional stability of thick filaments in activated skeletal muscle depends on sarcomere length: evidence for the role of titin filaments. Journal of cell biology 105, 2217-2223.

Huijing, P. A., 1999a. Muscle as a collagen fiber reinforced composite material: Force transmission in muscle and whole limbs. Journal of Biomechanics 32, 329-345.

Huijing, P. A., 1999b. Muscular force transmission: A unified, dual or multiple sytem? A review and some explorative experimental results. Archives of Physiology and Biochemistry 170, 292-311.

Huijing, P. A. (2000). In vivo, force is transmitted from muscle also at other locations than the tendons: Extramuscular myofascial force transmisison. 5th Annual Congress of the European College of Sports Science, Jyvaskyla, Finland, University of Jyvaskyla.

Huijing, P. A. and Baan, G. C., 2001a. Extramuscular myofascial force transmission within the rat anterior tibial compartment: Proximo-distal differences in muscle force. Acta Physiologica Scandinavica 173, 1-15.

Huijing, P. A. and Baan, G. C., 2001b. Myofascial force transmission causes interaction between adjacent muscles and connective tissue: Effects of blunt dissection and compartmental fasciotomy on length force characteristics of rat extensor digitorum longus muscle. Archives of Physiology and Biochemistry 109, 97-109.

Huijing, P. A. and Baan, G. C., 2003. Myofascial force transmission: muscle relative position and length determine agonist and synergist muscle force. Journal of Applied Physiology 94, 1092-1107.

Huijing, P. A., Baan, G. C. and Rebel, G., 1998. Non myo-tendinous force transmission in rat extensor digitorum longus muscle. Journal of Experimental Biology 201, 682-691.

Huijing, P. A., Nieberg, S. M., vd Veen, E. A. and Ettema, G. J., 1994. A comparison of rat extensor digitorum longus and gastrocnemius medialis muscle architecture and length-force characteristics. Acta Anatomica 149, 111-120.

Huxley, A. F., 1957. Muscle structure and theories of contraction. Prog. Biophys. Biophys. Chem. 7.

Huyghe, J. M., van Campen, D. H., Arts, T. and Heethaar, R. M., 1991a. The constitutive behaviour of passive heart muscle tissue: a quasi- linear viscoelastic formulation. Journal of Biomechanics 24, 841-849.

Huyghe, J. M., van Campen, D. H., Arts, T. and Heethaar, R. M., 1991b. A two-phase finite element model of the diastolic left ventricle. Journal of Biomechanics 24, 527-538.

Jaspers, R. T., Brunner, R., Pel, J. J. M. and Huijing, P. A., 1999. Acute effects of intramuscular aponeurotomy on rat GM: Force transmission, muscle force and sarcomere length. Journal of Biomechanics 32, 71-79.

Jenkyn, T. R., Koopman, B., Huijing, P., Lieber, R. L. and Kaufman, K. R., 2002. Finite element model of intramuscular pressure during isometric contraction of skeletal muscle. Physics in Medicine and Biology 47, 4043-4061.

Johansson, T., Meier, P. and Blickhan, R., 2000. A finite-element model for the mechanical analysis of skeletal muscles. Journal of Theoretical Biology 206, 131-49.

Leiden, J. M., 1997. The genetics of dilated cardiomyopathy, emerging clues to the puzzle. New England Journal of Medicine 337, 1080-1081.

Li, Z. M., Zatsiorsky, V. M. and Latash, M. L., 2000. Contribution of the extrinsic and intrinsic hand muscles to the moments in finger joints. Clinical Biomechanics 15, 203-211.

Lindhard, J., 1931. Der Skeletmuskel und seine Funktion. Ergebntsse der Physiologie 33, 22-557.

Loeb, G. E., Pratt, C. A., Chanaud, C. M. and Richmond, F. J., 1987. Distribution and innervation of short, interdigitated muscle fibers in parallel-fibered muscles of the cat hindlimb. Journal of Morphology 191, 1-15.

Maas, H., Baan, G. C. and Huijing, P. A., 2001. Intermuscular interaction via myofascial force transmission: effects of tibialis anterior and extensor hallucis longus length on force transmission from rat extensor digitorum longus muscle. Journal of Biomechanics 34, 927-940.

Maas, H., Baan, G. C. and Huijing, P. A. (2002). The relative position of extensor digitorum longus muscle, kept at constant length, affects isometric force exerted at its proximal and distal tendons: effects of extramuscular myofascial force transmission. 12 th International Conference on Mechanics in Medicine and Biology, Lemnos, Greece.

Maruyama, K., 1994. Connectin, an elastic protein of striated muscle. Biophys Chem 50, 73-85.

Menke, A. and Jockusch, H., 1991. Decreased osmotic stability of dystrophin-less muscle cells from the mdx mouse [see comments]. Nature 349, 69-71.

Menke, A. and Jockusch, H., 1995. Extent of shock-induced membrane leakage in human and mouse myotubes depends on dystrophin. Journal of Cell Science 108, 727-733.

Ohlendieck, K., 1996. Towards an understanding of the dystrophin-glycoprotein complex: linkage between the extracellular matrix and the membrane cytoskeleton in muscle fibers. European Journal of Cell Biology 69, 1-10.

Pardo, J. V., Pittenger, M. F. and Craig, S. W., 1983a. Subcellular sorting of isoactins: selective association of gamma actin with skeletal muscle mitochondria. Cell 32, 1093-1103.

Pardo, J. V., Siliciano, J. D. and Craig, S. W., 1983b. A vinculin-containing cortical lattice in skeletal muscle: transverse lattice elements ("costameres") mark sites of attachment between myofibrils and sarcolemma. Proceedings of the National Academy of Sciences of the United States of America 80, 1008-1012.

Pasternak, C., Wong, S. and Elson, E. L., 1995. Mechanical function of dystrophin in muscle cells. Journal of cell biology 128, 355-361.

Patel, T. J. and Lieber, R. L., 1997. Force transmission in skeletal muscle: from actomyosin to external tendons. Exercise and Sport Science Review 25, 321-363.

Petrof, B. J., Shrager, J. B., Stedman, H. H., Kelly, A. M. and Sweeney, H. L., 1993. Dystrophin protects the sarcolemma from stresses developed during muscle contraction. Proceedings of the National Academy of Sciences of the United States of America 90, 3710-3714.

Podolsky, R. J., 1964. The maximum sarcomere length for contraction of isolated myofibrils. Journal of Physiology 170, 110-123.

Purslow, P. P. and Trotter, J. A., 1994. The morphology and mechanical properties of endomysium in series-fibred muscles: variations with muscle length. Journal of Muscle Research Cell Motility 15, 299-308.

Ramsey, R. W. and Street, S. F., 1940. The isometric length-tension diagram of isolated skeletal muscle fibers of the frog. Journal of Cellular and Comparative Physiology 15, 11-34.

Rekveldt, M. G. C., Finite element modeling of aponeurotomy (MSc thesis). Enschede, The Netherlands: University of Twente, 1999.

Riewald, S. A. and Delp, S. L., 1997. The action of the rectus femoris muscle following distal tendon transfer: does it generate knee flexion moment? Developmental Medicine and Child Neurology 39, 99-105.

Shear, C. R. and Bloch, R. J., 1985. Vinculin in subsarcolemmal densities in chicken skeletal muscle: localization and relationship to intracellular and extracellular structures. The Journal of Cell Biology 101, 240-256.

Street, S. F., 1983. Lateral transmission of tension in frog myofibers: a myofibrillar network and transverse cytoskeletal connections are possible transmitters. Journal of Cellular Physiology 114, 346-364.

Street, S. F. and Ramsey, R. W., 1965. Sarcolemma: transmitter of active tension in frog skeletal muscle. Science 149, 1379-1380.

Tidball, J. G., 1983. The geometry of actin filament-membrane associations can modify adhesive strength of the myotendinous junction. Cell Motil 3, 439-447.

Tidball, J. G., 1991. Force transmission across muscle cell membranes. Journal of Biomechanics 24, 43-52.

Trinick, J., 1991. Elastic filaments and giant proteins in muscle. Curr Opin Cell Biol 3, 112-119.

Trombitas, K., Jin, J. P. and Granzier, H., 1995. The mechanically active domain of titin in cardiac muscle. Circulation Research 77, 856-861.

Trotter, J. A., 1990. Interfiber tension transmission in series-fibered muscles of the cat hindlimb. Journal of Morphology 206, 351-361.

Trotter, J. A., 1991. Dynamic shape of tapered skeletal muscle fibers. Journal of Morphology 207, 211-223.

Trotter, J. A., 1993. Functional morphology of force transmission in skeletal muscle. A brief review. Acta Anatomica (Basel) 146, 205-222.

Trotter, J. A. and Purslow, P. P., 1992. Functional morphology of the endomysium in series fibered muscles. Journal of Morphology 212, 109-122.

van der Linden, B. J. J. J., Mechanical modeling of muscle functioning (PhD thesis). Enschede, The Netherlands: University of Twente, 1998.

Vankan, W. J., Huyghe, J. M., Janssen, J. D. and Huson, A., 1996. A 3-D finite element model of blood perfused rat gastrocnemius medialis muscle. European Journal of Morphology 34, 19-24.

Vankan, W. J., Huyghe, J. M., van Donkelaar, C. C., Drost, M. R., Janssen, J. D. and Huson, A., 1998. Mechanical blood-tissue interaction in contracting muscles: a model study. Journal of Biomechanics 31, 401-409.

Worton, R., 1995. Muscular dystrophies: diseases of the dystrophin-glycoprotein complex. Science 270, 755-756.

Chapter 2

Three-dimensional finite element modeling of skeletal muscle using a two-domain approach: Linked fiber-matrix mesh model

Abstract

In previous applications of the finite element method in modeling mechanical behavior of skeletal muscle, the passive and active properties of muscle tissue were lumped in one finite element. Although this approach yields increased understanding of effects of force transmission, it does not support an assessment of the interaction between the intracellular structures and extracellular matrix. In the present study, skeletal muscle is considered in two domains: (1) the intracellular domain and (2) extracellular matrix domain. The two domains are represented by two separate meshes that are linked elastically to account for the trans-sarcolemmal attachments of the muscle fibers' cytoskeleton and extracellular matrix. With this approach a finite element skeletal muscle model is developed, which allows force transmission between these domains with the possibility of investigating their interaction as well as the role of the trans-sarcolemmal systems.

The model is applied to show the significance of myofascial force transmission, by investigating possible mechanical consequences due to any missing link within the trans-sarcolemmal connections such as found in muscular dystrophies. This is realized by making the links between the two meshes highly compliant at selected intramuscular locations. The results indicate the role of extracellular matrix for a muscle in sustaining its physiological condition. It is shown that if there is an inadequate linking to the extracellular matrix, the myofibers become deformed beyond physiological limits due to the lacking of mechanical support and impairment of a pathway of force transmission by the extracellular matrix. This leads to calculation of a drop of muscle force and if the impairment is located more towards the center of the muscle model, its effects are more pronounced. These results indicate the significance of non-myotendinous force transmission pathways.

Introduction

The finite element method (FEM) is a powerful tool for modeling mechanics of skeletal muscle. In an earlier work, a 3-D finite element mesh was mapped on a reconstructed geometry of a gastrocnemius medialis muscle of rat to study the mechanical behavior of blood-perfused muscle tissue (e.g. Donkelaar et al., 1996; Vankan et al., 1996). Subsequently Vankan and coworkers (1998) developed a finite element model of blood perfused biological tissue, which contains a transversely isotropic, non-linearly elastic description of deforming muscle tissue. Finite element modeling of heart muscle tissue was also done in the same group (e.g. Huyghe et al., 1991b; Huyghe et al., 1991a). van der Linden and colleagues (1998) developed a muscle element and built a 2D-muscle finite element model. Recently, Johansson and coworkers (2000) developed a 3D-muscle element in a similar way.

Skeletal muscle tissue is composed of activatable muscle fibers and a passive matrix of connective tissues that houses them. Muscle can be represented as an extensive 3D set of endomysial tunnels within which the myofibers operate (e.g. Trotter and Purslow, 1992). Although a certain general knowledge has existed for a long time that myofibers are connected to the extracellular matrix and neighboring muscles (e.g. Pond, 1982), this knowledge has not generally been used in physiological experiments on muscle to consider the role of these connections in *force transmission* explicitly (e.g. Heslinga and Huijing, 1993; Hawkins and Bey, 1997). On the other hand, some specific work showed that the linked intracellular and extracellular matrix domains interact mechanically (e.g. Street, 1983; Trotter and Purslow, 1992). The multimolecular complexes (Berthier and Blaineau, 1997) connecting sarcomeres to elements of the subsarcolemmal cytoskeleton and from there to trans-sarcolemmal molecules provide a route of force transmission to the extracellular matrix. Force transmission from the full perimeter surface of myofibrils onto the extracellular matrix was evident in a number of experimental studies (e.g. Huijing et al., 1998; Huijing, 1999a; Huijing, 1999b). This transmission has not been considered in skeletal muscle models (e.g. van der Linden et al., 1998; Denoth and Danuser, 2001) other than in some FEM work (e.g. van der Linden, 1998; Johansson et al., 2000), which accounted for myofascial force transmission mechanism implicitly as the passive and active properties of muscle were lumped in one finite element. In the present model, skeletal muscle is considered explicitly as two separate domains: (1) the intracellular domain and (2) extracellular matrix domain. To account for the transmembranous attachments, the two domains are linked elastically. This way of modeling allows assessment of force transmission and interaction between these domains. The goal of the present paper is to introduce this model and present a first application to show the significance of intramuscular myofascial force transmission. The modeled conditions involve altered or inadequate linking of the domains. Such conditions may be found in pathologies such as muscular dystrophies.

Methods

The Model

Two 3D-elements developed were introduced into ANSYS 5.5.1 FEM software as user-defined elements. One of these elements represents the extracellular matrix, which includes the basal lamina and connective tissue components such as endomysium and perimysium (*extracellular matrix element*). A second element accounts for the muscle fibers (*myofiber element*). The elements have eight nodes, linear interpolation functions and a large deformation analysis formulation. A 3D local coordinate system representing the fiber, cross-fiber (normal to the fiber direction), and thickness directions is used. The stress formulation, $\underline{S}$ based on Second Piola–Kirchoff definition constitutes the derivative of the strain energy density function, *W* with respect to the Green–Lagrange strain tensor, $\mathrm{d}\underline{L}^{G}$

$$\underline{S} = \frac{dW}{d\underline{L}^{G}} \tag{2.1}$$

Extracellular matrix element

The strain energy density function mechanically characterising the extracellular matrix includes two parts:

$$W = W_1 + W_2 \tag{2.2}$$

The first part represents the non-linear and anisotropic material properties (Huyghe et al., 1991a):

$$W_1 = W_{ij}(\varepsilon_{ij}) \quad \text{where} \tag{2.3}$$

$$W_{ij}(\varepsilon_{ij}) = \mathrm{k}.(\mathrm{e}^{a_{ij}.\varepsilon_{ij}} - \mathrm{a}_{ij}.\varepsilon_{ij}) \quad \text{for} \quad \varepsilon_{ij} > 0 \quad \text{or}$$
$$W_{ij}(\varepsilon_{ij}) = -W_{ij}\left(\left|\varepsilon_{ij}\right|\right) \quad \text{for} \quad \varepsilon_{ij} < 0 \text{ and } i \neq j \tag{2.4}$$

ε_{ij} are the Green-Lagrange strains in the local coordinates. The indices $i = 1\ldots3$ and $j = 1\ldots3$ represent the local cross-fiber, fiber and thickness directions respectively. a_{ij} and *k* are constants (Table 1). The resulting stress-strain curves are shown in Fig.1a.

The second part includes a penalty function to account for the constancy of muscle volume.

$$W_2 = \lambda_s.(I_3 - 1)^2 + \lambda_f.(I_3^{avg} - 1)^2 \qquad (2.5)$$

where I_3 is the third invariant (determinant) of the Right Cauchy-Green strain tensor and is a measure for the local volume for each Gaussian point. To conserve the local volumes (i.e I_3 equals unity), the element is considered as incompressible solid. In contrast, if the weighted mean of all I_3`s per element, (I_3^{avg}) is kept as unity, the element is considered to be a fluid. Using the penalty parameters λ_s (for the solid volume) and λ_f (for the fluid volume) (Table 1), the emphasis given for each part can be manipulated.

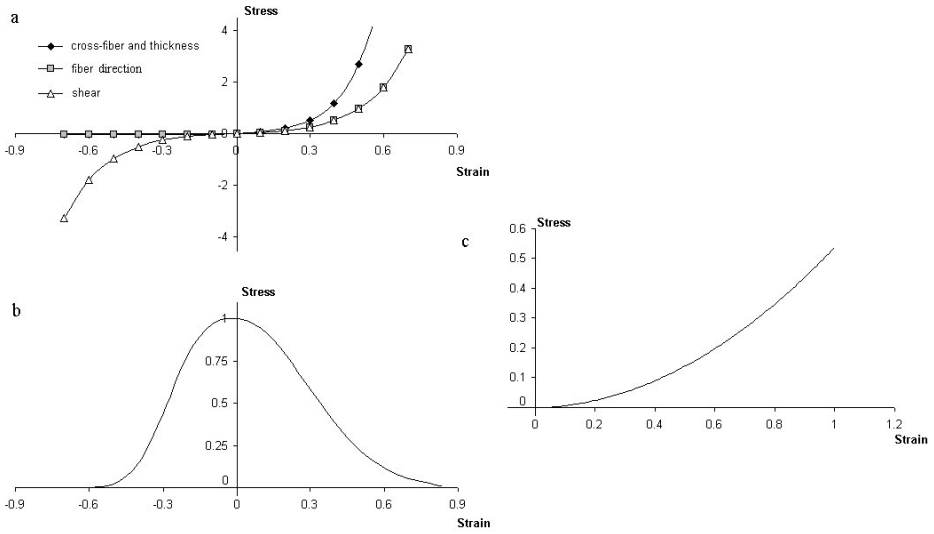

Fig.1. The stress-strain relations representing the mechanical behavior of the muscle tissue. (a) Passive non-linear and anisotropic material properties of the extracellular matrix element in the local coordinates. (b) Active stress-strain properties of the myofiber element representing the contractile apparatus, which is only valid for the local fiber direction. (c) Mechanical properties representing the titin filaments which is dominating the passive resistance in the myofiber element valid, also only in the local fiber direction. The curves in parts (b) and (c) are scaled to the maximum value of active contractile stress to make them compatible. The stresses are normalized and dimensionless.

Myofiber element

Maximally activated muscle is studied and within the muscle fibers, sarcomeres are assumed to have identical material properties. The force-velocity characteristics are not considered due to the isometric nature of the present work. The total stress for the intracellular domain ($\sigma_{22\,\mathrm{f}}$) is a Cauchy stress acting only in the local fiber direction and is the sum of the active

stress of the contractile elements ($\sigma_{22contr}$) and the stress due to intracellular passive tension (σ_{22icp}).

Table 1. Values and definitions of the constants used in the formulations

Constant	Value	Definition
k	0.05	Initial passive stiffness (eqn 2.4)
a_{11}	8.0	Passive cross-fiber direction stiffness, $a_{11} = a_{33}$ (eqn 2.4)
a_{22}	6.0	Passive fiber direction stiffness (eqn 2.4)
a_{12}	6.0	Passive fiber-cross-fiber shear stiffness, $a_{12}=a_{23}=a_{31}$ (eqn 2.4)
λ_s	10.0	Weight factor in the penalty function for the solid volume (eqn 2.5)
λ_f	80.0	Weight factor in the penalty function for the fluid volume (eqn 2.5)
b_1	30.0	Coefficient for the stress-strain relation of the contractile elements (eqn 2.6)
b_2	-6.0	Coefficient for the stress-strain relation of the contractile elements (eqn 2.6)
b_3	1	Coefficient for the stress-strain relation of the contractile elements (eqn 2.6)
t_1	0.522	Coefficient for the stress-strain relation of the intracellular passive elements (eqn 2.7)
t_2	0.019	Coefficient for the stress-strain relation of the intracellular passive elements (eqn 2.7)
t_3	-0.002	Coefficient for the stress-strain relation of the intracellular passive elements (eqn 2.7)

To define the active length-force characteristics, an exponential function (Fig.1b) was fit to the experimental data of small rat GM fiber bundles (Zuurbier et al., 1995). This function is scaled such that at optimum length, the fiber direction strain (ε_{22}) is zero and the maximal stress value is unity.

$$\sigma_{22contr}(\varepsilon_{22})=b_3 e^{b_2\varepsilon_{22}^3} \quad \text{for } \varepsilon_{22}>0 \text{ or}$$
$$\sigma_{22contr}(\varepsilon_{22})=b_3 e^{b_1\varepsilon_{22}^4} \quad \text{for } \varepsilon_{22}<0 \qquad (2.6)$$

where b_1, b_2 and b_3 are constants (Table 1)

The source of intracellular passive tension is the intra-sarcomeric cytoskeleton (Trombitas et al., 1995), which is composed of several proteins. In this work titin is considered to play the dominant role. Experimental tension-sarcomere length data (Trombitas et al., 1995) for a single rabbit skeletal muscle fiber was fitted using a parabolic

function (Fig.1c) and scaled to make it compatible to the stress-strain characteristics of the contractile part.

$$\sigma_{22\,icp}(\varepsilon_{22}) = t_1\varepsilon_{22}^2 + t_2\varepsilon_{22} + t_3 \qquad \text{and}$$
$$\sigma_{22icp}(\varepsilon_{22}) = 0 \quad \text{for} \quad \varepsilon_{22} < 0 \tag{2.7}$$

where t_1, t_2 and t_3 are constants (Table 1)

Aponeurosis Element

To represent the aponeurosis, a standard element with a hyperelastic mechanical formulation (HYPER58) from the element library of ANSYS 5.5.1 is used.

Linked fiber-matrix mesh model

Within the biological context, one *muscle element* is defined to represent a segment of a bundle of muscle fibers with identical material properties, its connective tissues and the links between them. This is realized as a linked system of connective tissue and myofiber elements. A schematic 1D-representation of an arrangement of these muscle elements is shown in Fig.2a.

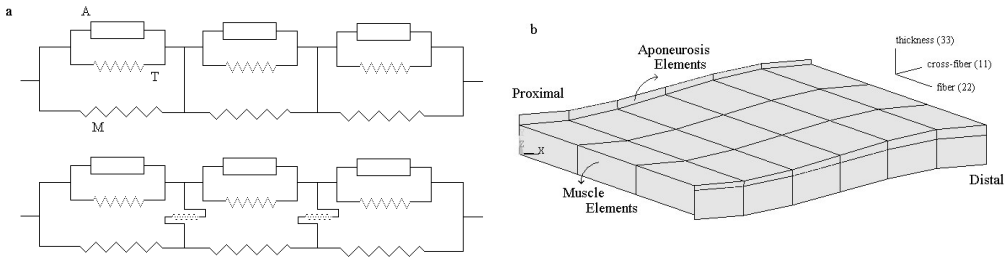

Fig.2. (a) 1D-Schematic representation of an arrangement of muscle elements. The intracellular domain, which is composed of the active contractile elements (A) and intracellular passive cytoskeleton (T), can be linked to the extracellular matrix domain (M) rigidly (upper panel), or elastically (lower panel). (b) The geometry of the muscle model is defined by the contour of a longitudinal slice of the isolated rat medial gastrocnemius muscle belly. The model is composed of three in series and six in parallel muscle elements. The initial muscle length is 30.3 mm. The 3D local coordinate system representing the fiber, cross-fiber (direction perpendicular to the fiber direction) and thickness directions, used for the analysis and presentation of the results is shown. Proximal and distal ends of the model were restrained in all directions. The nodes at the lower surface of the model were constrained to move in the thickness direction.

In the *linked fiber-matrix mesh model*, the extracellular matrix domain is represented by a mesh of extracellular matrix elements (*matrix mesh*). In the same space, a separate mesh of

myofiber elements is built to account for the intracellular domain (*fiber mesh*). The two meshes are rigidly connected to single layers of aponeurosis elements at the myotendinous connection sites and are linked elastically at the intermediate nodes. The elastic links are maintained as adjustable in stiffness to allow manipulation of the interaction. The links are represented by the spring element COMBIN39, one of the standard elements of ANSYS 5.5.1, which is set to be longitudinal and have linear stiffness characteristics.

The geometry of the model is shown in (Fig.2b). The collection of elements in series represents a big muscle fascicle. All aponeurosis elements have identical properties but an increasing stiffness is introduced towards the tendons using a variable thickness in the fiber-cross fiber plane.

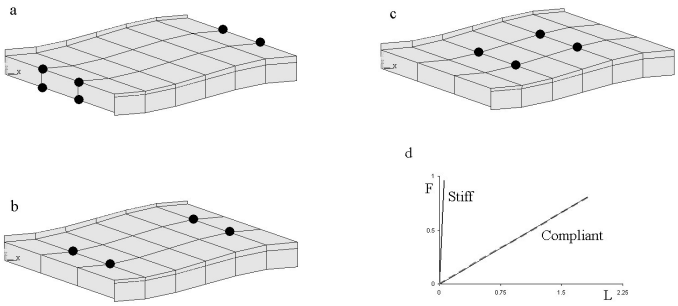

Fig.3. The compliant links at selected locations within the muscle model. The locations indicated in part (a) are referred to as case A, part (b) are as case B and (c) are as case C. Comparison of the normalized length-force curves of the stiff and compliant links as a measure of their relative stiffness is given in part (d).

A first application of the linked fiber-matrix mesh model

The functioning and integrity of skeletal muscle fibers is directly related to their being efficiently anchored to the extracellular environment (e.g. Berthier and Blaineau, 1997). Dystrophin is a subsarcolemmal protein participating in such linking and is thought to play the major role in force transduction (Ingber, 1991) as well as force transmission (Wang et al., 1993). In order to show the significance of such transmission, the linking stiffness was manipulated at selected locations within the modeled muscle (Fig.3) such that at 8 of the total 28 nodes links were made much more compliant than the highly stiff remainder links. Dystrophin deficiency can lead to such pathological conditions that may be caused by diseases, muscular dystrophies (e.g. Campbell, 1995; Jung et al., 1996; Ohlendieck, 1996) or by eccentric contractions in genetically healthy muscle (e.g. Komulainen et al., 1998). As the solutions for the nodes are interpolated linearly over the elements, decreased linking stiffness represents the missing or altered connection between the two domains along the full length of fibers.

Results

High stiffness links

As a control case, (case S), all the links between the two meshes were made highly stiff. The calculated total muscle length-force characteristics provide a sufficiently good comparison to experimental data (Meijer et al., 1998). However, the modeled forces cover a wider length range, and above optimum length, they are higher than the experimental ones (Fig.4).

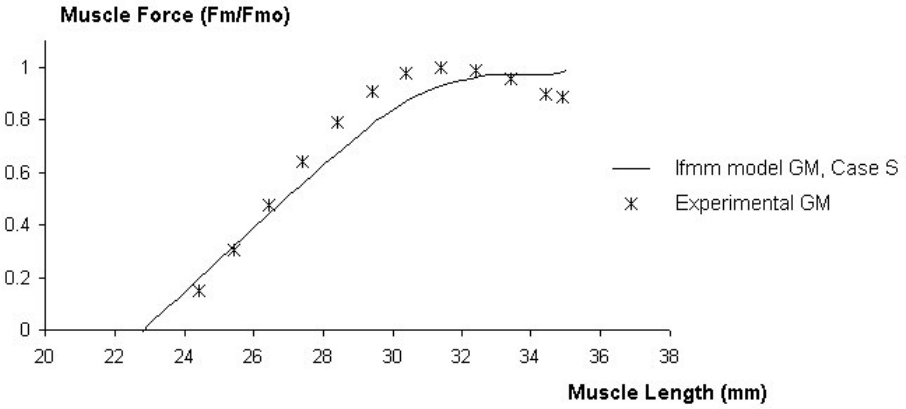

Fig.4. The isometric muscle length-total force curves for isolated rat medial gastrocnemius muscle (GM). Case S is the control case for the linked fiber matrix mesh model (lfmm model) with all links being highly stiff. Experimental GM data is adopted from (Meijer et al., 1998). The muscle force (Fm) is normalized for optimum force (Fmo). Initial muscle length is 30.3 mm.

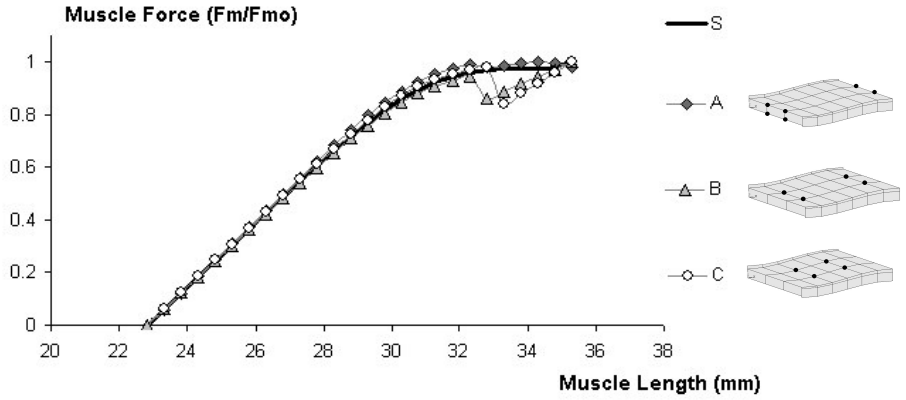

Fig.5. The muscle length-total force curves. S is the control case with all links being highly stiff. For the other three cases, the links at the nodes of intramuscular locations A, B and C are compliant. The muscle force (Fm) is normalized for optimum force (Fmo). Initial muscle length is 30.3 mm.

Lower stiffness links at selected intramuscular locations

A comparison of modeled muscle length-force characteristics with stiff (case S) and compliant links (cases A, B and C) is shown in Fig.5. For the lower length range, not much difference was found as a result of manipulation of linking stiffness. In contrast, for compliant links at certain intramuscular locations, the high length range (i.e., $l_{ma} > l_{mao} + 2\,\text{mm}$) yielded drops in force accompanying small changes of isometric length. This drop is enhanced, as the compliant link locations are more towards the middle of the muscle belly while little effect is seen if they are at the periphery.

The reason for the force drop can be understood from the stress (presented as Cauchy stresses: $\underline{\sigma}$) and strain distribution comparisons in the fiber mesh (Fig.6) for two muscle lengths: The length just below that at which the force drop occurs and the actual length of force drop. For case C, such comparison reveals a sizable overall decrease of total fiber direction stress (σ_{22f}). At the lower length, σ_{22f} approximates unity throughout the fiber mesh (Fig 6a), but it reaches much lower values locally at the higher length (Fig.6b). Distribution of ε_{22} is highly uniform at the lower length (Fig.6c) while very high strains occur near the compliant link locations at the force drop length (Fig.6d). These locally high strains reach values (over unity) for which very small (or zero) active stresses are calculated (see Fig.1b). The high negative strains observed also lead to lower stress in the fiber direction. This decrease in stress at higher length generates the force drop.

The stress within the fiber mesh ascribable to the contractile elements ($\sigma_{22\text{contr}}$) and intra-sarcomeric cytoskeleton ($\sigma_{22\text{icp}}$) is compared for these two lengths (Fig.7). For the lower length, both $\sigma_{22\text{contr}}$ (Fig.7a) and $\sigma_{22\text{icp}}$ (Fig.7b) distributions are almost uniform approximating values arround unity and zero respectively. However, at the higher length, $\sigma_{22\text{contr}}$ shows substantial decreases (up to zero) (Fig.7c) while $\sigma_{22\text{icp}}$ attains high values (Fig.7d) at the same locations. This suggests that sarcomeres are stretched locally to lengths higher than maximal filament overlap length, which phenomenon is known as popped sarcomeres (Morgan, 1990).

The effect of location of intervention is assessed through the strain distributions in the fiber direction and the shear between the fiber and cross-fiber directions (Fig.8) at the highest isometric length considered. For case S, the fiber mesh shear strain is quite uniform however; increased distributions are found for the cases from A to C (Fig.8a, left column). This leads to shear strain distributions ranging from negative to sizable positive values, as the interventions are more central.

The lengths of myofiber elements are monitored from the fiber direction strains (Fig.8b, left column). Case A, displays differences in distributions compared to case S but the

remarkable effects of the interventions are clearly visible in cases B and C. In these cases, strains reach quite low and very high values, indicating that there are overly lengthened and shortened elements in the fiber mesh. The resulting length differences are clearly visible in the deformed shapes of the fiber mesh.

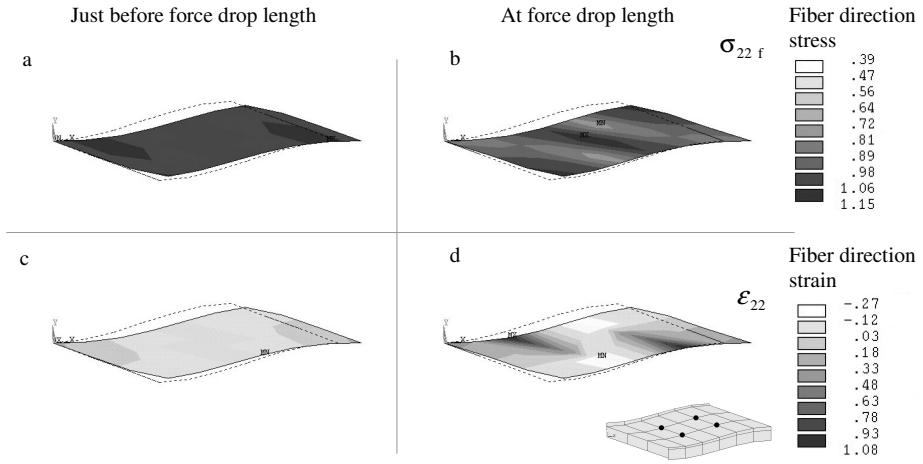

Fig.6. The total stress and strain distributions for the fiber mesh, in the fiber direction at high muscle lengths, with compliant links. (a) and (b) The total stress is the sum of the active stress of the contractile elements and the stress due to the passive intra-sarcomeric cytoskeleton. (c) and (d) Strain distributions of the fiber mesh for the fiber (22) direction. Stress and strain distributions are shown for two muscle lengths equal to 32.8 mm and 33.3 mm respectively. The higher length is the length at which the force drop was found and the lower length is just below it. Results are shown for the case with compliant links located intramuscularly (case C, marked with dots, in inset). The dotted line contour indicates muscle geometry at the initial length.

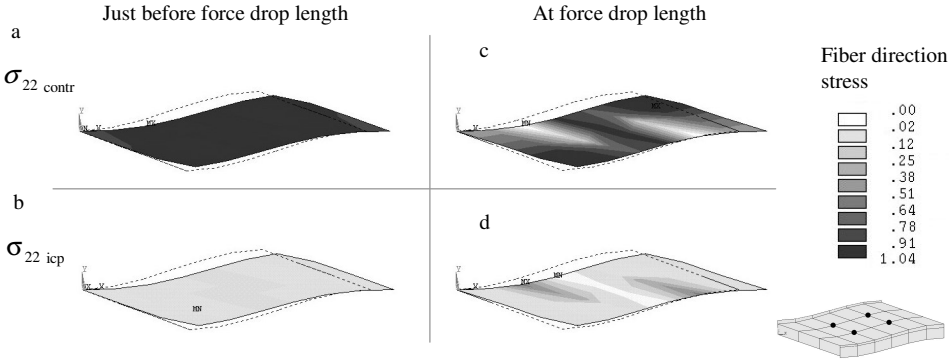

Fig.7. Contributions to total stress by active contractile elements and the passive intra-sarcomeric cytoskeleton. (a) and (b) Distributions of $\sigma_{22\,\mathrm{contr}}$ and $\sigma_{22\,\mathrm{icp}}$ respectively ,at the length which is just below that of the force drop (32.8 mm). (c) and (d) Distributions of $\sigma_{22\,\mathrm{contr}}$ and $\sigma_{22\,\mathrm{icp}}$ at the force drop length (33.3 mm). Results are shown for the case with compliant links located intramuscularly (case C, marked with dots, in inset). The dotted line contour indicates muscle geometry at the initial length.

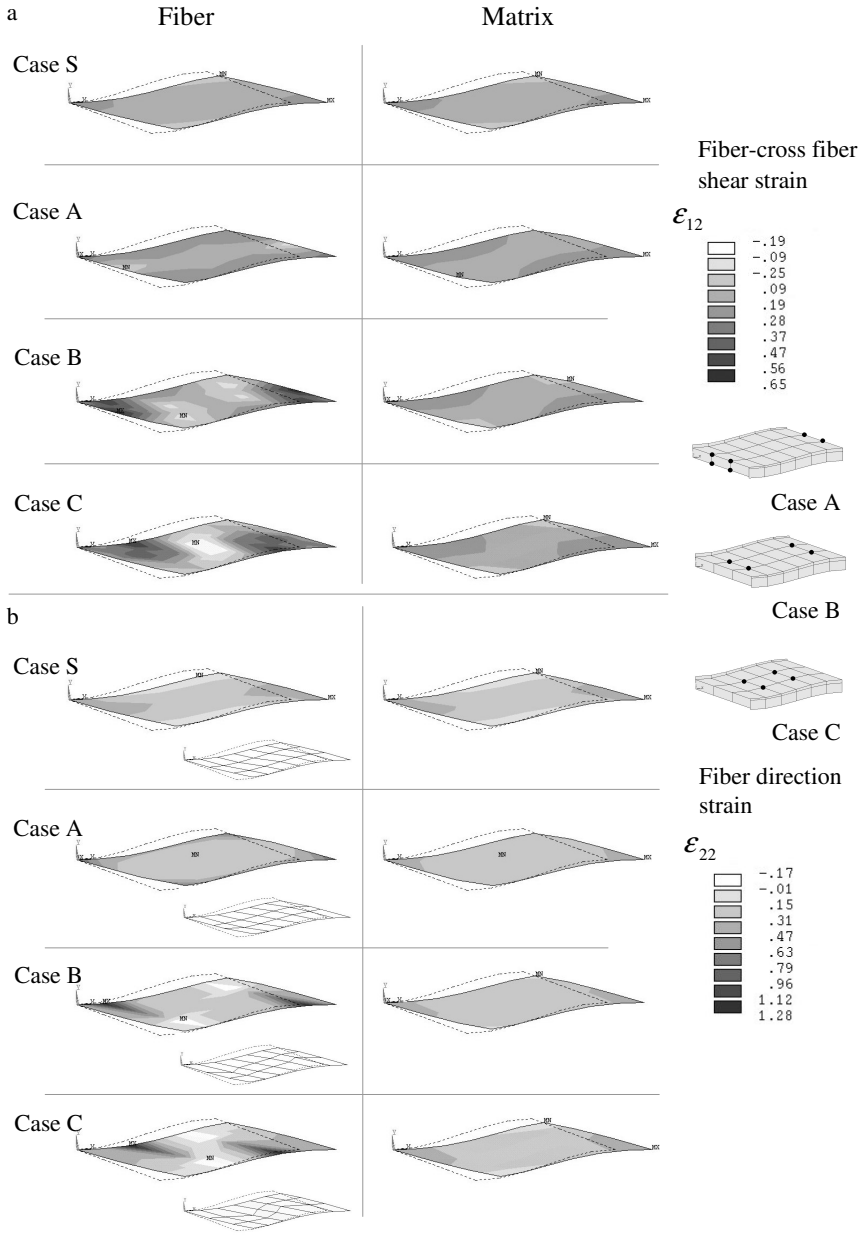

Fig.8. The effect of the location of compliant links on the fiber direction and shear strain distributions. (a) The shear strain (12) between fiber and cross-fiber directions for the control case (Case S) and the cases with local compliant links (Cases A, B and C). (b) The fiber (22) direction strains for all cases. The actual deformed shapes of the fiber mesh are also shown as insets below the strain distributions. All distributions in the left column are for the fiber mesh while the right column shows results for the extracellular matrix. The locations of the compliant links are indicated by dots at the right hand side of the figure. The fiber and shear strain distributions are shown for all cases at the highest length (35.3 mm).

Comparing the matrix meshes of the pathological cases, some limited differences in shear strains are visible (Fig.8a, right column) which almost completely disappears for fiber direction strains (Fig.8b, right column). The differences between the matrix meshes of case S and the pathological cases are also very limited especially in the fiber direction. The matrix mesh is highly stiff, as it does not display big strain variations regardless of the stiffness and location of the links between the two meshes. Also note that there are hardly any differences between the fiber and matrix mesh strain for case S (compare Fig.8a and b top panels).

The loads on a representative link (at a location belonging to case C, Fig.9) show that, at most muscle lengths, link loads are similar. However, the link is exposed to a dramatic increase in force at a specific high isometric length, independent of its stiffness. The reason for this is the shear in fiber and cross-fiber directions. The matrix mesh is sufficiently stiff to bare this shear but the fiber mesh tends to deform as shown above. This causes the link loads to increase in both cases. However, in case S, the much stiffer link handles the increase without really extending which keeps the fiber and matrix meshes at a very similar state of strain distribution. These results show that the extreme deformations in the fiber mesh for the cases with compliant links are induced by the muscle geometry. The specific geometry, resulting from the mechanical equilibrium of the continuum, is dominated by the shear.

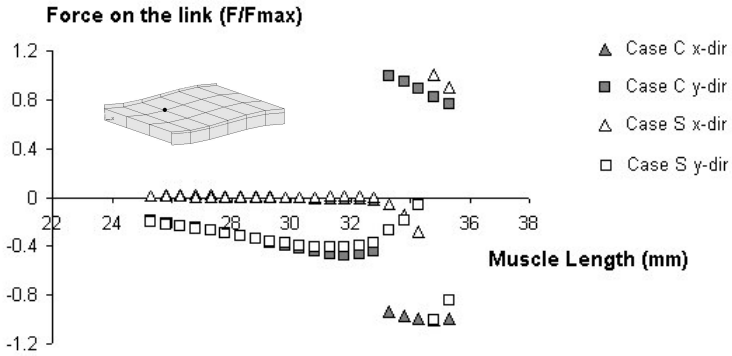

Fig.9 An example of forces on a link of the meshes. Forces are shown for the link at the specified location (see the dot in inset). For case C this link is compliant and for case S it is highly stiff. The forces in global x and y-directions are plotted as a function of isometric muscle length.

Discussion

The model

A 3D-muscle model with two-domain approach was developed which consists of two elastically linked meshes occupying the same space. Earlier, the bi-domain concept was

used in a nonmechanical application, modeling of a cylindrical, multicellular bundle for studying action potential propagation in cardiac muscle by Henriquez and Plonsey (1990). A bi-domain model based finite element formulation of anisotropic myocardium coupled with a boundary element method representation of the surrounding isotropic volume conductor was also described recently (Fischer et al., 2000) for a magneto- and electrocardiographic problem. Our method to link two mechanical domains with different properties represented by 3-D self-developed elements to carry on a finite element analysis of skeletal muscle mechanics is novel.

The relative success in calculation of length-force characteristics by the present model is similar to that of van der Linden (1998). Scaling of both curves to their own optimum forces and possible differences in the initial sarcomere length distributions cause differences between model and experimental data. Over-estimation of passive characteristics leads to the differences above the optimum length. Despite the lumped consideration of active and passive properties, model of van der Linden (1998) supported increased understanding in functional morphology of pennate muscle (e.g. Huijing, 1998), intramuscular force transmission (e.g. Huijing, 1999a) and acute effects of tenotomy (Huijing et al., 1998) and aponeurotomy (e.g. Jaspers et al., 1999). The present model provides a better representation of the muscle tissue and is promising especially to study myofascial force transmission.

The role of the extracellular matrix in force transmission

In the present study the rigid connections between the in series myofiber elements and to the aponeuroses ensure the myotendinous force transmission pathway. Additionally, the elastic links between the fiber and extracellular matrix domains provide the model with an explicit mechanism of myofascial force transmission. An in situ muscle was modeled which was isolated from its surrounding tissues. In such a case, the endomysial apparatus as well as myo-tendinous pathways transmit force exclusively onto the tendons. Note that within the model, all molecular elements constituting possible myofascial pathways are lumped in the linking element characteristics.

A significant model result was the drops in muscle force following small changes of isometric length in the high length range. No experimental length force curves are available for dystrophic muscle. Therefore, the hypothesis for a force drop needs to be tested. However, it was shown that, if muscle of young dystrophic animals is immobilized and prevented from attaining high lengths, the effects of the disease are limited (e.g. Wirtz et al., 1988; Brocks et al., 1992; Mokhtarian et al., 1999). Note that the model results show a force drop of approximately 25% (at muscle length = 32.8 mm) and more pronounced strain distributions, if all linking elements are made compliant (not presented). The force drop is caused by an overall decrease in the total stress σ_{22f} in the fiber mesh. This was due to a

combination of very high positive or negative strains in the fiber direction, that were found near compliant links in the fiber mesh. Such high, positive fiber direction strains are interpreted as popped sarcomeres which terminology was proposed by Morgan (1990). In his study Morgan modeled a single muscle fiber as a set of in series sarcomeres, which has some random property variation. His conclusion was that in this condition some sarcomeres will be stretched to a length providing no overlap between thick and thin filaments, and the tension is borne by passive components. However, he did not take into account myofascial force transmission. The present model results show that despite the assumption of sarcomeres with identical properties, myofascial force transmission allows distribution of strain within fibers and muscle. Note that, for the case of homogeneous mechanical properties of both passive and active muscle components, our model does not yield results that can be interpreted as popped sarcomeres, if extracellular matrix support for the myofibers is adequate.

The geometrical changes in the muscle model dominated by the shear between the fiber and cross-fiber directions cause the high local strains arising at high muscle lengths leading to the external muscle force drop. It is a matter of the stiffness of the meshes or the links between them to withstand such deformations. It is clear that the matrix mesh is stiffer than the fiber mesh as it exhibits no exaggerated deformation even at the presence of local compliant links. The important role of the linking stiffness is also clear as highly stiff links can prevent the fiber mesh from such deformation (Fig.8). The fiber mesh strongly depends on the extracellular matrix mesh to preserve a physiological shape. The only interface able to provide the fiber domain with such mechanical guidance and a path of force transmission is apparently its trans-sarcolemmal connections to the extracellular matrix domain.

Conclusions

The present model provides a new means of studying skeletal muscle mechanics and myofascial force transmission, allowing an improved representation of muscle tissue. It yields a detailed analysis of local strain and stress, which is not feasible in experimental work. The model is designed in such a way that extra- and intermuscular myofascial force transmission phenomena can be incorporated and studied in the future. The application in this study indicates the functional significance of intramuscular myofascial force transmission mechanism in addition to myotendinous force transmission.

References

Berthier, C. and Blaineau, S., 1997. Supramolecular organization of the subsarcolemmal cytoskeleton of adult skeletal muscle fibers. A review. Biology of the Cell 89, 413-434.

Brocks, L., Wirtz, P., Loermans, H. and Binkhorst, R., 1992. Effects of early immobilization on the functional capacity of dystrophic (ReJ 129 dy/dy) mouse leg muscles. International Journal of Experimental Pathology 73, 223-229.

Campbell, K. P., 1995. Three muscular dystrophies: loss of cytoskeleton-extracellular matrix linkage. Cell 80, 675-679.

Denoth, J. and Danuser, G.,2001. Does it pop, hop, or even stop? New views on sarcomere stability. Proceedings of the XVIII th Congress of the International Society of Biomechanics, Zurich, Switzerland.

Donkelaar, C. C. v., Drost, M. R., Mameren, H. v., Tuinenburg, C. F., Janssen, J. D. and Huson, A., 1996. Three-Dimensional reconstruction of the rat triceps surae muscle and finite element mesh generation of the gastrocnemius medialis muscle. European Journal of Morphology 34, 31-37.

Fischer, G., Tilg, B., Modre, R., Huiskamp, G. J., Fetzer, J., Rucker, W. and Wach, P., 2000. A bidomain model based BEM-FEM coupling formulation for anisotropic cardiac tissue. Annals of Biomedical Engineering 28, 1229-1243.

Hawkins, D. and Bey, M., 1997. Muscle and tendon force-length properties and their interactions in vivo. Journal of Biomechanics 30, 63-70.

Henriquez, C. S. and Plonsey, R., 1990. Simulation of propagation along a cylindrical bundle of cardiac tissue--I: Mathematical formulation. IEEE Transactions on Bio-Medical Engineering 37, 850-860.

Heslinga, J. W. and Huijing, P. A., 1993. Muscle length-force characteristics in relation to muscle architecture: a bilateral study of gastrocnemius medialis muscles of unilaterally immobilized rats. European Journal of Applied Physiology and Occupational Physiology 66, 289-298.

Huijing, P. A., 1998. Muscle the motor of movement: Properties in function, experiment and modelling. Journal of Electromyography and Kinesiology 8, 61-77.

Huijing, P. A., Baan, G. C. and Rebel, G., 1998. Non myo-tendinous force transmission in rat extensor digitorum longus muscle. Journal of Experimental Biology 201, 682-691.

Huijing, P. A., 1999a. Muscle as a collagen fiber reinforced composite material: Force transmission in muscle and whole limbs. Journal of Biomechanics 32, 329-345.

Huijing, P. A., 1999b. Muscular force transmission: A unified, dual or multiple sytem? A review and some explorative experimental results. Archives of Physiology and Biochemistry 170, 292-311.

Huyghe, J. M., van Campen, D. H., Arts, T. and Heethaar, R. M., 1991a. A two-phase finite element model of the diastolic left ventricle. Journal of Biomechanics 24, 527-538.

Huyghe, J. M., van Campen, D. H., Arts, T. and Heethaar, R. M., 1991b. The constitutive behaviour of passive heart muscle tissue: a quasi- linear viscoelastic formulation. Journal of Biomechanics 24, 841-849.

Ingber, D., 1991. Integrins as mechanochemical transducers. Current Opinion in Cell Biology 3, 841-848.

Jaspers, R. T., Brunner, R., Pel, J. J. M. and Huijing, P. A., 1999. Acute effects of intramuscular aponeurotomy on rat GM: Force transmission, muscle force and sarcomere length. Journal of Biomechanics 32, 71-79.

Johansson, T., Meier, P. and Blickhan, R., 2000. A finite-element model for the mechanical analysis of skeletal muscles. Journal of Theoretical Biology 206, 131-149.

Jung, D., Duclos, F., Apostol, B., Straub, V., Lee, J. C., Allamand, V., Venzke, D. P., Sunada, Y., Moomaw, C. R., Leveille, C. J., Slaughter, C. A., Crawford, T. O., McPherson, J. D. and Campbell, K. P., 1996. Characterization of delta-sarcoglycan, a novel component of the oligomeric sarcoglycan complex involved in limb-girdle muscular dystrophy. The Journal of Biological Chemistry 271, 32321-32329.

Komulainen, J., Takala, T. E., Kuipers, H. and Hesselink, M. K., 1998. The disruption of myofibre structures in rat skeletal muscle after forced lengthening contractions. Pflugers Archiv : European Journal of Physiology 436, 735-741.

Meijer, K., Koopman, H. J. F. M., Grootenboer, H. J. and Huijing, P. A.,1998. Shortening history effects in maximally and sub-maximally stimulated muscle. Third World congress of Biomechanics, Sapporo, Japan.

Mokhtarian, A., Lefaucheur, J. P., Even, P. C. and Sebille, A., 1999. Hindlimb immobilization applied to 21-day-old mdx mice prevents the occurrence of muscle degeneration. Journal of Applied Physiology 86, 924-931.

Morgan, D. L., 1990. New insights into the behavior of muscle during active lengthening. Biophysical Journal 57, 209-221.

Ohlendieck, K., 1996. Towards an understanding of the dystrophin-glycoprotein complex: linkage between the extracellular matrix and the membrane cytoskeleton in muscle fibers. European Journal of Cell Biology 69, 1-10.

Pond, C. M., 1982. The importance of connective tissue within and in between muscles. The Behavioral and Brain Sciences 5, 562.

Street, S. F., 1983. Lateral transmission of tension in frog myofibers: a myofibrillar network and transverse cytoskeletal connections are possible transmitters. Journal of Cellular Physiology 114, 346-364.

Trombitas, K., Jin, J. P. and Granzier, H., 1995. The mechanically active domain of titin in cardiac muscle. Circulation Research 77, 856-861.

Trotter, J. A. and Purslow, P. P., 1992. Functional morphology of the endomysium in series fibered muscles. Journal of Morphology 212, 109-122.

van der Linden, B. J., Koopman, H. F., Huijing, P. A. and Grootenboer, H. J., 1998. Revised planimetric model of unipennate skeletal muscle: a mechanical approach. Clinical Biomechanics 13, 256-260.

van der Linden, B. J. J. J. Mechanical modeling of muscle functioning (PhD thesis). Enschede, The Netherlands: University of Twente, 1998.

Vankan, W. J., Huyghe, J. M., Janssen, J. D. and Huson, A., 1996. A 3-D finite element model of blood perfused rat gastrocnemius medialis muscle. European Journal of Morphology 34, 19-24.

Vankan, W. J., Huyghe, J. M., van Donkelaar, C. C., Drost, M. R., Janssen, J. D. and Huson, A., 1998. Mechanical blood-tissue interaction in contracting muscles: a model study. Journal of Biomechanics 31, 401-409.

Wang, N., Butler, J. P. and Ingber, D. E., 1993. Mechanotransduction across the cell surface and through the cytoskeleton. Science 260, 1124-1127.

Wirtz, P., Loermans, H. M., de Haan, A. F. and Hendriks, J. C., 1988. Early immobilization of hindleg muscles of dystrophic mice: short-term and long-term effects. Journal of the Neurological Sciences 85, 293-307.

Zuurbier, C. J., Heslinga, J. W., Lee-de Groot, M. B. and Van der Laarse, W. J., 1995. Mean sarcomere length-force relationship of rat muscle fibre bundles. Journal of Biomechanics 28, 83-87.

Chapter 3

Finite element modeling of intermuscular interactions and myofascial force transmission

Abstract

A finite element muscle model to study the principles of intermuscular myofascial force transmission is developed. The results obtained explain force differences at the distal and proximal tendons of muscles that have mechanical interaction. This is in agreement with experimental findings in other recent studies. The strain distributions found along the fiber direction indicate intermuscular myofascial force transmission. A consequence is that active force generated within one muscle may be exerted at the tendon of another muscle.

Introduction

Performing the complex task of controlled bodily movements requires the transmission of the force generated by the skeletal muscles onto the skeleton. Although for this transmission, the myotendinous junction is widely accepted to be the major site, rather recently the transmission from the muscle fibers onto the intramuscular connective tissue has been proven to be important as well (Street, 1983; Trotter and Purslow, 1992; Hijikata et al., 1993; Huijing et al., 1998; Huijing, 1999a). Referring to this kind of transmission as myofascial force transmission, Huijing (Huijing, 1999b) suggested that force could be transmitted from the muscle by this path as well (extramuscular myofascial force transmission). Recent experiments revealed significant changes in the length-force characteristics of rat extensor digitorium longus (EDL) muscle on interference with (Huijing and Baan, 2001) or interactions with the surrounding extramuscular tissues. It was also shown that adjacent muscles interact mechanically (Maas et al., 2001).

In the present work, the two-domain finite element muscle model described recently (Yucesoy et al., 2002) is extended to include the principles of intermuscular myofascial force transmission. In experimental work on the subject, the muscle is not accessible for local strain measurements, as it has to remain surrounded by compartmental connective tissues. This modeling study aims at providing such analysis of local strain to enhance understanding of this concept.

Methodology

A 3D-finite element muscle model (linked fiber-matrix mesh model: lfmm model) with a two-domain approach was developed (Yucesoy et al., 2002). This model consists of two meshes that are linked elastically representing the extracellular matrix (matrix mesh) and muscle fiber domains (fiber mesh), which occupy the same space. These two meshes are built using earlier developed myofiber or extracellular matrix elements that are introduced into the finite element program ANSYS 5.5.1 as user defined elements. The two meshes are rigidly connected to single layers of elements representing the muscles' aponeurosis, for which a standard element, HYPER58 from the element library of ANSYS 5.5.1 is used.

In the present study, using the same methods, a model representing whole EDL isolated from the surrounding connective tissues was built. As a subsequent step, two of such models were connected: the corresponding nodes of the matrix meshes of the two models were linked elastically. Such links represent the intermuscular connections, providing a means to show the principles of mechanical interaction between the two muscles and a pathway for intermuscular force transmission.

To assess the principles of such interaction and force transmission, one EDL model referred to as restrained muscle was kept at a low length (Δlm = 2.5 mm below the original length), while the other model (referred to as lengthened muscle) was lengthened from this low length up to 1.5 mm over the original length (Fig. 1). Throughout the analysis, both modeled muscles were maintained maximally activated. The length-force characteristics of the isolated model will be compared to experimental data for EDL in such conditions. Stress and strain distributions of the isolated model and the model with intermuscular links will be compared as well.

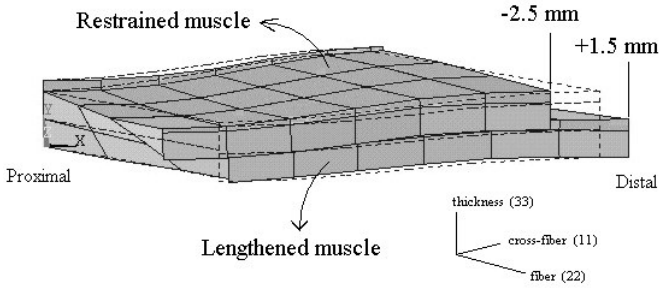

Fig.1. The deformed shape of the model. The model consists of two EDL models. One that is *restrained* at a low length (i.e. 2.5 mm shorter than the initial length), which has interaction with another EDL model that is *lengthened* distally (from Δlm = –2.5 mm to Δlm = 1.5 mm). Muscular geometry at the initial muscle length (lm = 28.7 mm) is represented by dotted lines. A 3D local coordinate system is used for the analysis and presentation of the results.

Results

Isolated EDL Model

The length- total force characteristics of modeled isolated EDL and experimental data (Huijing and Baan, 2001) are shown in Fig. 2. The model forces are maximally 5% above or below the experimental ones suggesting a fairly good agreement. For the highest lengths considered, the model forces remain high whereas the experimental force decreases with increasing length. This could be due to over estimated passive length-force characteristics of

the model as well as the, unrealistic modeling assumption of an initially uniform sarcomere distribution.

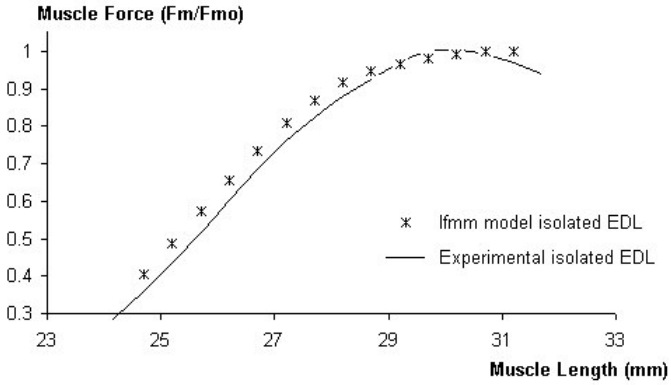

Fig.2. The isometric muscle length-total force curve for isolated rat EDL muscle. Experimental EDL data is adopted from (Huijing and Baan, 2001). The muscle force (Fm) is normalized for optimum force (Fmo). Initial muscle length equals 28.7 mm.

Model with Intermuscular Connections

The muscle length-total force characteristics of the lengthened and the restrained muscle, which have intermuscular links between their matrix meshes representing intramuscular collagen is presented in Fig. 3. Note that the distributions of strain and stress in the fiber mesh of the restrained muscle are provided for three lengths of the lengthened muscle (Fig. 4). At Δlm = -2.5 mm (i.e. both muscles are at the lowest length), the fiber direction strain (ε_{22}) does not exhibit variations, i.e. the lengths of sarcomeres in series within fibers are highly uniform (Fig. 4a). As the lengthened muscle reaches higher lengths (Δlm = +1.5 mm) this homogeneity is replaced by on average 10% longer sarcomeres at the distal end of muscle fibers than at their proximal end.

The consequences of these differences in strain are clearly visible on the fiber direction stresses (σ_{22}). If both muscles are at low length, the stresses along the fibers of the restrained muscle are rather uniform. As the adjacent muscle is lengthened, distributions of σ_{22} become apparent: at distal ends of fibers approximately 50% higher stresses are encounterd than their proximal ends.

For a further assessment of mechanics of interaction between the muscles, the fiber direction strains and stresses within the fiber mesh at the highest length studied (i.e. Δlm =

+1.5 mm) are considered for the lengthened muscle of the modeled pair, in comparisson to the isolated EDL model (Fig. 5). A clear difference in strain distributions between the two muscles is visible (Fig. 5a). Except for the minor distributions in the most proximal part of the isolated muscle (which is ascribable to the asymmetric EDL muscle geometry), the strains are highly uniform over the whole fiber mesh. In contrast, for the lengthened muscle with intermuscular connections to the restrained muscle, a high level of variation in ε_{22} distribution is seen: The sarcomeres along the proximal ends of the muscle fibres are approximately 20% shortened, while towards the distal ends, their lengths gradually increase, such that the sarcomeres at most distal end are up to 67% longer.

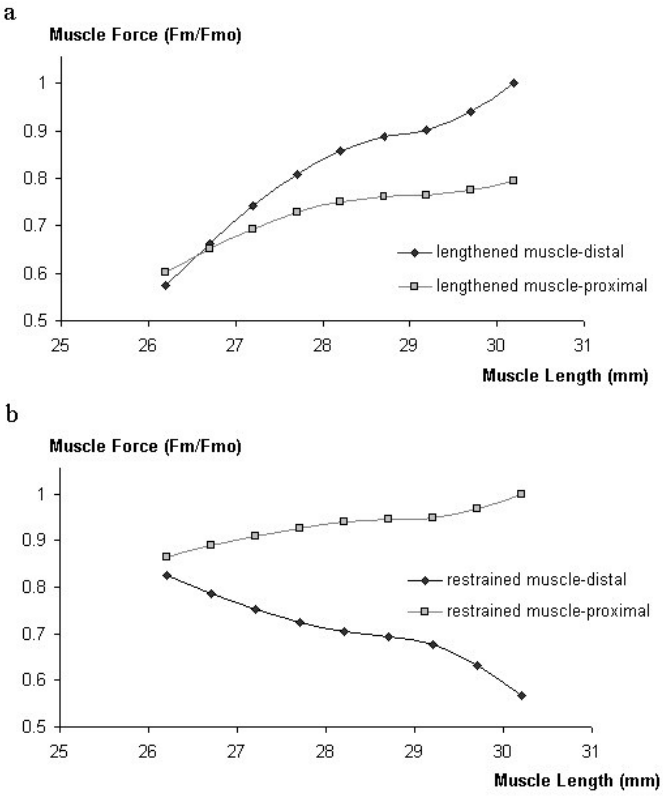

Fig.3. Comparison of proximal and distal forces of the modeled EDL muscles. (a) Length-total force curves for the lengthened muscle. The muscle force (Fm) is normalized with respect to optimum distal force (Fmo). (b) Total force for the restrained muscle as a function of the lengthened muscles' length. The muscle force is normalized for optimum proximal force. Initial muscle length equals 28.7 mm

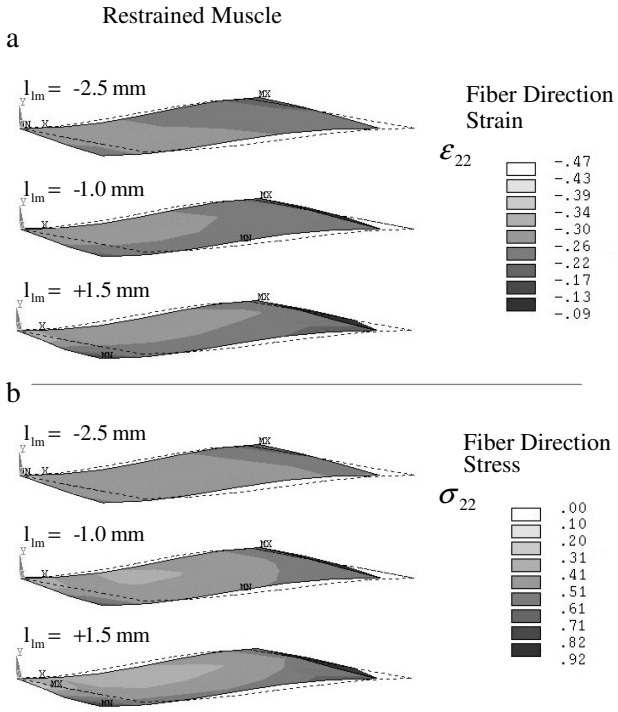

Fig.4. Distributions of fiber direction strain and stress for the fiber mesh of the restrained muscle as a function of the length of the lengthened muscle. (a) Distributions of fiber strain at three muscle lengths. (b) Distributions of fiber stress at three muscle lengths. The dotted line contour indicates muscle geometry at the initial length.

The differences between the muscles are also remarkable for the fiber direction stresses (Fig. 5b). In agreement with the strain distributions for the isolated muscle, the σ_{22} values are highly uniform (i.e. approximating unity all over the fiber mesh). However, the lengthened muscle of the pair exhibits a sizable variation in σ_{22} distribution, ranging from aproximately 0.80 to 0.50. In that muscle stress decreases from the proximal end of the muscle fibres towards their distal ends. Also note that the mean stress for the isolated muscle (which is approximately unity) is significantly higher than that of the lengthened muscle with intermuscular connections. Although σ_{22} does attain values arround unity at certain limited locations, stress values over the major part of the fiber mesh are much lower. As fiber direction stress in the fiber mesh is the dominating factor determining muscle force, this result is highly interesting since the distal forces of the lengthened muscle are higher than that of the isolated muscle throughout the length range and at this particular length (Fig.

6). Such higher forces in spite of the lower mean stresses can be explained by intermuscular myofascial force transmission from the restrained muscle to the lengthened one.

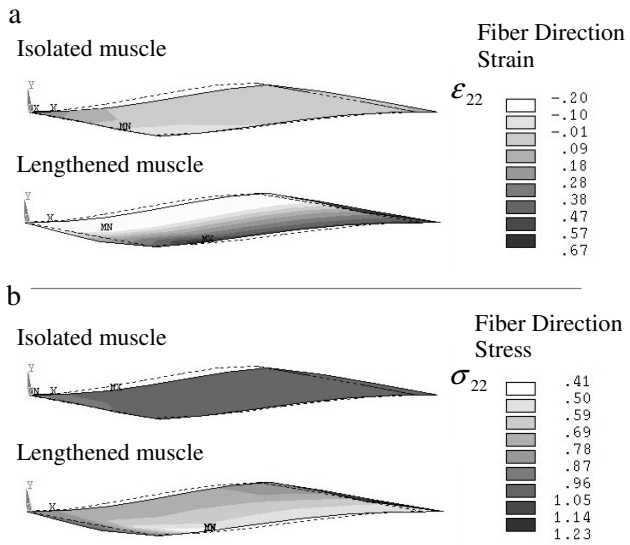

Fig.5. Comparison of strain and stress distributions for the fiber mesh of the lengthened and isolated muscles. (a) Strain distributions of the fiber mesh for the fiber (22) direction. (b) Stress distributions of the fiber mesh for the fiber (22) direction. Both muscles are represented at the high length (Δlm = +1.5mm). The dotted line contour indicates muscle geometry at the initial length.

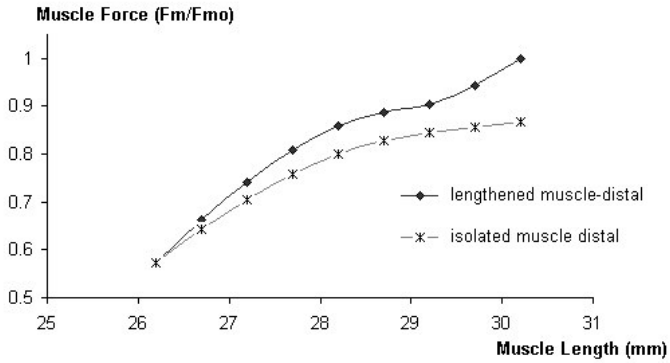

Fig.6. Comparison of length-total distal force curves of modeled muscle with intermuscular connections and isolated muscles. Muscle force (Fm) is normalized for optimum force (Fmo) of the muscle with intermuscular connections.

Discussion

Connective tissue network and force transmission

Muscle can be represented as an extensive 3D set of organized endomysial tunnels, within which the myofibers operate (Trotter and Purslow, 1992). The identification of intramuscular force transmission from the lateral perimeter surface of myofibers onto the connective tissue network (myofascial force transmission) is relatively recent and limited. However, various studies indicated (Street, 1983; Trotter and Purslow, 1992) or experimentally confirmed (Street, 1983; Danowski et al., 1992; Trotter and Purslow, 1992; Huijing et al., 1998; Huijing, 1999a; Huijing, 1999b) such force transmission and suggested an important functional significance of the connective tissue network. This endomysial network is continuous with the perimysium system and can be regarded as a continuous system of tunnels or tubes as well. In addition, the muscular epimysium is continuous with this system as well as with the connective tissue of adjacent muscles in addition to other elements of the compartment in which the muscles operate (e.g. Huijing, 1999a; Huijing and Baan, 2001). Therefore, in vivo there is an additional route for force transmission out off the muscle, which completely bypasses the tendon of the muscle that was the source of the generated force (Huijing, 1999a; Huijing, 2000; Huijing and Baan, 2001). In the majority of the earlier work on muscle functioning, muscles are investigated isolated from their surrounding (e.g. Faulkner et al., 1982; Street, 1983; Huijing et al., 1994; Jaspers et al., 1999). Such a type of experiment eliminates any possible mechanism of inter or extra-muscular force transmission from or to the muscle studied.

Results of the model

The model developed in this study provides the possibility to interpret effects of myofascial force transmission between two maximally activated muscles with a set of elastic links between their matrix meshes representing their intramuscular connections. A finite element muscle model with such an approach is novel. The remarkable result of the analysis is the significant differences between the distal and proximal forces of both of the restrained and lengthened muscles. These differences are such that for almost all of the length range considered, the distal forces of the lengthened muscle are higher than the proximal forces. This proximo-distal force difference increases with increasing muscle length. For the restrained muscle, the distal force decreases as the lengthened muscle reaches higher lengths. These results are highly compatible with the very recent findings in experimental work exploring intermuscular interaction via myofascial force transmission within rat hind limb. In their study investigating the effects of blunt dissection and compartmental fasciatomy on rat EDL length-force characteristics, Huijing and Baan (Huijing and Baan, 2001) showed that a systematic manipulation of the extra and inter-muscular connective tissue structures

altered proximal EDL force remarkably. These changes were decreases in force and changes in the muscle optimum length, as a result of decreased inter and extra-muscular interactions as EDL was dissected further. This indicates the importance of extramuscular connective tissue in force transmission.

The advantage of the present model is its capability to examine the mechanics by analysis of local stress and strain distributions. Such distributions reveal that even though the restrained muscle is fixed at a constant low length, the fiber mesh of the restrained muscle exhibits strain variations along the fiber direction as the second muscle is lengthened (Fig. 4). This is reflected on the fiber direction stresses of the same muscle.

The model results show that such distributions are also present in the lengthened muscle of the adjacent pair (Fig. 5), while the isolated muscle model exhibits highly uniform stress and strain distributions. As mean fiber direction stress within the fiber mesh is considerably lower for the lengthened muscle than for the isolated muscle, the higher distal forces associated with the lengthened muscle indicate that active force generated within one muscle may be exerted at the tendon of another muscle by intermuscular myofascial force transmission. This tendency of 'focusing' of active forces of adjacent muscles on the distal tendon of a distally lengthened muscle is a remarkable conclusion for which further experimental confirmation will be sought in the anterior tibial compartment muscles of rat hind limb.

Conclusion

Present application of the linked fiber matrix mesh model reveals the principles of the significant role of intermuscular myofascial force transmission on the mechanical behavior of a muscle in an in vivo situation. In agreement with experimental findings, it clearly demonstrates the altered length force characteristics with respect to the isolated situation and increases the understanding of the in vivo mechanics. The conclusion that active force generated within one muscle may be exerted at the tendon of another muscle by intermuscular myofascial force transmission is one of the remarkable results of this analysis.

References

Danowski, B. A., Imanaka-Yoshida, K., Sanger, J. M. and Sanger, J. W., 1992. Costameres are sites of force transmission to the substratum in adult rat cardiomyocytes. The Journal of Cell Biology 118, 1411-1420.

Faulkner, J. A., McCully, K. K., Carlson, D. S. and McNamara, J. A., Jr., 1982. Contractile properties of the muscles of mastication of rhesus monkeys (Macaca mulatta) following increase in muscle length. Archives of Oral Biology 27, 841-845.

Hijikata, T., Wakisaka, H. and Niida, S., 1993. Functional combination of tapering profiles and overlapping arrangements in nonspanning skeletal muscle fibers terminating intrafascicularly. Anatomical Record 236, 602-610.

Huijing, P. A., 1999a. Muscle as a collagen fiber reinforced composite material: Force transmission in muscle and whole limbs. Journal of Biomechanics 32, 329-345.

Huijing, P. A., 1999b. Muscular force transmission: A unified, dual or multiple sytem? A review and some explorative experimental results. Archives of Physiology and Biochemistry 170, 292-311.

Huijing, P. A. (2000). In vivo, force is transmitted from muscle also at other locations than the tendons: Extramuscular myofascial force transmisison. 5th Annual Congress of the European College of Sports Science, Jyvaskyla, Finland, University of Jyvaskyla.

Huijing, P. A. and Baan, G. C., 2001. Myofascial force transmission causes interaction between adjacent muscles and connective tissue: Effects of blunt dissection and compartmental fasciotomy on length force characteristics of rat extensor digitorum longus muscle. Archives of Physiology and Biochemistry 109, 97-109.

Huijing, P. A., Baan, G. C. and Rebel, G., 1998. Non myo-tendinous force transmission in rat extensor digitorum longus muscle. Journal of Experimental Biology 201, 682-691.

Huijing, P. A., Nieberg, S. M., vd Veen, E. A. and Ettema, G. J., 1994. A comparison of rat extensor digitorum longus and gastrocnemius medialis muscle architecture and length-force characteristics. Acta Anatomica 149, 111-120.

Jaspers, R. T., Brunner, R., Pel, J. J. M. and Huijing, P. A., 1999. Acute effects of intramuscular aponeurotomy on rat GM: Force transmission, muscle force and sarcomere length. Journal of Biomechanics 32, 71-79.

Maas, H., Baan, G. C. and Huijing, P. A., 2001. Intermuscular interaction via myofascial force transmission: effects of tibialis anterior and extensor hallucis longus length on force transmission from rat extensor digitorum longus muscle. Journal of Biomechanics 34, 927-940.

Street, S. F., 1983. Lateral transmission of tension in frog myofibers: a myofibrillar network and transverse cytoskeletal connections are possible transmitters. Journal of Cellular Physiology 114, 346-364.

Trotter, J. A. and Purslow, P. P., 1992. Functional morphology of the endomysium in series fibered muscles. Journal of Morphology 212, 109-122.

Yucesoy, C. A., Koopman, H. J. F. M., Huijing, P. A. and Grootenboer, H. J., 2002. Three-dimensional finite element modeling of skeletal muscle using a two-domain approach: Linked fiber-matrix mesh model. Journal of Biomechanics 35, 1253-1262.

Chapter 4

Extramuscular myofascial force transmission:
Experiments and finite element modeling

Abstract

The specific purpose of the present study was to show that extramuscular myofascial force transmission affects muscular mechanics substantially. The experimental conditions included distal lengthening of rat extensor digitorium longus (EDL) muscle with extramuscular connections exclusively. Muscle forces exerted at proximal and distal tendons were measured. A finite element model of EDL including the muscles' extramuscular connections was used to assess the effects of extramuscular myofascial force transmission on muscular mechanics, primarily to test if such effects lead to distribution of length of sarcomeres within muscle fibers. Furthermore, the role of the connective tissues of the neurovascular tract in extramuscular myofascial force transmission was studied.

EDL isometric forces measured at the distal and proximal tendons were significantly different ($F_{dist} > F_{prox}$, ΔF approximates maximally 40 % of the proximal force). The model results show that extramuscular myofascial force transmission causes distributions of strain in the fiber direction (shortening in the proximal, lengthening in the distal ends of fibers) at higher lengths. This indicates significant length distributions of sarcomeres arranged in series within muscle fibers. Stress distributions found are in agreement with the higher distal force measured, meaning that the muscle fiber is no longer the unit exerting equal forces at both ends. Dissecting the extramuscular connections, to leave only the tissues of the proximal neurovascular tract intact (as in most in situ muscle experiments) caused no statistically significant changes in the length-force characteristics (i.e. proximo-distal force differences were maintained). This shows that the connective tissues of the neurovascular tract play a major role in extramuscular myofascial force transmission.

We conclude that extramuscular myofascial force transmission has major effects on muscle functioning.

Introduction

Transmission of the force generated by the sarcomeres, from the full perimeter surface of the myofibers onto the intramuscular connective tissue has been emphasized by some authors (e.g. Street, 1983; Trotter and Purslow, 1992; Danowski et al., 1992; Hijikata et al., 1993; Huijing et al., 1998; Huijing, 1999a; Yucesoy et al., 2002). Such transmission was referred to as myofascial force transmission (Huijing, 1999b). It should be noted that the perimysium and epimysium, neurovascular tracts, compartmental boundaries and even the general fascia surrounding the limb are continuous with the endomysial system of tunnels or tubes within which the muscle fibers operate (Huijing, 1999b; Huijing and Baan, 2001a; 2001b; Maas et al., 2001). Such connective tissue organization creates connections of muscle fibers to the surrounding structures, which allows myofascial force transmission.

In recent experiments, inter- and extramuscular myofascial force transmission was shown to significantly affect muscle length-force characteristics determined after proximal lengthening of rat EDL (Huijing and Baan, 2001a; 2001b; Maas et al., 2001). These findings and the continuity of intra- and extramuscular connective tissues lead to the hypothesis that myofascial force transmission could cause distribution of length of sarcomeres arranged in series within muscle fibers. The first goal of the present work was to show that extramuscular myofascial force transmission exclusively has substantial effects on muscular mechanics: (1) the effects on isometric EDL force exerted at proximal and distal tendons were assessed experimentally, after distal lengthening. (2) A finite element model of EDL muscle including the muscles' extramuscular connections was used primarily to test the hypothesis regarding distribution of length of sarcomeres.

During the full course of a myological experiment in situ, the minimal condition is to keep blood supply and innervation of a muscle intact as much as possible. However, blood vessels and nerves are embedded in the connective tissues of the neurovascular tract. Despite such remaining extramuscular connections, a muscle "in situ" is commonly (e.g. Huijing et al., 1994; Frueh et al., 2001) considered as "isolated" from its surroundings. It is expected that this tract also allows extramuscular myofascial force transmission. The second goal of the present work is to test this hypothesis.

Methods

I Experimental Study

Surgical procedures

Surgical and experimental procedures were in strict agreement with the guidelines and regulations concerning animal welfare and experimentation set forth by Dutch law, and approved by a Committee on Ethics of Animal Experimentation at the Vrije Universiteit, Amsterdam.

Male Wistar rats (n = 5, body mass = 304.4 ± 3.5 g) were anaesthetized by intraperitoneally injected urethane solution (initial dose: 1.2 mg 100 g^{-1} body mass, extra doses if necessary: maximally 1.5 mg). A heated water pad was used to prevent hypothermia and the ambient temperature (22 ± 0.5 °C) and air humidity (80 ± 2%) were kept constant (for details see Huijing and Baan, 2001a). Muscle and tendon tissue was further prevented from dehydration by regular irrigation with isotonic saline.

The left anterior crural compartment, which consists of the tibialis anterior (TA), extensor digitorum longus (EDL) and extensor hallucis longus (EHL) muscles, was exposed by removing the skin and most of the biceps femoris muscle. Subsequently the compartment was opened and the TA, and EHL muscles were removed, leaving EDL and its extramuscular connections to the surrounding tissues intact.

With the knee joint at 90° and the ankle joint at 90° (referred to as reference position), the four distal tendons of EDL were tied together. Matching markers were placed on the distal tendons and on a fixed location on the lower leg. Subsequently, the distal tendon complex was cut as distally as possible and removed from their retinaculae near the ankle joint (after cutting the transverse crural ligament and cruciate ligament). The foot was attached to a plastic plate with tie wraps.

The femoral compartment was opened to detach the proximal tendon of EDL from the femur and to secure the femur (at a knee angle of 90°) with a metal clamp. A Kevlar thread (4% elongation at a break load of 800 N) was tied to the combined distal EDL tendons and the proximal EDL tendon with a suture. The Kevlar threads were later connected to force transducers that were aligned with the muscle line of pull (Hottinger Baldwin, maximal output error < 0.1 %, compliance of 0.0048mm N^{-1}). The sciatic nerve was dissected, leaving the peroneus communis nerve branch intact. The tibial nerve and the sural branch of the sciatic nerve were cut. The sciatic nerve was cut as proximally as possible and placed on a pair of silver electrodes and covered by a saline wetted piece of tissue, which was covered by a small piece of latex.

Experimental procedures

The footplate was positioned in such a way that the ankle angle was in maximal plantar flexion. The knee angle was maintained at 90°. The proximal EDL tendon was displaced by 2 mm in the distal direction with respect to its reference position at which location it was kept throughout the experiment. To determine the muscle length-force characteristics, isometric EDL force was measured at various muscle–tendon complex lengths. Before each isometric contraction, these lengths were attained by moving exclusively the distal EDL force transducer with 1 mm increments starting at muscle active slack length (i.e. the length at which active force approaches zero) until approximately 2 mm over the optimum length.

After each tetanic contraction the muscle was allowed to recover below active slack length for 2 minutes.

The sciatic nerve was stimulated supra-maximally using a pair of silver electrodes connected to a constant current source (3 mA, pulse width 100 μs). Two twitches were evoked and followed by a tetanic contraction after 300 ms (pulse train 400 ms, frequency 100 Hz). Simultaneously, images of the muscle in passive and active state were recorded using a digital camera (DVC, JAI CV−M10, shutter speed 1/50 s).

To avoid possible artifacts due to differences force measurement systems (e.g. force transducers and amplifiers), prior to the experiment the two force transducers to be used for measurement of EDL forces were connected to each other using a compliant spring. The output recorded with the identical measurement system as used in the animal experiment revealed that the slope of the regression line (r^2 = 0.999) of the simultaneously measured forces deviated 0.6 % from the expected 45°. This leads to the conclusion that any force differences between the two transducers greater than 0.6 % should not be ascribed to the measurement system used. The timing of stimulation of the nerve, A/D conversion (12−bit A/D converter, sampling frequency 1000 Hz, resolution of force 0.01 N), and photography were controlled by a microcomputer.

These experimental procedures were applied in two conditions:

A. First the extramuscular connective tissue associated with EDL was left intact as much as possible.

B. Subsequently, the extent of the connective tissue sheet which plays a role in connecting the muscle to the compartment was dissected, to leave only the tissues of the neurovascular tract (for images see Huijing and Baan, 2001a; Maas et al., 2001) intact. This tract is composed of connective tissues as well as blood vessels and nerves that are essential to keep a muscle in physiological conditions. Therefore, this is a common condition in muscle experiments in situ after dissection from other muscles and connective tissues.

Processing of experimental data and statistics

Data for total muscle force (F_{mt}) in relation to muscle tendon complex length (l_{oi}) were fitted by a polynomial function

$$y = b_0 + b_1x + b_2x^2 + b_3x^3 + b_4x^4 + \ldots + b_nx^n,$$

where y represents F_{mt} and x represents l_{oi}. b_0, $b_1 \ldots b_n$ are coefficients determined in the fitting process. Polynomials that best described the experimental data were selected (see below). These polynomials were used for averaging of data and calculation of standard errors.

In the fitting procedure one-way analysis of variance (ANOVA) (Neter et al., 1996) was used to select the lowest order of the polynomials that still added a significant improvement of the description of changes of muscle tendon complex length and muscle force data for EDL. Two-way analysis of variance (ANOVA) was performed to test for length effects and for differences between the EDL force measured at the proximal and distal tendons. Bonferroni post–hoc tests were carried out to identify the significance of proximo–distal force difference at each l_{oi} (Neter et al., 1996). Differences were considered significant at $p<0.05$.

II. Modeling Study

A 3D-finite element muscle model (linked fiber-matrix mesh model: lfmm model) with a two-domain approach was developed (Yucesoy et al., 2002). In summary, this model consists of two meshes occupying the same space that are linked elastically representing the extracellular matrix domain (matrix mesh) and intracellular domain (fiber mesh). The two meshes are built using the self-programmed "myofiber" or "extracellular matrix" elements (Yucesoy et al., 2002) that are introduced as user defined elements into the finite element program ANSYS 5.7.1. The elements have eight nodes, linear interpolation functions and a large deformation analysis formulation. A 3D local coordinate system representing the fiber, cross-fiber (normal to the fiber direction), and thickness directions is used. For the myofiber element, the total stress that acts only in the local fiber direction is the sum of the active stress of the contractile elements and the stress due to intracellular passive tension. It is assumed that, at initial muscle length and passive state, the sarcomeres arranged in series within muscle fibers have identical lengths and material properties. The extracellular matrix element incorporates a strain energy density function that accounts for the non-linear and anisotropic material properties and the constancy of muscle volume.

Within the biological context, one muscle element is defined to represent a segment of a bundle of muscle fibers with identical material properties, its connective tissues and the links between them. This is realized as a linked system of extracellular matrix and myofiber elements. Both matrix and fiber meshes are rigidly connected to single layers of elements forming the muscles' proximal and distal aponeurosis. To represent the aponeuroses, a standard 3D, 8-node element HYPER58, from the element library of ANSYS 5.7.1 was used. This element has a hyperelastic mechanical formulation for which the strain energy density function is defined using the Mooney-Rivlin material law. For the elastic links between the two meshes, which represent the transmembranous attachments of the cytoskeleton and extracellular matrix, another standard element COMBIN39 was used. This is a 2-node spring element, which is set to be uniaxial and have linear stiffness characteristics.

The geometry of the model (Fig.1) is currently defined by the contour of a longitudinal slice at the middle of the isolated rat EDL muscle belly. Three muscle elements in series and six in parallel fill this slice. Therefore any collection of three muscle elements arranged in series represents a big muscle fascicle. All aponeurosis elements have identical mechanical properties but using a variable thickness in the fiber-cross fiber plane, the increasing cross-sectional area of the aponeurosis toward the tendon (Zuurbier et al., 1994) is accounted for.

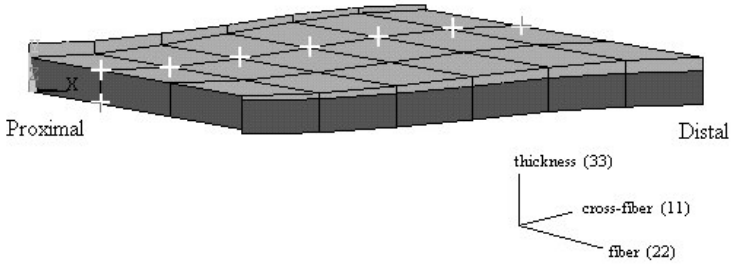

Fig.1. The geometry of the muscle model. The geometry is defined by the contour of a longitudinal slice of the rat extensor digitorum longus (EDL) muscle belly. The muscle model is composed of three in series and six in parallel muscle elements. A 3D local coordinate system is used for the analysis and presentation of the results. At the nodes indicated with a white "+" sign the extramuscular connections are made.

A. Model of EDL with extramuscular connections

For the present application, the lfmm model was extended to include extramuscular connections of EDL muscle to the tibia via surrounding connective tissues. Using spring elements, these connections were realized by linking a set of nodes of the matrix mesh (Fig. 1) to a set of fixed points, representing the 'mechanical ground'. In the experiments of the present study, the locations of the extramuscular connections of EDL muscle were determined to be at one-third of the fascicle length from the most proximal side of each muscle fascicle. For the extramuscular linking elements the spring element COMBIN39 was used with longitudinal force-deflection capability and linear stiffness characteristics. A suitable stiffness (k) was determined for these elements that provides a sufficiently good agreement between the experimental and modeled muscle forces. This model is referred to as model of EDL with extramuscular connections.

The corresponding fixed points of the mechanical ground and the nodes of the model were at identical locations initially (i.e., muscle length = 28.7 mm, and before moving any of the tendon ends). Mimicking the experimental conditions, first the proximal end of the modeled EDL was displaced 2 mm distally, which introduced a stretch of the extramuscular

linking elements. This end was then fixed at that position. The isometric analysis was carried out after displacing the distal end of the modeled EDL.

B. Model of EDL with minimal extramuscular connections

In the second part of the experimental study, the connective tissues providing the extramuscular connections of the EDL muscle were dissected to a maximum possible extent, without endangering circulation and innervation. The remaining connective tissue is the proximal part of the extramuscular connections of EDL, which consists of less than half of the complete tissue structure. To investigate the functional significance of the remaining connective tissue, most of the extramuscular linking elements were removed from the model. Only the first three proximal linking elements were remained. For these elements, a suitable stiffness value was determined that maintains the agreement between the experimental and modeled muscle forces after the second part of the experimental study. This model is referred to as model of EDL with minimal extramuscular connections.

The remaining connective tissue structure, which supports the blood vessels and nerves, is crucial for maintaining a physiological situation for the in situ muscle. Despite such connections, in situ muscle is generally considered to be to be isolated from its surroundings. In order to distinguish these two conditions, in addition to the model with minimal extramuscular connections, an isolated EDL model (i.e., a model of EDL muscle, from which all extramuscular linking spring elements were removed) was used. The results of the model with minimal extramuscular connections are compared to those of the isolated model.

Results

EDL with extramuscular connections

The length-total force characteristics for EDL muscle with intact extramuscular connections, as determined experimentally, as well as calculated using the lfmm model are compared in Fig.2. The experimental data reveal significant differences between EDL forces measured at the distal and proximal tendons (Fig.2a). After distal lengthening of EDL, distal isometric force is higher than proximal forces throughout almost all of the muscle length range studied. This proximo-distal EDL force difference increases as a function of the muscle length to a maximum value of almost 0.8 N (i.e. approximately 40% of the proximal force). The experimental and modeled forces agree quite well (Fig.2b), as long as a suitable stiffness (k) is selected for extramuscular links from the range of values given in Table 1. The model indicates that the extramuscular connections cause the proximo-distal force differences. Table 1, also provides estimates of goodness of fit between modeled and experimental data: RMSD represents the root mean squared deviation of model data from experimental data. The values with the superscript * indicate the linking stiffness selected for the results presented. Cells above and below, show values for stiffer and for more compliant links,

respectively. Fig.2b includes a comparison of the experimental and modeled passive forces. The distal passive forces of the model are over-estimated. A remarkable result is build up of passive forces well before optimum muscle length is reached. Both experimental and modeled passive proximal forces indicate that the proximal tendon of the muscle remains slack even at high muscle lengths.

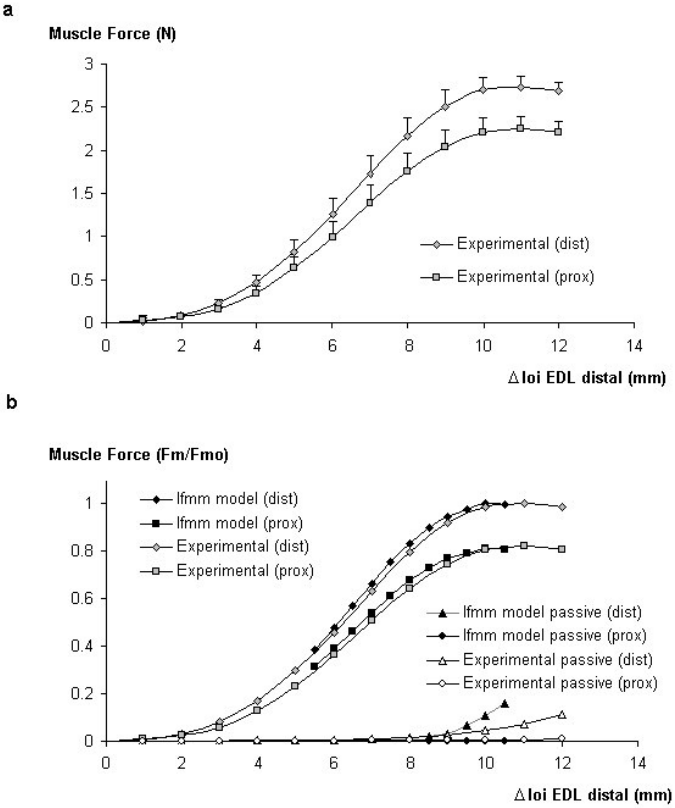

Fig.2. The isometric muscle length-total force curve for rat EDL muscle with extramuscular connections. (a) Absolute values of the experimental total muscle force at the proximal and distal tendons of the EDL muscle tendon complex expressed as a function of deviation (Δloi) from the active slack length. Mean results and standard errors of the mean (n=5) are shown. (b) Comparison of the experimental data and model data for muscle force (Fm) normalized for optimal force (Fmo).

For selected muscle lengths, fiber direction strain and stress distributions in the fiber mesh are shown in Fig.3. Strain as a measure of change of length, reflects lengthening (positive strain) or shortening (negative strain) of sarcomeres. Note that zero strain in the model represents the undeformed state of sarcomeres (i.e., sarcomere length ≅ 2.5 μm) in the passive condition, at initial muscle length (28.7 mm). Therefore, the strain distributions indicate distributions of length of sarcomeres arranged in series within muscle fibers. At low as well as high lengths (Fig.3a, b, c), a considerable distribution of strain throughout the

muscle is calculated. Note however, that, at low muscle length (Fig.3a), strains along the muscle fibers are more uniform (i.e. distributions are limited to a few percent). In contrast, at higher lengths (Fig.3b and c), increasing strain distributions are found within muscle fibers. The strain values for the proximal sarcomeres of muscle fibers are negative, whereas in distal sarcomeres of the same fibers positive strains are encountered (Fig.3c).

Table 1. Goodness of fit of model results to experimental data for EDL with intact extramuscular connections.

	Distal length-force characteristics	Proximal length-force characteristics
k	RMSD	RMSD
0.267	0.0429	0.0606
0.133	0.0365	0.0252
0.067*	0.0279*	0.0279*
0.033	0.0272	0.0432
0.017	0.0256	0.0513

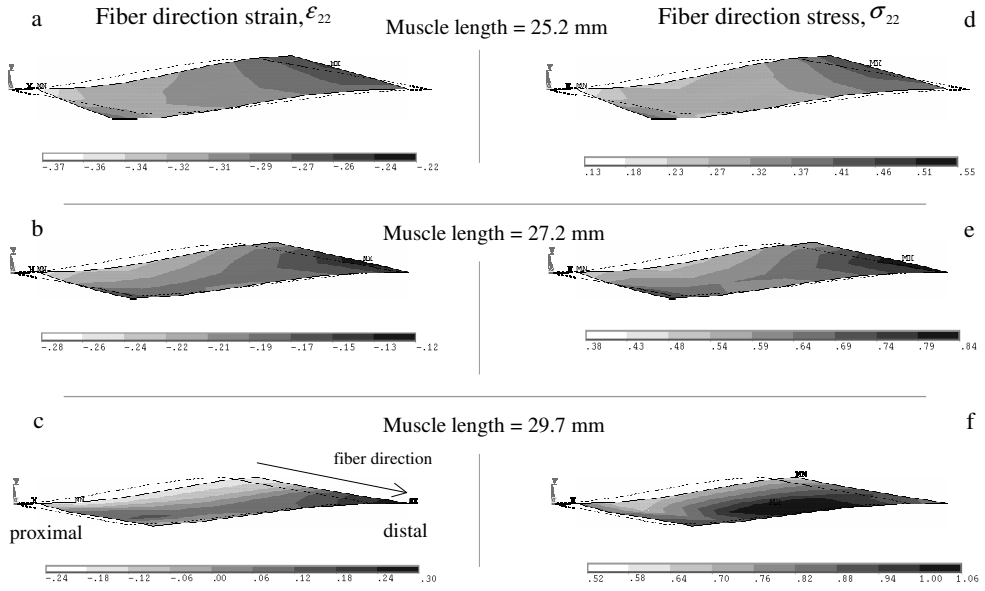

Fig.3. Stress and strain distributions for the fiber mesh of the EDL model with extramuscular connections at selected muscle lengths. (a) (b) and (c) Strain distributions of the fiber mesh for the fiber (22) direction. (d) (e) and (f) Stress distributions of the fiber mesh for the fiber (22) direction. The distributions are shown for the muscle lengths 25.2 mm, 27.2 mm and 29.7 mm (i.e. Δloi = 6 mm, Δloi = 8 mm and Δloi = 10.5 mm respectively). The dotted line contour indicates muscle geometry at the initial length. The fiber direction as well as the proximal and distal ends of the muscle is shown in part (c).

Fig.7 shows a comparison of the nodal strains plotted in parallel rows, to illustrate the in series distribution of sarcomere lengths within muscle fibers. At low muscle length the strains plotted at nodal positions for different rows are highly similar (Fig.7a). This shows that the distribution of length of sarcomeres in series is minimal. However, at high lengths, the strain plots for different rows are substantially heterogeneous (Fig.7b and c). This shows the enhanced distribution of sarcomere lengths as a function of increased extramuscular myofascial force transmission. Accordingly, distribution of stress along the fiber direction increases as a function of muscle length (Fig.3d, e and f). At high length (Fig. 3f) the stress at the proximal side of the muscle fibers is approximately 50% lower than the stress at their distal side. These results show that the extramuscular connections of the muscle lead to substantial local strain and stress distributions, not only for the whole muscle, but also for the sarcomeres arranged in series within muscle fibers, without affecting mechanical stability.

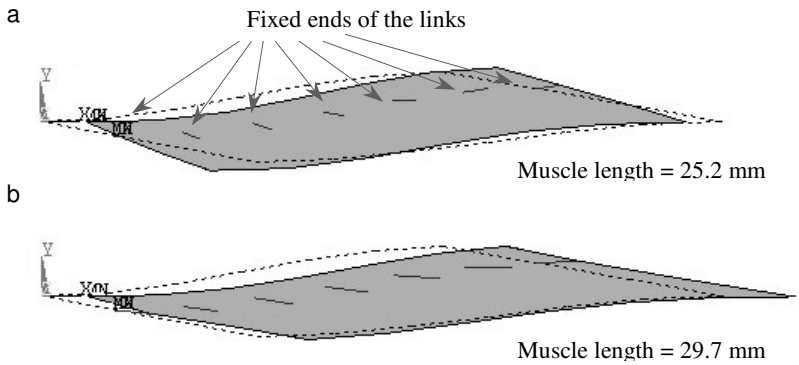

Fig.4. Comparison of length and orientation of the spring elements representing the modeled muscles' extramuscular connections. (a) At the lowest length studied. (b) At the highest length studied. The locations of the fixed ends of the links are indicated by arrows in (a). The dotted line contour indicates muscle geometry at the initial length.

The forces acting in the direction of line of pull of the muscle include the distal and proximal muscle forces, as well as the component of total force exerted on the extramuscular links in that direction. The deformed shapes of the extramuscular linking elements, indicating the magnitude and direction of the extramuscular force, are shown in Fig.4. Distal lengthening of the muscle leads to stretching of the extramuscular links (Fig.4a and b). Distally located links are stretched more than proximal links and rotated more in distal direction. Each spring element applies a certain force on the muscle in proximal direction. Therefore total extramuscular link force is directed towards the proximal side. For the force equilibrium in the present conditions, the sum of the proximal force and the total extramuscular link force must be equal to the distal force (i.e., the proximo-distal force

difference is equal to the total extramuscular link force). Note that this total link force increases, as the muscle is distally lengthened. Such increase explains the increasing proximo-distal force difference in favor of the distal force as a function of the distal muscle lengthening.

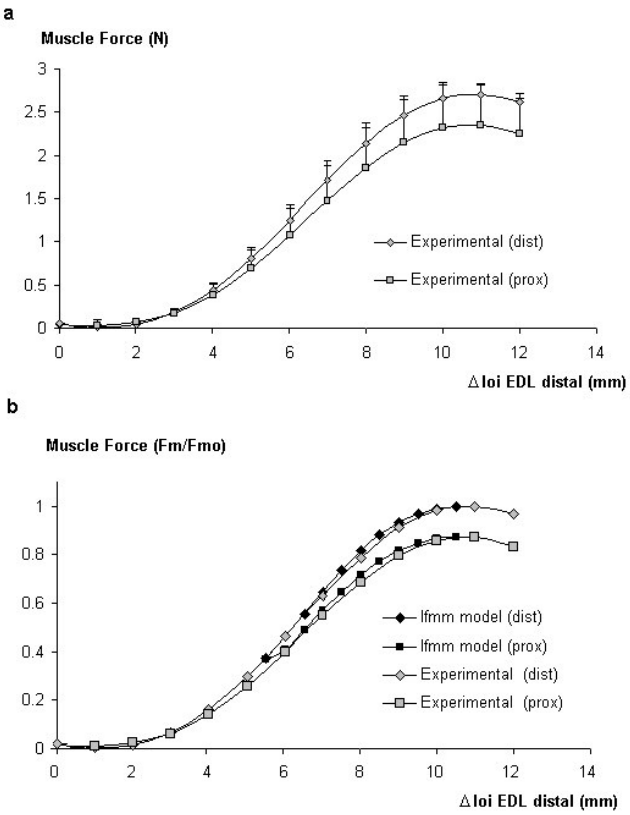

Fig.5. The isometric muscle length-total force curve for rat EDL muscle with minimal extramuscular connections. (a) Absolute values of the experimental total muscle force at the proximal and distal tendons of the EDL muscle tendon complex expressed as a function of deviation (Δloi) from the active slack length. Mean results and standard errors of the mean (n=5) are shown. (b) Comparison of the experimental data to the model predictions for which the muscle force (Fm) is normalized for optimum force (Fmo).

EDL with minimal extramuscular connections

Fig.5 shows the experimental and modeled length-total force characteristics of EDL muscle with minimal extramuscular connections. It shows maintained significant proximo-distal force differences (Fig.5a), featuring higher distal forces than proximal forces. Statistical analysis indicates that the differences between experimental length-force data of EDL with

full and minimal intact extramuscular connections are not significant. Fig.5b shows that after making the remaining extramuscular linking elements stiffer, the modeled and experimental forces agreed well (k = 0.286 unit force/mm is used for minimal extramuscular connections case whereas, k = 0.067 unit force/mm was the selected value for the previous case). These results indicate that the proximal connective tissues dominate the extramuscular effects. The most proximal neurovascular tract (a collagen fiber reinforced structure containing nerves and blood vessels) is likely to be a major factor at that location.

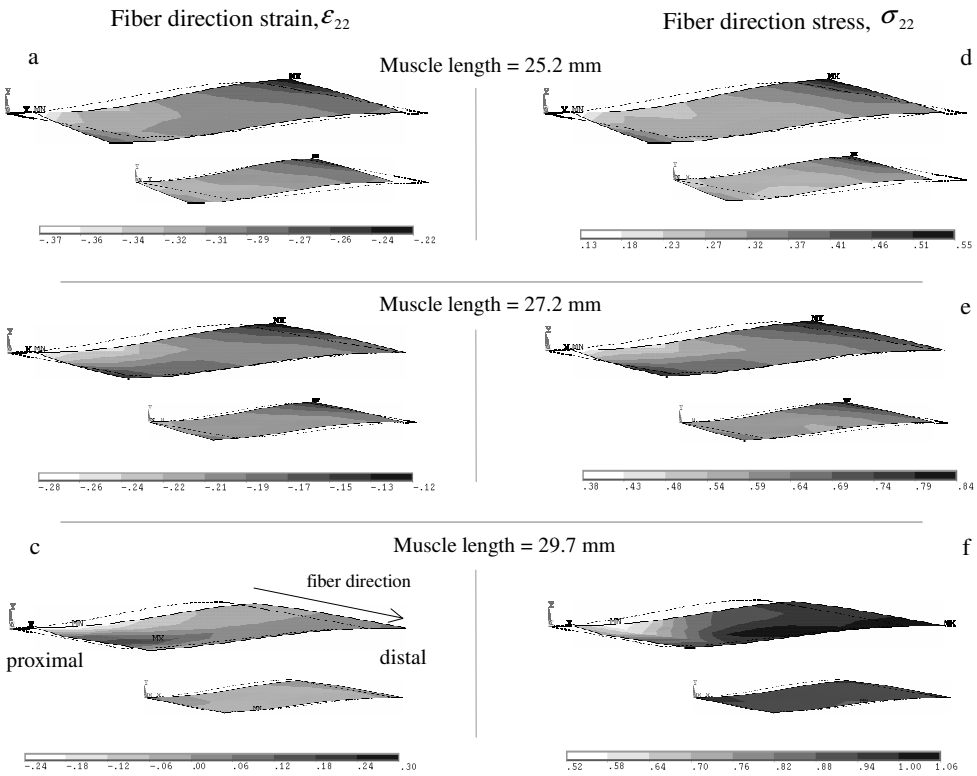

Fig.6. Stress and strain distributions for the fiber mesh of the model of EDL with minimal extramuscular connections (bigger contours) compared to the distributions of isolated EDL model (smaller contours) at selected muscle lengths. (a) (b) and (c) Strain distributions of the fiber mesh for the fiber (22) direction. (d) (e) and (f) Stress distributions of the fiber mesh for the fiber (22) direction. The distributions are shown for the muscle lengths 25.2 mm, 27.2 mm and 29.7 mm (i.e. Δloi = 6 mm, Δloi = 8 mm and Δloi = 10.5 mm respectively). The dotted line contour indicates muscle geometry at the initial length. The fiber direction as well as the proximal and distal ends of the muscle is shown in part (c) in the upper panel.

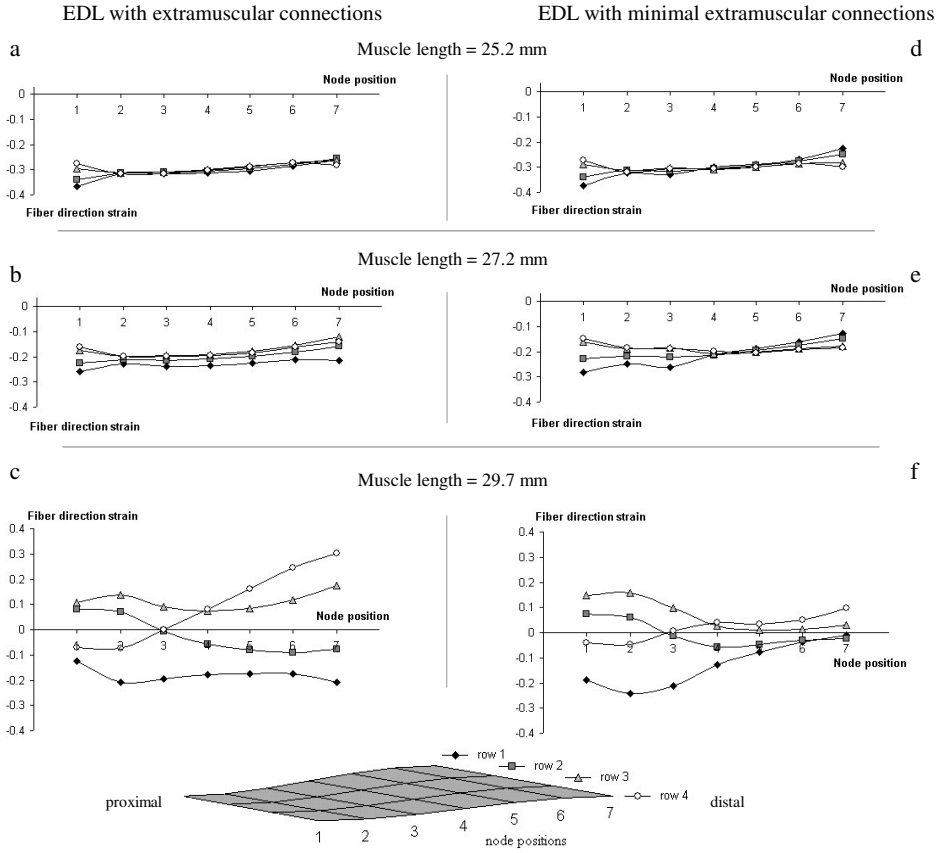

Fig.7. Comparison of the nodal strains plotted in parallel rows. The fiber direction strains within the fiber mesh are plotted in four parallel rows of nodes numbered from 1 to 7 (i.e., from proximal to distal side, lower panel). The differences between the strain plots provide a measure of distribution of length of sarcomeres arranged in series within muscle fibers. (a) (b) and (c) Strain plots for EDL with extramuscular connections, shown for the muscle lengths 25.2 mm, 27.2 mm and 29.7 mm (i.e. for Δloi = 6 mm, Δloi = 8 mm and Δloi = 10.5 mm) respectively. (d) (e) and (f) Strain plots for EDL with minimal extramuscular connections, shown for the muscle lengths 25.2 mm, 27.2 mm and 29.7 mm (i.e. for Δloi = 6 mm, Δloi = 8 mm and Δloi = 10.5 mm) respectively. Note that the strain values for the lower and upper surfaces of the model are identical as both faces have identical extramuscular connections. Strain is defined as the ratio of the change in length to the original length. Zero strain in the model is assumed to represent the undeformed state of sarcomeres (i.e., sarcomere length ≅ 2.5 μm) in the passive condition, at initial muscle length (28.7 mm). Positive strain shows lengthening and negative strain shows shortening of the sarcomeres with respect to this undeformed state.

Fig.6 shows the local strain and stress distributions within the fiber mesh of EDL with minimal extramuscular connections, for identical muscle lengths as considered above (Fig.3). The smaller size contours represent the isolated EDL model. These distributions illustrate that if the muscle is fully isolated (no extramuscular connections) no significant

strain or stress variation within muscle fibers occurs. For the muscle with minimal extramuscular connections, in the distal half of the muscle belly, both strains and stresses along the muscle fibers are rather uniform while the proximal half displays sizable distributions. The distributions of length of sarcomeres in series within muscle fibers of the proximal half of the muscle increase as the muscle length is higher (Fig.6a, b and c). At low muscle length, the similarity of the strains plotted at nodal positions for different rows (Fig.7d) indicates a minimal distribution of sarcomere lengths. In contrast, the increased heterogeneity between strain plots for different rows shows the enhanced distribution of sarcomere lengths at high muscle lengths (Fig.7e and d). Fig.6d, e and f show that the distribution of fiber direction stress within muscle fibers at the proximal half of the muscle becomes higher as a function of muscle length. At high length, this distribution is so substantial, that the stress at the distal end of the most proximal fibers is nearly twice as high as the stress at their proximal end (Fig.6f). These results show that due to even the minimal extramuscular connections significant proximo-distal force differences and local distributions of strain and stress are maintained.

In summary, the present experimental results confirmed that extramuscular myofascial force transmission has a major effect on the length-force characteristics of a muscle leading to significant force differences between the proximal and distal ends. The model results showed that as the muscle is lengthened distally, it is increasingly loaded in proximal direction by its extramuscular connections, which causes significant distributions of length of sarcomeres arranged in series within muscle fibers. As a result, stress distributions occur leading to the exertion of proximal and distal muscle forces, which ensure the mechanical equilibrium. This indicates that within a muscle with extramuscular connections, compartmentalization of sarcomeres occurs across muscle fibers indicating that the muscle fiber is no longer a unit exerting equal forces at both ends. Furthermore our present results showed that the minimal extramuscular connections necessary to keep a muscle within physiological ranges causes highly similar effects on muscle mechanics to the effects caused by the full extramuscular connections. This suggests that a muscle in situ should be distinguished from an isolated muscle.

Discussion

Inter- and extramuscular myofascial force transmission

Only some recent studies indicate effects of inter- and extramuscular myofascial force transmission. For example an attempt to verify effects of distal tendon transfer of the rectus femoris muscle, believed to be the conversion of it from a knee extensor to a knee flexor revealed that rectus femoris still generated a knee extension moment (Riewald and Delp, 1997). However, in those studies, myofascial force transmission was not accounted for which has been shown recently to have significant effects. Significant differences were

found for the simultaneously measured proximal and distal forces of EDL muscle within the intact anterior tibial compartment (Huijing, 1999b; 2000). A study investigating the effects of blunt dissection and compartmental fasciotomy (Huijing and Baan, 2001b) showed that a systematic manipulation of the extra and inter-muscular connective tissue structures altered the muscle length-force characteristics. Huijing and Baan (2001a) measured isometric EDL force after proximal EDL lengthening while TA, EHL as well as EDL were simultaneously and maximally activated. They found significant proximo-distal differences of active and passive EDL force. Experiments focused on intermuscular myofascial force transmission also showed unequal proximal and distal EDL forces (Maas et al., 2001). Our present study on EDL with extramuscular connections exclusively, studied the simplest level of interaction of a muscle with its surroundings.

Distribution of length of sarcomeres arranged in series within muscle fibers

The intramuscular connective tissues interact mechanically with the myofibers (e.g. Danowski et al., 1992; Huijing, 1999b) through the multimolecular trans-sarcolemmal systems (e.g. for a review see Berthier and Blaineau, 1997). This allows transmission of force, generated within myofibers, onto the extracellular matrix. Such transmission is an important determinant of the distribution of sarcomere lengths in series within muscle fibers. Results of a finite element modeling study on isolated muscle (Yucesoy et al., 2002) support this conclusion. In that work it was demonstrated that if there is an inadequate linking of sarcomeres to the extracellular matrix (as occurs in muscular dystrophies), at high muscle lengths the myofibers may be deformed beyond physiological limits. The intramuscular connective tissues are continuous with extramuscular connective tissues. Therefore we hypothesized that extramuscular myofascial force transmission can cause sarcomere length distributions. Our modeling results show sizeable distributions of fiber direction strain, indicating length distributions of sarcomeres in series within muscle fibers and therefore verify the hypothesis. Our results also show distribution of mean sarcomere length of different fibers. The principles effects of such distributions were discussed previously (e.g. Edman et al., 1993; Huijing, 1998).

Passive Forces

Both experimental and modeling parts of the present study show interesting results regarding passive force. For an isolated muscle, passive force is due to the tensile resistance of the muscle tissue only. The present results show that the distal passive forces start building up already at lengths lower than optimum muscle length. This happens because the extramuscular connections cause a certain passive resistance at those lengths. It is also interesting that while the distal EDL passive force increases the proximal force remains near

zero. This shows that any tensile loading of the proximal part of the passive muscle is prevented by the extramuscular connections.

Connective tissues supporting the neurovascular tract

Length-force data of EDL with minimal extramuscular connections was not significantly different from that of EDL with fully intact extramuscular connections. This shows that the mechanical properties of the extramuscular connections are not homogeneous but the tissues of the proximal neurovascular tract are stiffer due to the collagen-reinforced structure (for anatomical details see Huijing, 1999a; Huijing and Baan, 2001a). Therefore, we conclude that the proximal neurovascular tract dominates the extramuscular connections within the rat anterior tibial compartment.

Relative position of a muscle with respect to its surroundings

The extramuscular connective tissue sheet connects EDL all along the muscle to the tibia, part of interosseal membrane and anterior intermuscular septum (for images see Huijing and Baan, 2001a; Maas et al., 2001). This sheet defines the anatomical path of the extramuscular myofascial force transmission. This path will be favoring the force measured at the tendon of the muscle that is repositioned in order to introduce the lengthening. However, the connective tissues of the neurovascular tract, which are shown to be stiffer than the remainder of the sheet, composes approximately the proximal one third of the complete sheet and enters EDL on its proximal side. This suggests that the extramuscular myofascial effects may not be identical after equal distal or proximal lengthening.

In previous experiments with rat EDL within intact anterior tibial compartment (Maas et al., 2001; Huijing and Baan, 2001a), isometric force was measured exclusively after "proximal lengthening" and yielded higher proximal EDL forces than distal forces. It should be noted that the conditions of those experiments included intermuscular interactions as well. Presently we found higher distal EDL forces than proximal forces. This is due to the fact that the muscle was lengthened distally. Explorative modeling of proximal lengthening of EDL with extramuscular connections (not presented here) yields higher proximal forces for most of the muscle length range. These arguments show that relative position of a muscle with respect to its surroundings is expected to be a major determinant of the force exerted at proximal and distal tendons.

Truly isolated muscle and muscle in situ

Despite the large body of earlier experimental work on muscle, only a few studies show evidence for extramuscular myofascial effects. One reason for that may be that in the majority of the earlier work, muscle tissues were investigated in experimental conditions which eliminate structures possibly involved in mechanisms of inter- or extra-muscular force

transmission (e.g. Faulkner et al., 1982; Huijing et al., 1994; Jaspers et al., 1999; Street, 1983). Such conditions were referred to as either “isolated” or “in situ”. However, it is necessary to clearly distinguish these conditions. If a muscle is isolated, the extramuscular connective tissues are completely dissected, whereas for a muscle in situ, the tissues of the major neurovascular tract are always left intact. Isolation of a muscle leads to identical proximal and distal forces and only very limited distribution of sarcomere length, which are caused by intramuscular myofascial force transmission. In contrast, for muscle in situ, our present results show that proximal and distal forces are unequal and a significant distribution of sarcomere length takes place within muscle fibers. The majority of the earlier experimental work was performed on muscles in situ, with measurement of muscle force only at one of the tendons. This approach was based on the implicit assumption that the conditions for an in situ muscle are not different than that of an isolated muscle. Our results show that due to the dominance of the extramuscular effects by the remaining extramuscular connections of the major neurovascular tract, such an assumption is not tenable. Therefore it seems likely that, the earlier experiments were affected also by extramuscular myofascial force transmission.

Limitations and implications of this study

The results of the present study show significant effects of extramuscular myofascial force transmission on muscle functional characteristics. Nevertheless, it should be noted that, the conditions experimentally imposed are not completely physiological: (1) Experimental were performed with maximal activation of the muscle, whereas this is hardly the case vivo. The level of activation will change the stiffness of the muscular tissues and is expected to effect extramuscular mechanical interaction. This needs to be studied in the future. (2) In the course of distal lengthening, the surrounding connective tissues of EDL muscle were kept in their original positions. Our results suggest that a major determinant of the myofascial effects is the relative position of a muscle with respect to its surroundings. However, in vivo, not only the muscle studied, but also some of the surrounding connective tissues (particularly joint related connective tissues) and muscles may change position with joint motion. Therefore, studies aimed at identification of the in vivo relative positions of muscles with respect to each other and their surroundings for given tasks, are indicated.

Our model results, featuring mechanical equilibrium of a continuum that represents the muscle tissue, confirm our hypothesis on distribution of lengths of sarcomeres due to extramuscular myofascial force transmission. However, such distributions have not been validated experimentally. It should be noted that doing this for a whole muscle surrounded by compartmental connective tissues and other muscles is very difficult. A possibility could be using ultrasound techniques to show length distributions within muscle fascicles.

The extramuscular force, which is equal to the proximo-distal force difference, is in the direction of line of pull. EDL is a muscle of intermediate degree of pennation. Therefore only the component of the extramuscular force, which acts in the fiber direction, leads to the sarcomere length distributions. This component is smaller than the actual extramuscular force. However, for a parallel fibered muscle, the fiber direction, extramuscular force and the line of pull could be aligned. In that case even more effects of myofascial force transmission may be expected.

Using spring elements with linear stiffness and identical properties representing the intact extramuscular connections must be considered as a significant simplification. However, this approach indicated that the remaining links for the minimally connected condition should be stiffer in order to show the experimental effects of the intact connections on length-force characteristics. In future modeling, the mechanical properties of the linking elements should be defined accordingly and possible nonlinear behavior should be accounted for.

In this study, significantly lower force was found at the proximal tendon of the distally lengthened muscle as a result of extramuscular myofascial force transmission. For a biarticular muscle that is lengthened distally, this would reduce the moment at the proximal joint and may have important functional consequences.

The variations of sarcomere lengths within fibers related to myofascial force transmission is expected to have effects on muscle force production as well as length range between active slack and optimum lengths. An increased distribution of mean sarcomere length of different fibers was shown to improve the muscle length range (Willems and Huijing, 1994). Intermuscular myofascial effects are also expected to contribute to sarcomere length distributions (for an explorative modeling work see Yucesoy et al., 2001).

In conclusion, effects of extramuscular myofascial force transmission on muscular mechanics are quite large, at least in our experimental and modeling conditions. They are characterized by EDL proximo-distal muscle force differences in both active and passive conditions. Present model results show that extramuscular myofascial force transmission leads to distributions of strain in the direction of the muscle fibers. This indicates substantial length distributions of sarcomeres arranged in series within muscle fibers. The resulting stress distributions (higher stress was found in the distal half of the muscle fibers) are in agreement with the experimental and modeled proximo-distal force difference in favor of the distal force. Our present results also draw the attention to the differences between truly isolated muscles and in situ muscle caused by the collagen reinforced neurovascular tract, which dominate the extramuscular effects. Note that for the in vivo situation, intermuscular effects will have to be taken into account as well.

References

Berthier, C. and Blaineau, S. (1997): Supramolecular organization of the subsarcolemmal cytoskeleton of adult skeletal muscle fibers. A review. *Biology of the Cell* 89: 413-434.

Danowski, B. A., Imanaka-Yoshida, K., Sanger, J. M. and Sanger, J. W. (1992): Costameres are sites of force transmission to the substratum in adult rat cardiomyocytes. *The Journal of Cell Biology* 118: 1411-1420.

Edman, K. A., Caputo, C. and Lou, F. (1993): Depression of tetanic force induced by loaded shortening of frog muscle fibres. *The Journal of Physiology* 466: 535-552.

Faulkner, J. A., McCully, K. K., Carlson, D. S. and McNamara, J. A., Jr. (1982): Contractile properties of the muscles of mastication of rhesus monkeys (Macaca mulatta) following increase in muscle length. *Archives of Oral Biology* 27: 841-845.

Frueh, B. R., Gregorevic, P., Williams, D. A. and Lynch, G. S. (2001): Specific force of the rat extraocular muscles, levator and superior rectus, measured in situ. *The Journal of Neurophysiology* 85: 1027-1032.

Hijikata, T., Wakisaka, H. and Niida, S. (1993): Functional combination of tapering profiles and overlapping arrangements in nonspanning skeletal muscle fibers terminating intrafascicularly. *Anatomical Record* 236: 602-610.

Huijing, P. A., Nieberg, S. M., vd Veen, E. A. and Ettema, G. J. (1994): A comparison of rat extensor digitorum longus and gastrocnemius medialis muscle architecture and length-force characteristics. *Acta Anatomica* 149: 111-120.

Huijing, P. A. (1998): Muscle the motor of movement: Properties in function, experiment and modelling. *Journal of Electromyography and Kinesiology* 8: 61-77.

Huijing, P. A., Baan, G. C. and Rebel, G. (1998): Non myo-tendinous force transmission in rat extensor digitorum longus muscle. *Journal of Experimental Biology* 201: 682-691.

Huijing, P. A. (1999a): Muscle as a collagen fiber reinforced composite material: Force transmission in muscle and whole limbs. *Journal of Biomechanics* 32: 329-345.

Huijing, P. A. (1999b): Muscular force transmission: A unified, dual or multiple sytem? A review and some explorative experimental results. *Archives of Physiology and Biochemistry* 170: 292-311.

Huijing, P. A.,2000. In vivo, force is transmitted from muscle also at other locations than the tendons: Extramuscular myofascial force transmisison. 5th Annual Congress of the European College of Sports Science, Jyvaskyla, Finland, University of Jyvaskyla.

Huijing, P. A. and Baan, G. C. (2001a): Extramuscular myofascial force transmission within the rat anterior tibial compartment: Proximo-distal differences in muscle force. *Acta Physiologica Scandinavica* 173: 1-15.

Huijing, P. A. and Baan, G. C. (2001b): Myofascial force transmission causes interaction between adjacent muscles and connective tissue: Effects of blunt dissection and compartmental fasciotomy on length force characteristics of rat extensor digitorum longus muscle. *Archives of Physiology and Biochemistry* 109: 97-109.

Jaspers, R. T., Brunner, R., Pel, J. J. M. and Huijing, P. A. (1999): Acute effects of intramuscular aponeurotomy on rat GM: Force transmission, muscle force and sarcomere length. *Journal of Biomechanics* 32: 71-79.

Maas, H., Baan, G. C. and Huijing, P. A. (2001): Intermuscular interaction via myofascial force transmission: effects of tibialis anterior and extensor hallucis longus length on force transmission from rat extensor digitorum longus muscle. *Journal of Biomechanics* 34: 927-940.

Neter, J., M.H., K., Nachtsheim, C. J. and Wasserman, W., 1996. Applied Linear Statistical Models. Irwin, Homewood, IL.

Riewald, S. A. and Delp, S. L. (1997): The action of the rectus femoris muscle following distal tendon transfer: does it generate knee flexion moment? *Developmental Medicine and Child Neurology* 39: 99-105.

Street, S. F. (1983): Lateral transmission of tension in frog myofibers: a myofibrillar network and transverse cytoskeletal connections are possible transmitters. *Journal of Cellular Physiology* 114: 346-364.

Trotter, J. A. and Purslow, P. P. (1992): Functional morphology of the endomysium in series fibered muscles. *Journal of Morphology* 212: 109-122.

Willems, M. E. and Huijing, P. A. (1994): Heterogeneity of mean sarcomere length in different fibres: effects on length range of active force production in rat muscle. *European Journal of Applied Physiology and Occupational Physiology* 68: 489-496.

Yucesoy, C. A., Koopman, H. J. F. M., Huijing, P. A. and Grootenboer, H. J.,2001. Finite element modeling of intermuscular interactions and myofascial force transmission. 23rd Annual International Conference of the IEEE Engineering in Medicine and Biology Society, Istanbul, Turkey.

Yucesoy, C. A., Koopman, H. J. F. M., Huijing, P. A. and Grootenboer, H. J. (2002): Three-dimensional finite element modeling of skeletal muscle using a two-domain approach: Linked fiber-matrix mesh model. *Journal of Biomechanics* 35: 1253-1262.

Zuurbier, C. J., Everard, A. J., van der Wees, P. and Huijing, P. A. (1994): Length-force characteristics of the aponeurosis in the passive and active muscle condition and in the isolated condition. *Journal of Biomechanics* 27: 445-453.

Chapter 5

Effects of inter- and extramuscular myofascial force transmission on adjacent synergistic muscles: Assessment by experiments and finite element modeling

Abstract

The effects of inter- and extramuscular myofascial force transmission on muscle length force characteristics were studied in rat. Connective tissues at the bellies of the experimental synergistic muscles of the anterior crural compartment were left intact. Extensor digitorium longus (EDL) muscle was lengthened distally whereas; tibialis anterior (TA) and extensor hallucis longus (EHL) were kept at constant muscle-tendon complex length. Substantial differences were found in EDL force measured at the proximal and distal tendons (maximally 46 % of the proximal force). EDL with intact inter- as well as extramuscular connections had an increased length range between active slack and optimum length compared to EDL with extramuscular connections exclusively: optimum muscle length was shifted by more than 2 mm. Distal EDL lengthening caused the distal force exerted by TA+EHL complex to decrease (approximately 17% of the initial force). This indicates increased intermuscular myofascial force transmission from TA+EHL muscle complex to EDL muscle.

Finite element modeling showed that: (1) Inter- and extramuscular myofascial force transmission leads to a substantial distribution of the lengths of the sarcomeres arranged in series within muscle fibers. Distribution of stress within the muscle fibers showed that the muscle fiber cannot be considered as a unit exerting equal forces at both ends. (2) Increased heterogeneity of mean fiber sarcomere lengths (i.e., a “parallel” distribution of length of sarcomeres among different muscle fibers) is found, particularly at high muscle lengths. This also explains the shift in muscle optimum length to higher lengths.

It is concluded that inter- and extramuscular myofascial force transmission has substantial effects on muscle length-force characteristics.

Introduction

Myofascial force transmission (Huijing, 1999b) is transmission of force from the full perimeter surface of myofibrils onto the extracellular matrix (e.g. Street, 1983; Danowski et al., 1992; Trotter and Purslow, 1992; Hijikata et al., 1993; Huijing et al., 1998; Huijing, 1999a; Yucesoy et al., 2002b). The multimolecular complexes (e.g. Berthier and Blaineau, 1997) connecting sarcomeres to elements of the subsarcolemmal cytoskeleton, and from there via trans-sarcolemmal molecules to the extracellular matrix allow intramuscular myofascial force transmission. The intramuscular connective tissues are continuous with inter- and extramuscular connective tissues. Transmission of force from the extracellular matrix of a muscle to the extracellular matrix of an adjacent muscle through the direct connections between the muscles is referred to as *intermuscular myofascial force transmission*. Transmission of force from the extracellular matrix of a muscle to surrounding non-muscular elements of a compartment and bone is referred to as *extramuscular myofascial force transmission*. In recent experiments, the existence of inter- and extramuscular myofascial force transmission has been proved (Huijing and Baan, 2001a; Huijing and Baan, 2001b; Maas et al., 2001). Interpretation of these results yield hypotheses regarding effects of myofascial force transmission on muscle characteristics such as distributions of length of sarcomeres within muscle fibers. However, confirming these hypotheses experimentally for a whole muscle surrounded by compartmental connective tissues and by other muscles is presently impossible, as the free view of the muscle and its fibers in situ is obscured.

Recently, the rat extensor digitorium longus muscle (EDL) was studied with intact extramuscular connections exclusively (Yucesoy et al., 2002a). Some morphological and physiological questions were addressed using a finite element muscle model (Yucesoy et al., 2002b). Extramuscular myofascial force transmission was shown to cause significant distributions of sarcomere length. In the present work, an experimental study is reported in which the intermuscular connections of EDL muscle to other muscles within the anterior crural compartment were left intact together with its extramuscular connections. The goal is to identify the specific effects of intermuscular myofascial force transmission and integrated effects of inter- and extramuscular myofascial force transmission on muscle length-force characteristics by comparing the experimental data for these two conditions. Finite element muscle modeling is aimed at studying the mechanics of such transmission and to test the hypothesis that intermuscular myofascial force transmission alters distributions of length of sarcomeres within muscle fibers and muscle.

Methods

I Experimental Study

Surgical procedures

Surgical and experimental procedures were in strict agreement with the guidelines and regulations concerning animal welfare and experimentation set forth by Dutch law, and approved by a Committee on Ethics of Animal Experimentation at the Vrije Universiteit, Amsterdam.

Male Wistar rats (n = 5, body mass = 304.4 ± 3.5 g) were anaesthetized by intraperitoneally injected urethane solution (initial dose: 1.2 mg 100 g^{-1} body mass, extra doses if necessary: maximally 1.5 mg). To prevent hypothermia, the animals were placed on a heated water pad of approximately 37°C during surgery and experimentation. Ambient temperature (22 ± 0.5°C) and air humidity (80 ± 2%) were kept constant by a computer controlled air–conditioning system (Holland Heating). Muscle and tendon tissue was further prevented from dehydration by regular irrigation with isotonic saline.

The left anterior crural compartment, which consists of the tibialis anterior (TA), extensor digitorum longus (EDL) and extensor hallucis longus (EHL) muscles, was exposed by removing the skin and most of the biceps femoris muscle. Connective tissues at the bellies of TA, EHL and EDL were left intact to maintain the physiological relations of intra-, inter- and extramuscular connective tissues. With the knee joint at 90° and the ankle joint at 90° (referred to as a reference position), the four distal tendons of EDL were tied together. The distal tendons of TA and EHL were also tied to each other. Matching markers were placed on the distal tendons of EDL, TA and EHL, as well as on a fixed location on the lower leg. Subsequently, the distal EDL and TA+EHL tendon complexes were cut as distally as possible and removed from their retinaculae near the ankle joint (after cutting the transverse crural ligament and cruciate ligament). The foot was attached to a plastic plate with tie wraps.

The femoral compartment was opened to detach the proximal tendon of EDL from the femur and to secure the femur (at a knee angle of 90°) with a metal clamp. A Kevlar thread (4% elongation at a break load of 800 N) was tied to the combined distal EDL tendons, distal TA+EHL tendons and the proximal EDL tendon with a suture. The Kevlar threads were later connected to force transducers (Fig.1a) that were aligned with the muscle line of pull (Hottinger Baldwin, maximal output error < 0.1 %, compliance of 0.0048mm N^{-1}). The sciatic nerve was dissected, leaving the peroneus communis nerve branch intact. The tibial nerve and the sural branch of the sciatic nerve were cut. The sciatic nerve was cut as proximally as possible and placed on a pair of silver electrodes and covered by a saline wetted piece of tissue, which was covered by a small piece of latex.

Experimental procedures

The footplate was positioned in such a way that the ankle angle was in maximal plantar flexion. The knee angle was maintained at 90°. The origins of TA and EHL muscles were not manipulated in any way. TA+EHL complex was allowed to shorten distally to such a length that the distal TA+EHL force was equal to approximately 2 N. After that, also the position of distal tendons of the TA+EHL complex was kept constant. Therefore, the length of this muscle group was not altered during the experiment. The proximal EDL tendon was displaced by 2 mm in the distal direction with respect to its reference position at which location it was kept throughout the experiment. Isometric EDL force was measured at various muscle–tendon complex lengths and distal TA+EHL force was measured simultaneously. EDL was lengthened by moving exclusively the distal force transducer with 1 mm increments starting at muscle active slack length (i.e. the length at which active force approaches zero). After each tetanic contraction (all muscles were excited simultaneously) the muscles were allowed to recover for 2 minutes.

The sciatic nerve was stimulated supra-maximally using a pair of silver electrodes connected to a constant current source (3 mA, pulse width 100 μs). Two twitches were evoked and followed by a tetanic contraction after 300 ms (pulse train 400 ms, frequency 100 Hz). Simultaneously, images of the muscle in passive and active state were recorded using a digital camera (DVC, JAI CV–M10, shutter speed 1/50 s). The timing of stimulation, A/D conversion (12–bit A/D converter, sampling frequency 1000 Hz, resolution of force 0.01 N), and photography were controlled by a microcomputer.

Processing of experimental data and statistics

Data for total muscle force (F_{mt}) in relation to muscle tendon complex length (l_{oi}) were fitted by a polynomial function

$$y = b_0 + b_1x + b_2x^2 + b_3x^3 + b_4x^4 + \ldots + b_nx^n,$$

where y represents F_{mt} and x represents l_{oi}. b_0, $b_1 \ldots b_n$ are coefficients determined in the fitting process. Polynomials that best described the experimental data were selected by using one-way analysis of variance (ANOVA) (Neter et al., 1996), to be used for averaging of data and calculation of standard errors. One-way analysis of variance was also used in testing the length range of active force production. Two-way analysis of variance (ANOVA) was performed to test for length effects and for differences between the EDL force measured at the proximal and distal tendons. Bonferroni post–hoc tests were carried out to identify the significance of proximo–distal force difference at each l_{oi} (Neter et al., 1996). Differences were considered significant at $p<0.05$.

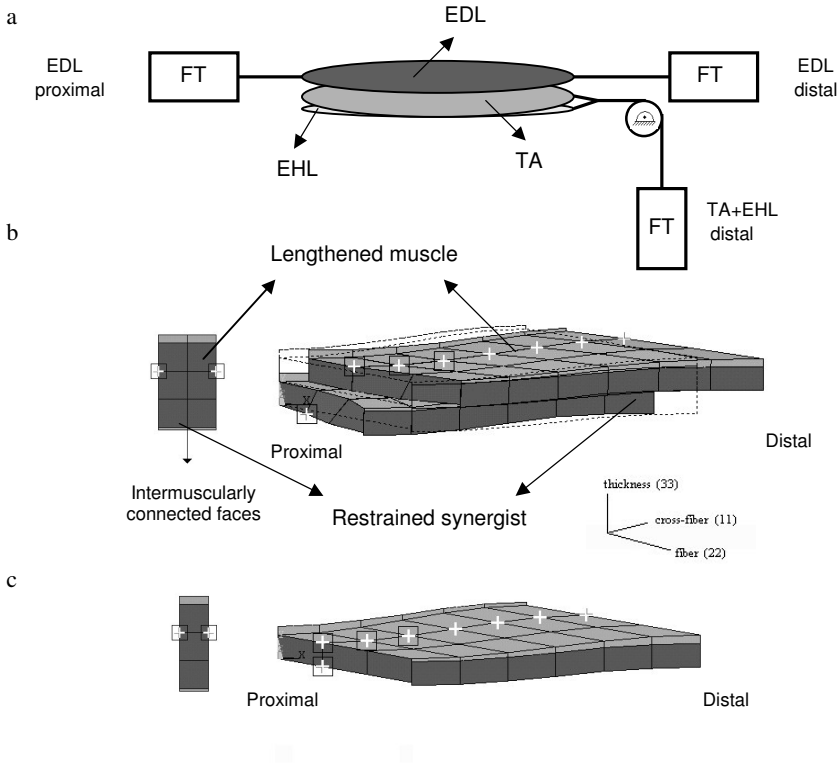

Fig.1. Schematic representation of the experimental setup and of the models. (a) The experimental setup. The Kevlar threads tied to the proximal and distal tendons of EDL, as well as to the tied distal tendons of TA+EHL complex were connected to force transducers (FT). (b) The models representing the intermuscularly connected synergists consist of two identical muscles. The geometry of both muscles is defined by the contour of a longitudinal slice of the rat extensor digitorum longus (EDL) muscle belly. Each muscle model is composed of three in-series and six in-parallel muscle elements. One of the models, is kept at a fixed low length (i.e. 3.0 mm shorter than its initial length), and is referred to as restrained synergist. This muscle is connected intermuscularly to the agonist muscle, which is lengthened distally, and referred to as lengthened muscle. Prior to distal lengthening, the proximal end of the agonist muscle was moved 2.0 mm in the distal direction, as in the experiment of the present study. Both of the models were also connected extramuscularly: the nodes of the matrix mesh marked by a white "+" sign have connections to mechanical ground. The nodes marked also by a black square have stiffer extramuscular connections. Muscular geometry at the initial muscle length is represented by dotted lines. A proximal view of the models in the undeformed state is shown on the left hand side. Locations of the inter- and extramuscular connections are indicated using the same symbols as in the view of the longitudinal plane. (c) The model of EDL muscle with extramuscular connections exclusively. The nodes of the matrix mesh marked by a white "+" sign have extramuscular connections to mechanical ground and the nodes marked also by a black square have stiffer connections. A proximal view in the undeformed state is shown on the left hand side. Also in this view the location of extramuscular connections of the model are marked. A 3D local coordinate system representing the fiber, cross-fiber (normal to the fiber direction), and thickness directions is used for the analysis and presentation of the model results.

II. Modeling Study

Using a two-domain approach, a 3D-finite element muscle model (linked fiber-matrix mesh model: lfmm model) was developed (Yucesoy et al., 2002b). This model consists of two meshes, occupying the same space, that are linked elastically. These meshes represent the extracellular matrix domain (matrix mesh) and intracellular domain (fiber mesh). The two meshes are built using the self-programmed "myofiber" and "extracellular matrix" elements (Yucesoy et al., 2002b) that are introduced as user defined elements into the finite element program ANSYS 5.7.1. For the myofiber element, the total stress that acts only in the local fiber direction is equal to the sum of the active stress of the contractile elements and the stress due to intracellular passive tension. It is assumed that, at initial muscle length in the passive state, the sarcomeres arranged in-series within muscle fibers have identical lengths and material properties. The extracellular matrix element incorporates a strain energy density function that accounts for the non-linear and anisotropic material properties and the constancy of muscle volume.

Within the biological context, one muscle element is defined to represent a segment of a bundle of muscle fibers with identical material properties, its connective tissues and the links between them. This is realized as a linked system of extracellular matrix and myofiber elements. Both matrix and fiber meshes are rigidly connected to single layers of elements forming the muscles' proximal and distal aponeurosis. To represent the aponeuroses, a standard element with a hyperelastic mechanical formulation (HYPER58) from the element library of ANSYS 5.7.1 was used. For the elastic links between the two meshes, which represent the transmembranous attachments of the cytoskeleton and extracellular matrix, a standard spring element (COMBIN39) was used. This element produces force in the direction of the deformation with linear stiffness characteristics.

In the present study, two models for which the geometry is defined by the contour of a mid-longitudinal slice of the rat EDL muscle belly were intermuscularly connected: the corresponding nodes of the matrix meshes of the two models were linked elastically (Fig.1b). The extramuscular connections of both models to the surrounding structures were also included: using spring elements, a set of nodes of the matrix mesh of each model were linked to a set of fixed points, representing 'mechanical ground'. Initially, the corresponding points of the mechanical ground and the nodes of the models were at identical locations (i.e., muscle length = 28.7 mm for both muscles, and before moving any of the tendon ends). The extramuscular connections of EDL muscle are located at approximately one-third of the fascicle length from the most proximal side of each fascicle (Huijing and Baan, 2001a). Embedded in this connective tissue, major nerves and blood vessels to the muscle and to the foot are found (neurovascular tract). Due to the collagen-reinforced structure, the proximal third of the extramuscular connective tissue sheet was shown to be much stiffer than the remainder of the sheet (Yucesoy et al., 2002a). This is taken into account in both models by

making the three most proximal extramuscular links stiffer than the other links. For both inter- and extramuscular links, the spring element COMBIN39 was used with linear stiffness characteristics. A suitable stiffness (k) was determined for the intermuscular elements that provides a sufficiently good agreement between the experimental and modeled muscle forces. For the extramuscular links, the stiffness values determined previously (Yucesoy et al., 2002a) were used (k = 0.286 unit force/mm for stiffer part and, k = 0.067 unit force/mm for the remaining links).

One of the modeled muscles was distally lengthened; this procedure models the EDL muscle in the experiment (referred to as the *lengthened muscle*). In the anterior crural compartment, EDL muscle is connected to the tibia only by extramuscular tissues such as the anterior intermuscular septum. As the tibia is located medially, the extramuscularly connected face of the lengthened muscle is referred to as the "medial face". Accordingly its intermuscularly connected face is referred to as the "lateral face".

The other model muscle, which was kept at a fixed length (3 mm shorter than the initial length) represents the TA+EHL muscle complex (referred to as the *restrained synergist*). Mimicking the experimental conditions, before distal lengthening, the proximal end of the lengthened muscle was displaced 2 mm distally, and was then fixed at that position. Throughout the analysis, both muscles were modeled as activated maximally.

Another EDL model with extramuscular connections exclusively was used in order to compare its results to the results of the lengthened muscle with both inter- and extramuscular connections. The extramuscular connections of this model were also represented by spring elements that link a set of nodes of the matrix mesh at medial and lateral faces (as described above) to mechanical ground (Fig1.c). Its proximal end was displaced 2 mm distally before distal lengthening and the activation was maximal.

Local strain, as a measure of change of length, reflects the lengthening or shortening of sarcomeres. Note that zero strain in the model represents the undeformed state of sarcomeres (i.e., sarcomere length ≅ 2.5 μm) in the passive condition. Fiber direction strain within the fiber mesh of the lfmm model was used to assess the non-uniformity of sarcomere lengths arranged in-series within muscle fibers (referred to as *serial distribution*). Mean fiber direction strain (mean of nodal strain values) was used to assess heterogeneity of mean sarcomere lengths of different fibers within the muscle (referred to as *parallel distribution*).

Results

Lengthened Muscle

Fig.2a and b shows superimposed examples of force time traces for EDL at four muscle lengths.

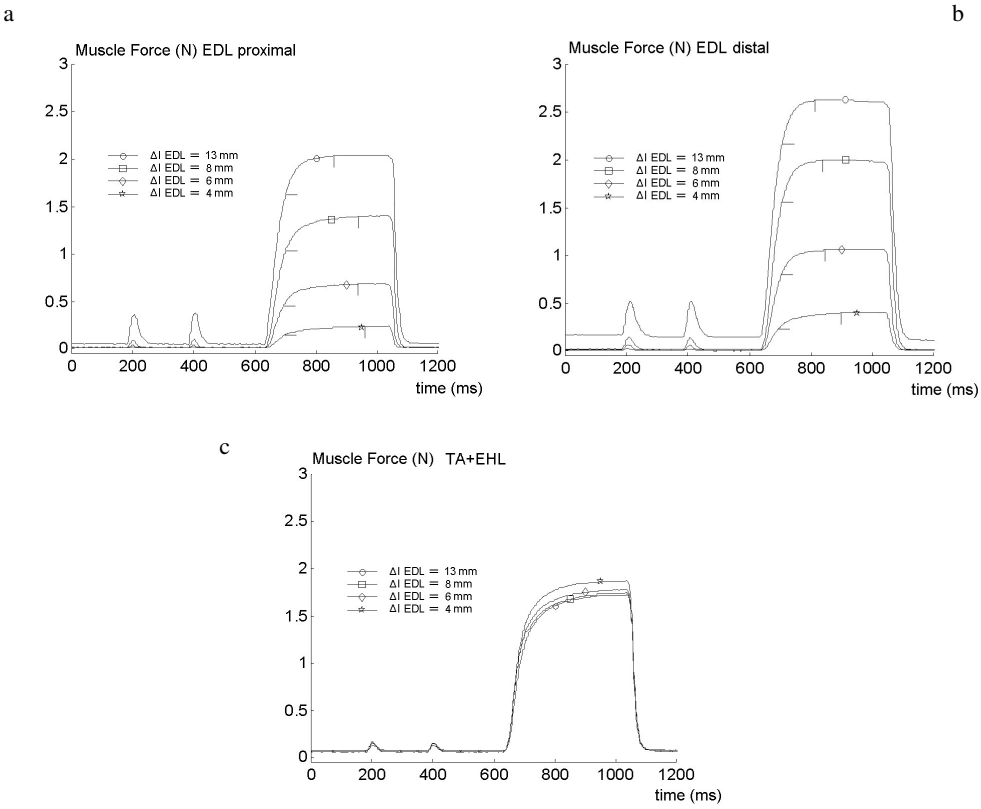

Fig.2. Typical examples of force time traces as measured at EDL proximal and distal tendons as well as at the distal tendon of the TA+EHL muscle complex. Superimposed traces recorded for an individual muscle at four EDL muscle lengths (a) proximal EDL force, (b) distal EDL force and (c) distal TA+EHL force. Note the proximo-distal EDL force differences at different muscle lengths (comparing panels a and b). The decrease in TA+EHL force as a function of increasing EDL length is apparent in panel (c). The creep phase (i.e., slow rise in force following the initial fast rise) for proximal and distal EDL force is indicated with short stripes in panels (a) and (b). The horizontal stripes mark the end of the fast rise in force therefore, the beginning of the creep phase. They are located at points on the force time traces, at which the slope of the curve changes such that the rate of increase in force becomes smaller. The vertical stripes mark the end of the slow rise of force therefore, the end of the creep phase. They are located at points on the force time traces at which the force reaches a maximum value and remains at a steady level. At higher EDL lengths, note the decrease in the duration of the creep phase whereas creep amplitude increases.

After distal lengthening, significant differences were found between isometric EDL forces measured at the distal and proximal tendons (Fig.3a). Except at very low lengths, distal isometric total EDL forces are higher than proximal forces. The proximo-distal force difference increases as a function of the muscle length to a maximum value of 0.95 N (i.e. approximately 46% of the proximal force). Similarly, the distal passive EDL forces are

higher than the proximal passive forces, which remain very low. In Fig.3b, the length-total force characteristics of EDL muscle with intact inter- and extramuscular connections are compared to that of EDL muscle with intact extramuscular connections exclusively (Yucesoy et al., 2002a). The length range of active force production between muscle slack and optimum lengths is significantly higher for EDL with intact inter- and extramuscular connections (12.7 ± 0.67 mm, mean ± SD) than that of EDL with extramuscular connections exclusively (10.2 ± 0.74 mm mean ± SD). Therefore, we hypothesize that with intact inter- and extramuscular connections, EDL will have increased heterogeneity of mean fiber sarcomere lengths compared to EDL with extramuscular connections exclusively. Also note that distal optimum force of EDL with intact inter- and extramuscular connections is higher than that of EDL with extramuscular connections exclusively. This is likely to be a result of intermuscular myofascial force transmission, i.e. force generated by sarcomeres of TA+EHL muscle complex is exerted at EDL tendon. The proximo-distal force difference is enhanced for EDL with intact inter- and extramuscular connections (Fig.3b) i.e., 46 % of its proximal force whereas the difference is maximally 22 % of the proximal force of EDL with extramuscular connections exclusively. This originates primarily from lower proximal forces exerted by EDL with intact inter- and extramuscular connections. Smaller differences are found comparing the distal forces of EDL for both conditions (Fig.3b).

The modeled forces agree reasonably well with the present experimental data (Fig.3c), provided that suitable stiffness values are selected for inter- and extramuscular linking elements. However, in contrast to modeled forces, at high lengths (i.e., Δl EDL > 11 mm) the experimental forces reach a plateau region. This is because, over optimum length, passive intramuscular connective tissues are modeled stiffer than that of the experimental muscle.

The strain distributions shown in Fig.4 are studied to address two points: (1) the intact inter- and extramuscular connections of EDL cause substantial serial distribution of sarcomere lengths within muscle fibers (2) parallel distribution within muscle is more pronounced for EDL with intact inter- and extramuscular connections compared to EDL with extramuscular connections exclusively.

Serial distribution of length of sarcomeres within muscle fibers

For EDL with inter- and extramuscular connections, the strain distributions of the medial face and the lateral face of the fiber mesh were different. However, Fig.4 shows for both faces that as muscle length increases (1) the range of the serial distribution increases i.e., the difference between the largest and smallest values of sarcomere lengths is higher and (2) more sarcomeres arranged in series within muscle fibers are at different lengths.

Distally Lengthened Muscle

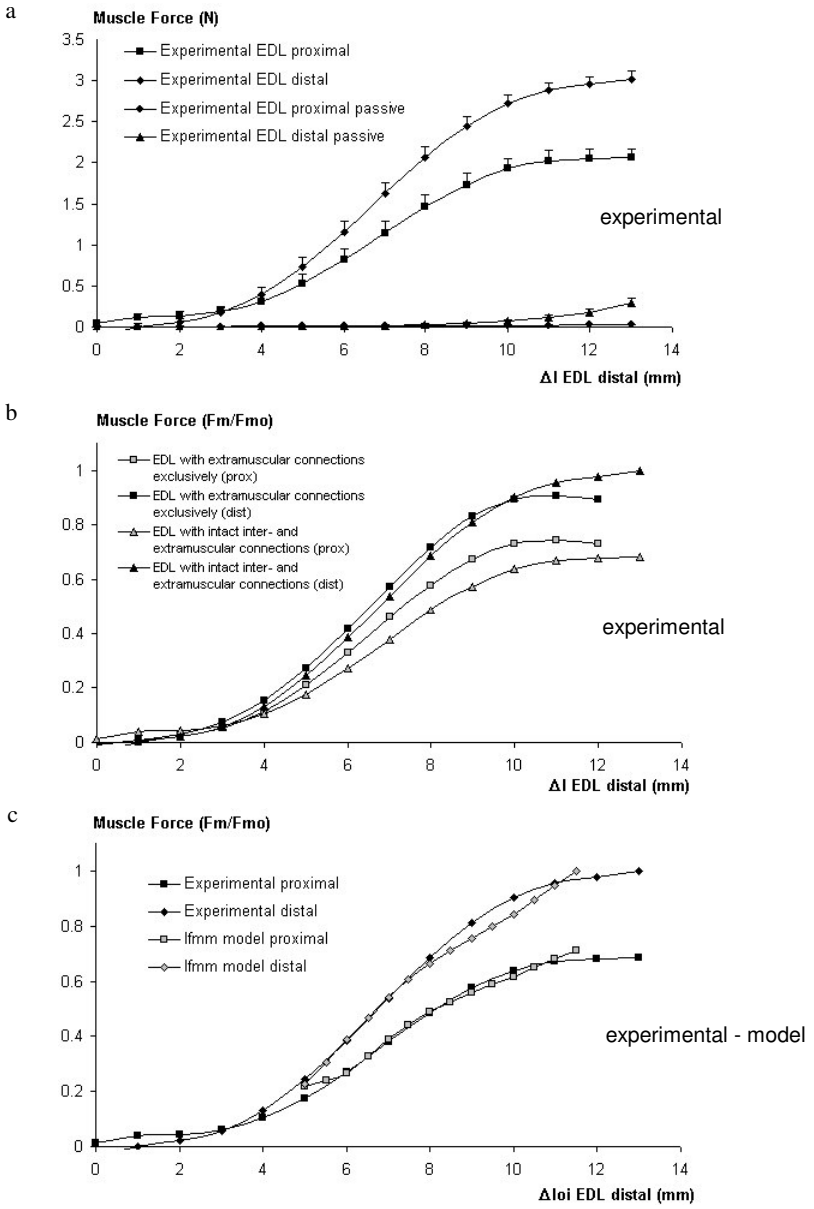

Fig.3. The isometric muscle length-force curves of EDL muscle. (a) Experimental total and passive muscle forces, measured at the proximal as well as distal tendons of the EDL muscle tendon complex after distal lengthening. Length is expressed as a function of deviation (Δl EDL) from active slack length. Mean results and standard errors of the mean (n=5) are shown. (b) Comparison of the length-total force characteristics of EDL muscle with intact inter- and extramuscular connections (present experimental data) to that of EDL muscle with extramuscular connections exclusively (Yucesoy et al., 2002a). Both sets of data are normalized for distal optimum force of EDL with intact inter- and extramuscular connections. (c) Comparison of experimental and modeled forces of the lengthened muscle (Fm) normalized for optimal force (Fmo).

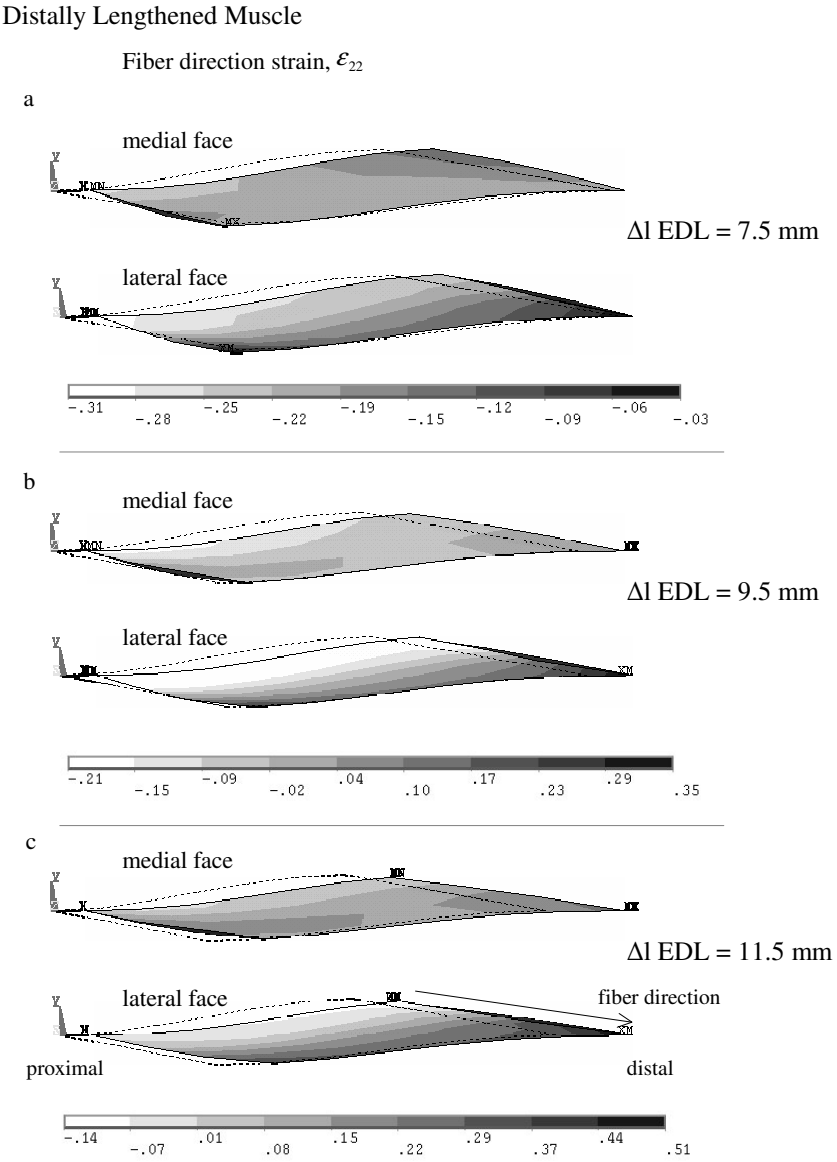

Fig.4. Distributions of fiber direction strain within modeled EDL muscle with intact inter- and extramuscular connections at selected muscle lengths. The Strain distributions within the fiber mesh are shown for (a) Δl EDL = 7.5 mm, (b) Δl EDL = 9.5 mm and (c) Δl EDL = 11.5 mm. The distributions at the medial face of this model are shown in the upper panels whereas the lower panels show the distributions in the lateral face. Length is expressed as a function of deviation (Δl EDL) from active slack length. The dotted line contour indicates muscle geometry at the initial length and position. Prior to distal lengthening, the proximal end of the muscle model was moved 2.0 mm in the distal direction, as in the experiment of the present study. The fiber direction as well as the proximal and distal ends of the muscle is shown in the lower panel of part (c).

Medial face. Due to the stiffer proximal extramuscular links, the strain distributions are more pronounced in the proximal part of the medial face (Fig.4a, b and c, upper panels). The sarcomeres located at the proximal ends of the muscle fibers are shorter than the ones located more distally. For example, within the most proximal fascicle at high length, the most proximally located sarcomeres remained slightly shortened (by 0.7 %) whereas the more distal sarcomeres are lengthened up to 22 % (Fig.4c, upper panel).

Lateral face. More pronounced strain distributions were found throughout the lateral face (Fig.4a, b and c, lower panels). The sarcomeres at the proximal ends of the muscle fibers are generally shorter than the ones located distally. At low length, the most distal parts of the muscle fibers show almost no length changes (i.e., strain values close to zero), although the proximal parts are shortened by up to 31% (Fig.4a lower panel). Even at high muscle lengths, the proximal ends of fibers remained shortened (by 14 %) while the most distally located sarcomeres are lengthened by up to 51% (Fig.4c lower panel). It is concluded that a major serial distribution of lengths of sarcomeres within muscle fibers does occur in EDL with intact inter- and extramuscular connections.

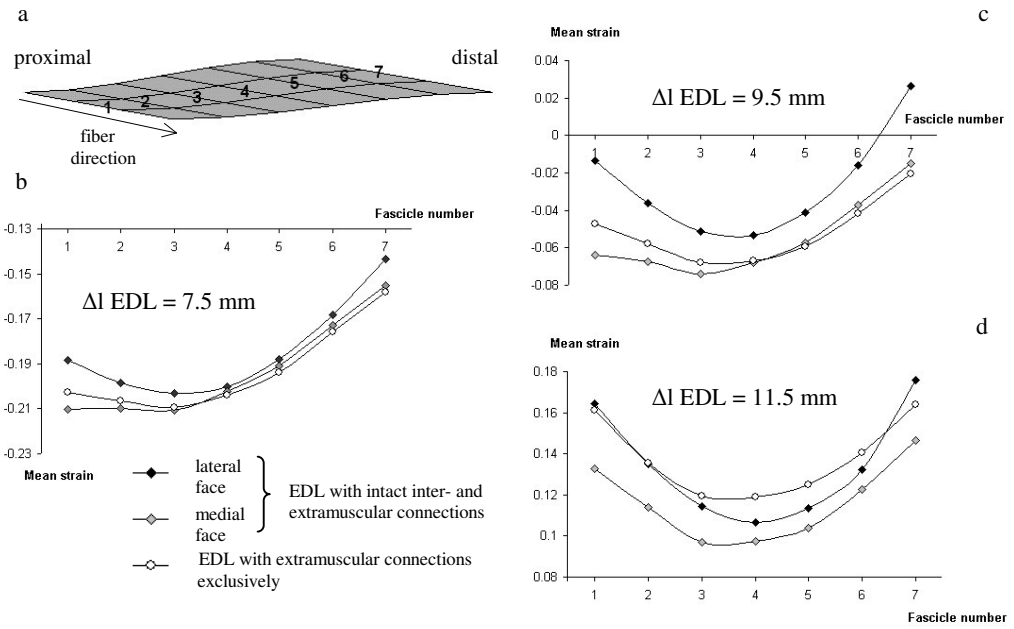

Fig.5. Distributions of mean fiber strains in fiber direction for EDL with intact inter- and extramuscular connections and for EDL with extramuscular connections exclusively. (a) Mean fiber direction strain was calculated at nodes of the myofiber elements (in the fiber mesh) in-series representing a muscle fascicle. Each fascicle is indicated by a number from 1 to 7. Mean fiber direction strains are plotted as a function of fascicle number for the selected EDL lengths: (b) Δl EDL = 7.5 mm, (c) Δl EDL = 9.5 mm and (d) Δl EDL = 11.5 mm. EDL length is expressed as a function of deviation (Δl EDL) from active slack length.

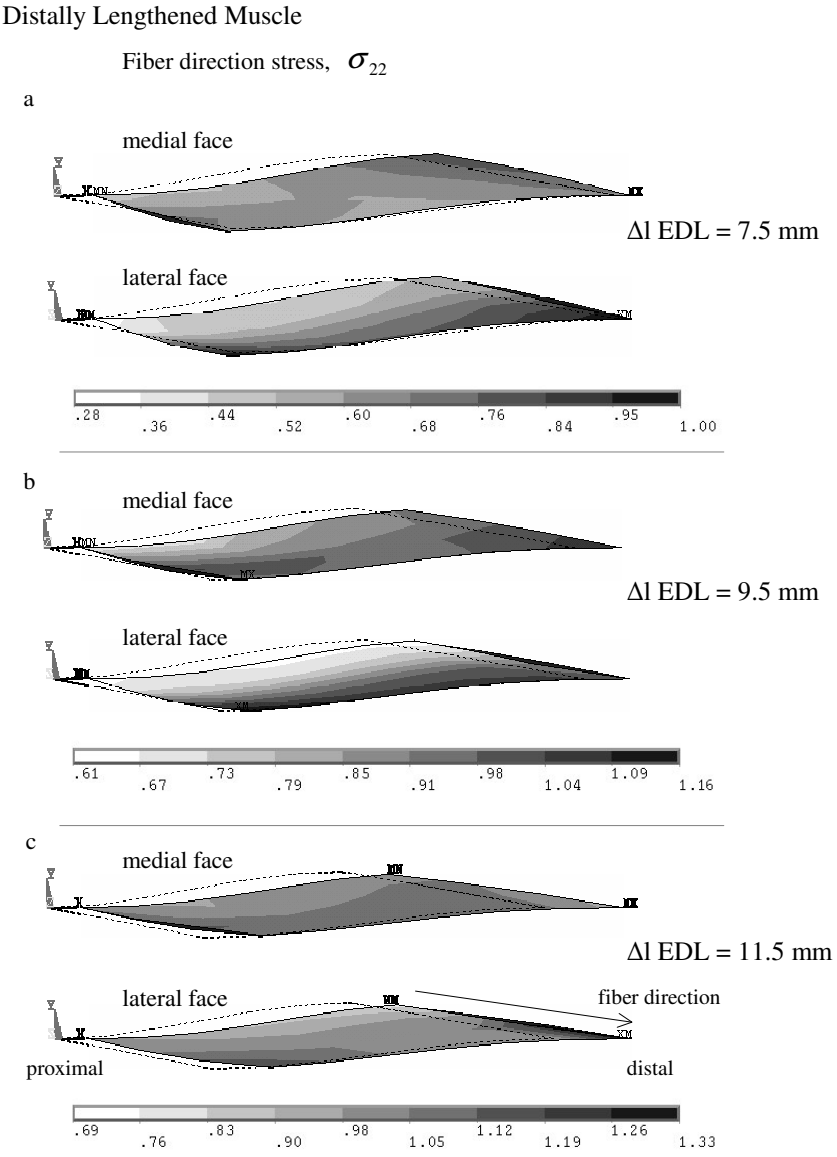

Fig.6. Stress distributions within the fiber mesh of the model of EDL. EDL was modeled with intact inter- and extramuscular connections at selected muscle lengths. The distributions in the fiber direction are shown for (a) Δl EDL = 7.5 mm, (b) Δl EDL = 9.5 mm and (c) Δl EDL = 11.5 mm. Length is expressed as a function of deviation (Δl EDL) from active slack length. Stress distributions in the medial face of this model are shown in the upper panels whereas the lower panels show the distributions in the lateral face. The dotted line contour indicates muscle geometry at the initial length and position. Prior to distal lengthening, the proximal end of the muscle model was moved 2.0 mm in the distal direction, as in the experiment of the present study. The fiber direction as well as the proximal and distal ends of the muscle is shown in the lower panel of part (c).

Parallel distribution of length of sarcomeres among different muscle fibers

For EDL with inter- and extramuscular connections, the differences in local strain between the lateral and medial faces are an additional indication for a sizable parallel distribution of length of sarcomeres. In Fig.5 the mean fiber direction strain distributions for different fascicle groups are shown for the medial and lateral faces of EDL with intact inter- and extramuscular connections, as well as for EDL with extramuscular connections exclusively. The collections of nodes along the longitudinal sides of myofiber elements represent fascicle groups (numbered from 1 to 7, Fig.5a). At all lengths studied, the mean strain values for the medial and lateral faces of EDL with intact inter- and extramuscular connections are clearly different for all fascicles (Fig.5b, c, and d). This is consistent with our hypothesis of increased heterogeneity of mean fiber sarcomere lengths for this muscle, particularly at high lengths. It explains the shift in optimum length to higher lengths (Fig.3).

For EDL with intact inter- and extramuscular connections, Fig.6 shows sizable fiber direction stress distributions. Reflecting the effects of sarcomere length distributions, stress in the fiber mesh is a significant determinant of muscle force exerted at each tendon. Differences in distributions of stress, apparent in the medial face and the lateral face are considerable: much more pronounced distributions of stress between the proximal and distal ends of muscle fibers are found in the lateral face (Fig.6a, b and c). A major model result is that the stress at the distal half of the muscle is higher in both faces. At lower length, the stress at proximal parts of the muscle fibers is as low as 0.28 in the lateral face (Fig.6a lower panel) due to sizably shortened sarcomeres. In contrast, the stress values remain as high as unity at the most distal ends of the muscle fibers, where change of sarcomere length is very limited. At Δl EDL = 9.5 mm, intense distributions of stress are found in the lateral face such that the stress at the distal end of the muscle fibers is nearly twice as high at their proximal end (Fig.6b lower panel). Similarly at high length, the stress at the distal half of the lateral face is higher, locally reaching very high values at the most distal end (Fig.6c lower panel). The higher stress found in the distal half of the muscle fibers is in agreement with the modeled as well as experimental proximo-distal force difference in favor of the distal force. We conclude that the muscle fiber cannot be considered as a unit, exerting equal forces at both ends since myofascial force transmission leads to distributions of force exerted along the muscle fibers.

Restrained Synergists

Fig.2c shows superimposed examples of force time traces for TA+EHL complex at four different EDL lengths.

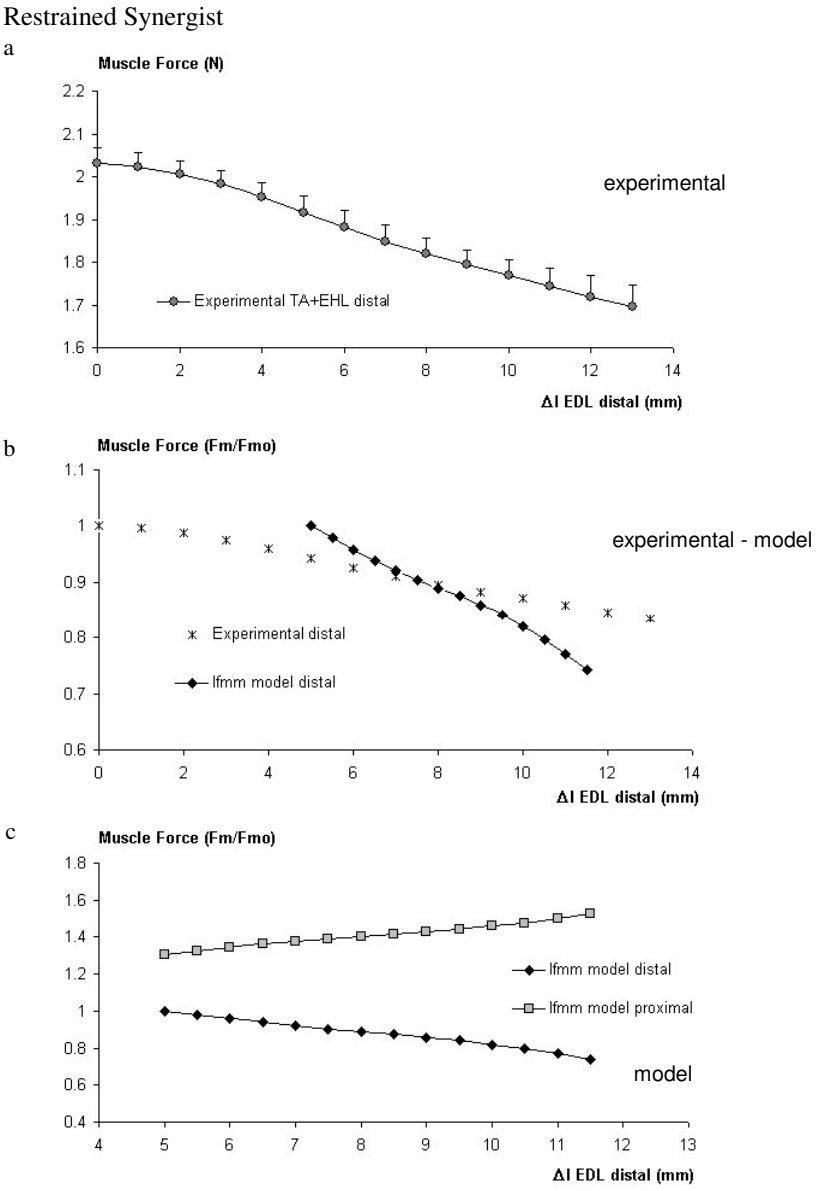

Fig.7. Experimental and modeled total force of the restrained synergists. (a) Experimental total muscle force measured at the tied distal tendons of tibialis anterior and extensor hallucis longus muscles (TA+EHL), shown as a function of EDL length. EDL length is expressed as a function of deviation (Δl EDL) from active slack length. Mean results and standard errors of the mean (n=5) are shown. (b) Experimental and modeled normalized distal forces of the restrained synergists. Both experimental and model data are normalized for their own initial value, i.e. the force exerted distally before EDL muscle was lengthened. (c) Modeled forces of the restrained synergist exerted at the distal and proximal ends. Forces are normalized for maximal calculated distal force, i.e. the force exerted distally before the adjacent muscle was lengthened.

A decrease of maximally 0.34 N, (approximately 17% of the initial force) in TA+EHL complex distal force is shown at higher EDL lengths (Fig.7a). Distal force of the modeled muscle (referred to as restrained synergist) decreases by maximally 20% of its initial force (Fig.7b) for the length range studied for the adjacent muscle. As the modeled synergist does not represent most morphological features of the actual TA+EHL complex, modeled forces identical to the experimental data are not expected. However, results of this model show the principles of the mechanical interaction of adjacent synergistic muscles. Proximal forces calculated for the restrained synergist, which could presently not be measured experimentally because of its attachment to bone deep within the intact anterior crural compartment, increased by maximally 13% (Fig.7c). This leads to an increased proximo-distal force difference. It is concluded that these results are explained solely by the effects of myofascial force transmission, as the altered muscle force is not ascribable to length changes of the whole restrained synergist.

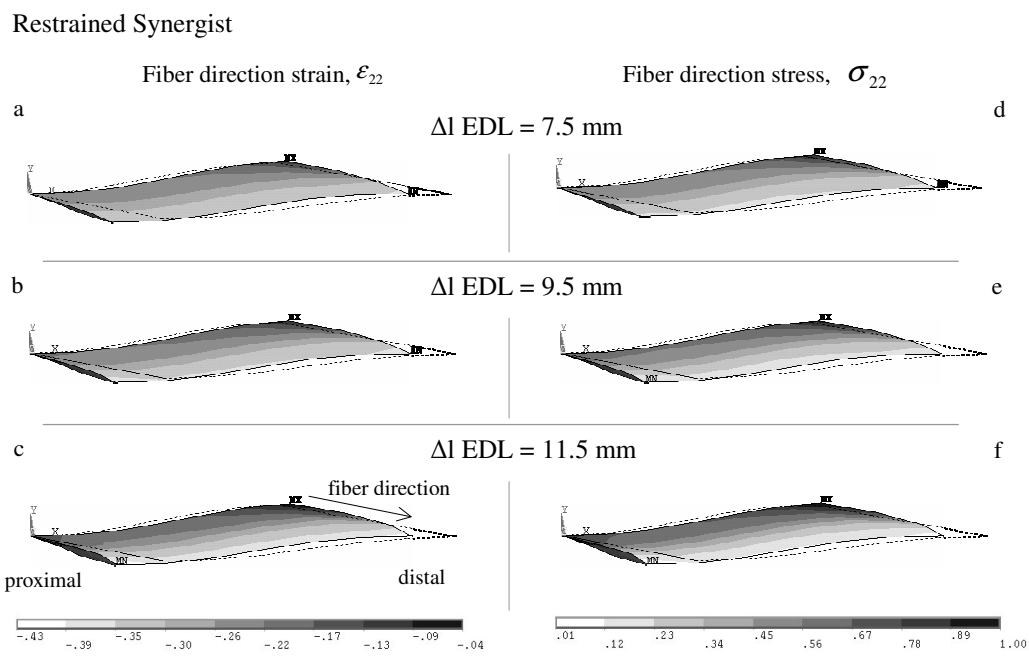

Fig.8. Stress and strain distributions in the fiber mesh of the modeled restrained synergists. Strain distributions (a) (b) and (c), stress distributions (d) (e) and (f) in the fiber direction, are shown at three EDL lengths (Δl EDL = 7.5 mm, Δl EDL = 9.5 mm and Δl EDL = 11.5 mm respectively. Length is expressed as a function of deviation (Δl EDL) from active slack length. The dotted line contour indicates muscle geometry at the initial length and position. The fiber direction as well as the proximal and distal ends of the muscle is shown in part (c) in the lower panel.

Substantial strain and stress distributions were found within the fiber mesh as a function of the length of the adjacent muscle. The sarcomeres located more proximally within muscle fibers are significantly longer than the ones located distally (Fig.8a, b and c). If the adjacent muscle is at higher lengths, this effect is more pronounced. At the highest length studied (Fig.8c), the distally located sarcomeres remained shortened. In contrast, myofascial force transmission causes the length of the more proximally located sarcomeres to be much higher (i.e., strain equals –22 % proximally whereas it is -43 % for the distal sarcomeres). Therefore, very low stress values are calculated for the distal ends of the muscle fibers (close to zero, Fig.8d, e and f). As a function of increased length of the adjacent muscle, stress increases in the proximal but decreases in the distal part of the muscle fibers (Fig.8d, e and f). This is in agreement with the decrease in distal muscle force measured experimentally.

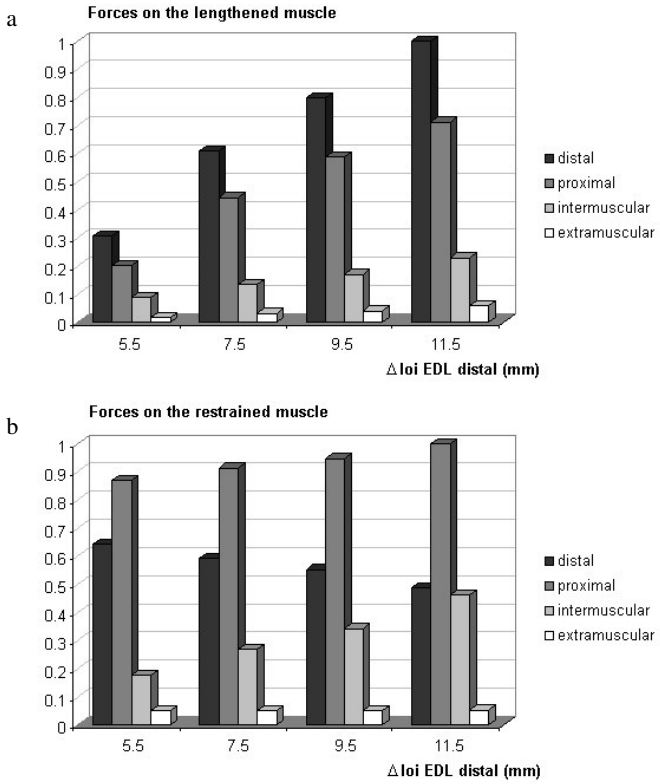

Fig.9. Forces acting on the modeled lengthened muscle and restrained synergist. (a) Forces acting on the lengthened muscle expressed at selected lengths of this muscle (Δl EDL). All forces are normalized for maximum distal force, i.e. the force exerted distally at the highest length studied. Note that both inter- and extramuscular forces are exerted in proximal direction. (b) Forces acting on the restrained synergist expressed at selected lengths of the lengthened muscle (Δl EDL). All forces are normalized for the force exerted proximally by the restrained muscle, at the highest length of the adjacent muscle studied. Note that both inter- and extramuscular forces are exerted in the distal direction. Length is expressed as a function of deviation (Δl EDL) from active slack length.

Inter- and extramuscular forces acting on the modeled muscles

Fig.9 shows the forces acting on the lengthened and restrained synergist models for selected lengths of the lengthened muscle. For the lengthened muscle, the sum of proximal muscle force and the inter- and extramuscular forces (which are also directed proximally), balance the force exerted at the distal end (Fig.9a). The intermuscular force constitutes the major part of the proximo-distal force difference (approximately 80 % of it at the high length). This explains why more pronounced sarcomere length distributions were found in the lateral face compared to the medial face for the lengthened muscle (Fig.4a, b and c). Both inter- and extramuscular forces increase as a function of muscle length. For the length range shown in Fig.9a, the increase in intermuscular force is approximately 39 % and in the extramuscular force is 30 %. The enhanced sarcomere length distributions at higher muscle lengths (Fig.4b and c) are caused by this.

For the restrained synergist, the sum of distal muscle force and the inter- and extramuscular forces (which are directed distally), balance the proximal muscle force (Fig.9b). As the relative position of the whole restrained synergist with respect to the surrounding tissues (mechanical ground in the model) was not altered, the extramuscular force remains nearly constant. However the intermuscular force increases (by approximately 39 % in the length range studied) as the adjacent muscle is lengthened distally. Note that the intermuscular forces acting on both muscles are identical in magnitude but opposite in direction. We conclude that the intermuscular connections play a dominant role in the enhancement of the distributions of strain and stress found in Fig.8.

Discussion

Effects on muscle length force characteristics

A major experimental result of the present study was the significant proximo-distal EDL force difference measured, after distal lengthening. Such force difference was reported recently for rat EDL muscle with intact inter- and extramuscular connections (Huijing and Baan, 2001a; Maas et al., 2001) for proximal lengthening. The proximal EDL force was shown to be higher than the distal force and the force difference was ascribed to the inter- and/or extramuscular myofascial force transmission. Note that, in the present study, after distal lengthening, the sign of the proximo-distal force difference was reversed favoring the distal force. Our model results show that the force difference is caused by the proximally directed forces acting on the muscle via its inter- and extramuscular connections. This confirms the role of myofascial force transmission. Moreover, the results regarding the TA+EHL complex reflect the effects of myofascial force transmission being independent of the muscle length, but not of changes of sarcomere length.

Keeping the intermuscular connections of EDL muscle intact along with its extramuscular connections allowed muscle optimum length to be significantly higher. In recent studies, systematic manipulation of the extra and inter-muscular connective tissue structures of EDL muscle (i.e., isolation of EDL gradually) yielded sizable differences in the length range for proximal lengthening (Huijing and Baan, 2001b; Huijing et al., 2003). These results indicate that the determinants of muscle length range of active force production, are not specific properties of muscle related only to filament overlap in sarcomeres, but are a function of the conditions in which the muscle is operating. Moreover, our present results suggest that insufficient stiffness of the intermuscular connective tissues may be a cause for an overly low muscle length range and therefore, for a limited range of joint motion.

For isolated muscle in situ, a higher length range due to heterogeneous mean fiber sarcomere lengths was argued to cause decreased optimum force (Huijing, 1996). However, the distal optimum force of EDL with intact inter- and extramuscular connections measured in the present study was higher than that of EDL with extramuscular connections exclusively. This is explained by intermuscular myofascial force transmission from TA+EHL muscle complex to EDL muscle. The study on the principles of intermuscular myofascial force transmission exclusively (Yucesoy et al., 2001) showed that the distal force of an intermuscularly connected muscle was significantly higher than that of an isolated muscle after identical distal lengthening. However, the mean fiber stress found in the isolated muscle was well above that of the intermuscularly connected muscle at high lengths. It is concluded that force generated within sarcomeres of one muscle may be exerted at a tendon of an adjacent synergist.

Distribution of sarcomere lengths

The continuity of intramuscular connective tissues to inter- and extramuscular connective tissues is expected to lead to distributions of sarcomere length arranged “in-series” within muscle fibers. The design of lfmm model allows testing this hypothesis (Yucesoy et al., 2002b). The present modeling results indicate substantial serial distributions of length of sarcomeres within muscle fibers. Moreover, significant stress differences at both ends of muscle fibers associated with sarcomere length distributions occur. We conclude that the muscle fiber should not be considered as a unit exerting equal forces at both ends but as a result of inter- and extramuscular myofascial force transmission a row of parallel sarcomeres located within different muscle fibers may be considered as a unit determining force exerted at a tendon.

Serial sarcomere length distribution (Wohlfart et al., 1977; Morgan et al., 2000) and heterogeneity of mean sarcomere length of different fibers (Willems and Huijing, 1994; Huijing, 1998) was shown to extend the muscle length range. Our present results confirm

the earlier findings and show that myofascial force transmission is a major contributor to such heterogeneity.

At high fiber lengths (i.e. with sarcomere active on the descending limb of the force-length curve), Julian and Morgan (1979a; 1979b) showed for isolated single frog muscle fibers, that a sizeable creep phase occurred on activation (i.e., in time a slow rise in force following the initial fast rise). Julian and Morgan reported creep to be positively correlated to variations in sarcomere lengths. Creep occurs as long as the shorter sarcomeres, with greater filament overlap (mainly at the fiber ends) shorten. This length effect increases the force of those sarcomeres until they reach full overlap. The longer sarcomeres arranged in series bear the higher force, because they are active on the eccentric part of their force-velocity curve. Julian and Morgan reported higher creep duration and amplitude at higher muscle fiber lengths.

In agreement with the results of Julian and Morgan, our present experimental results show that in EDL muscle active at higher lengths, creep amplitude increases (Fig.2) and our model results show that more sarcomeres arranged in series within muscle fibers are at different lengths. However, proximally directed inter- and extramuscular forces acting on EDL muscle create very different conditions from those found in isolated muscle fibers: even at higher muscle lengths, rather short sarcomeres active on the ascending limb of their force-length curve are found (Fig.4). Some effects of these different conditions are also apparent from our experimental results. In contrast to results of Julian and Morgan, we found, despite enhanced serial distribution of sarcomere lengths, a decreased duration of creep at higher EDL lengths. We suggest the following explanation: Due to the fact that equilibrium of forces has no longer to be attained for individual sarcomeres, but only for the unit of sarcomeres and their myofascial connections, stable conditions are reached sooner, allowing a more limited role of inter-sarcomere dynamics. In addition, since any lengthening and shortening of sarcomeres arranged in series will be distributed over a much higher number of sarcomeres, stable equilibrium of force can be attained faster.

We conclude that a major difference between the conditions of single muscle fibers and muscle fibers within their in vivo context is that, trough myofascial force transmission, the length of sarcomeres comprising a muscle fiber depend not only on interactions with sarcomeres arranged in series within the same fiber, but also on the lengths of adjacent myofascial structures and even on sarcomeres within the neighboring muscle fibers. Therefore, we hypothesize that myofascial force transmission, being the major cause of enhanced serial sarcomere length distributions, is likely to alter the role of inter-sarcomere dynamics in whole muscle.

However, it should be noted that, as our modeling approach was quasi-static, inter-sarcomere dynamics should be incorporated in the model before we are able to test the dominance of the role of myofascial force transmission on inter-sarcomere dynamics.

Interaction of inter- and extramuscular myofascial force transmission

In recent experiments, no significant effects of proximal EDL lengthening on distal force exerted by the restrained TA+EHL muscle complex could be shown (Huijing and Baan, 2001a). Extramuscular force transmission was concluded to dominate the myofascial effects suggesting that intermuscular force transmission remains close to a net value of zero. In contrast, the present modeling study showed that the proportion of extramuscular force in proximo-distal force difference is quite low (maximally 20%, Fig.9a). This suggests that the role of extramuscular force transmission may have been over emphasized in that study. However, proximal or distal lengthening could impose different effects on the interaction between inter- and extramuscular myofascial force transmission, which determines their relative proportions. This should be investigated.

Limitations and implications of this study

A significant determinant of the myofascial effects seems to be the relative position of a muscle with respect to its surroundings. However, in vivo, not only the muscle studied, but also the surrounding muscles may change length with joint motion. Differences in moment arm will contribute to relative movement. For bi- or polyarticular muscle, relative movement of muscles will be much larger. If myofascial force transmission would be found for antagonists, effects larger than described here may be found. Therefore, studies aiming at identification of the relative positions of in vivo muscles with respect to their surroundings, for given tasks are indicated.

The experimental conditions of the present study included maximal activation whereas this is hardly the case in vivo. The mechanical interaction between adjacent muscles and other structures strongly depends on the stiffness of the muscular tissues. Maximally activated muscle is stiffer than sub-maximally activated muscle. Therefore, level of activation is expected to significantly affect myofascial force transmission. This needs to be studied in the future.

Using linearly stiff spring elements to represent the inter- and extramuscular connections must be considered as a significant simplification. Such connective tissues feature non-linear length-force characteristics. The modeled effects of myofascial force transmission are expected to be more pronounced at lower lengths (because of a higher stiffness than reality), and less pronounced at higher lengths (because of a lower stiffness than reality). In future modeling, possible nonlinear behavior of the linking elements should be accounted for.

A recent study on unintended force exertion showed that production of isometric force with one, two, or three fingers caused the other fingers of the hand also to exert a certain force (Li et al., 2000). Our present results could be extrapolated to explain those findings. Moreover a possible role of myofascial effects on such pathologies as musicians arm and repetitive strain injury are indicated. Deformations due to length changes of only one

muscle, or even only a part of a muscle while all the surrounding muscles are restrained (as in the precision task of clicking the mouse button) may contribute to such conditions.

In conclusion, inter- and extramuscular myofascial force transmission has major effects on skeletal muscle mechanics. These effects include significant changes in the length-force characteristics such as proximo-distal force differences, altered muscle length range of active force production and higher muscle optimum force as a result of transmission of force from adjacent muscles. Myofascial interaction of a muscle with its surrounding structures and muscles causes substantial distributions of sarcomere lengths both for sarcomeres arranged in-series within myofibers and among myofibers arranged in-parallel. For muscle with intact inter- and extramuscular connections, serial sarcomere length distributions lead to unequal forces exerted at both ends of muscle fibers. This is consistent with the unequal forces exerted at proximal and distal tendons of the muscle. Both the parallel distributions and the serial distributions affect length range of force production and thus force exerted at different lengths.

References

Berthier, C. and Blaineau, S., 1997. Supramolecular organization of the subsarcolemmal cytoskeleton of adult skeletal muscle fibers. A review. Biology of the Cell 89, 413-434.

Danowski, B. A., Imanaka-Yoshida, K., Sanger, J. M. and Sanger, J. W., 1992. Costameres are sites of force transmission to the substratum in adult rat cardiomyocytes. The Journal of Cell Biology 118, 1411-1420.

Hijikata, T., Wakisaka, H. and Niida, S., 1993. Functional combination of tapering profiles and overlapping arrangements in nonspanning skeletal muscle fibers terminating intrafascicularly. Anatomical Record 236, 602-610.

Huijing, P. A., 1996. Important experimental factors for skeletal muscle modeling: non-linear changes of muscle length force characteristics as a function of degree of activity. European Journal of Morphology 34, 47-54.

Huijing, P. A., 1998. Muscle the motor of movement: Properties in function, experiment and modelling. Journal of Electromyography and Kinesiology 8, 61-77.

Huijing, P. A., 1999a. Muscle as a collagen fiber reinforced composite material: Force transmission in muscle and whole limbs. Journal of Biomechanics 32, 329-345.

Huijing, P. A., 1999b. Muscular force transmission: A unified, dual or multiple sytem? A review and some explorative experimental results. Archives of Physiology and Biochemistry 170, 292-311.

Huijing, P. A. and Baan, G. C., 2001a. Extramuscular myofascial force transmission within the rat anterior tibial compartment: Proximo-distal differences in muscle force. Acta Physiologica Scandinavica 173, 1-15.

Huijing, P. A. and Baan, G. C., 2001b. Myofascial force transmission causes interaction between adjacent muscles and connective tissue: Effects of blunt dissection and compartmental fasciotomy on length force characteristics of rat extensor digitorum longus muscle. Archives of Physiology and Biochemistry 109, 97-109.

Huijing, P. A., Baan, G. C. and Rebel, G., 1998. Non myo-tendinous force transmission in rat extensor digitorum longus muscle. Journal of Experimental Biology 201, 682-691.

Huijing, P. A., Maas, H. and Baan, G. C., 2003. Compartmental fasciotomy and isolating a muscle from neighboring muscles interfere with extramuscular myofascial force transmission within the rat anterior tibial compartment. Journal of Morphology 256, 306-321.

Julian, F. J. and Morgan, D. L., 1979a. The effect on tension of non-uniform distribution of length changes applied to frog muscle fibres. Journal of Physiology 293, 379-392.

Julian, F. J. and Morgan, D. L., 1979b. Intersarcomere dynamics during fixed-end tetanic contractions of frog muscle fibres. Journal of Physiology 293, 365-378.

Li, Z. M., Zatsiorsky, V. M. and Latash, M. L., 2000. Contribution of the extrinsic and intrinsic hand muscles to the moments in finger joints. Clinical Biomechanics 15, 203-211.

Maas, H., Baan, G. C. and Huijing, P. A., 2001. Intermuscular interaction via myofascial force transmission: effects of tibialis anterior and extensor hallucis longus length on force transmission from rat extensor digitorum longus muscle. Journal of Biomechanics 34, 927-940.

Morgan, D. L., Whitehead, N. P., Wise, A. K., Gregory, J. E. and Proske, U., 2000. Tension changes in the cat soleus muscle following slow stretch or shortening of the contracting muscle. Journal of Physiology 522 Pt 3, 503-513.

Neter, J., M.H., K., Nachtsheim, C. J. and Wasserman, W. (1996). Applied Linear Statistical Models. Irwin, Homewood, IL.

Street, S. F., 1983. Lateral transmission of tension in frog myofibers: a myofibrillar network and transverse cytoskeletal connections are possible transmitters. Journal of Cellular Physiology 114, 346-364.

Trotter, J. A. and Purslow, P. P., 1992. Functional morphology of the endomysium in series fibered muscles. Journal of Morphology 212, 109-122.

Willems, M. E. and Huijing, P. A., 1994. Heterogeneity of mean sarcomere length in different fibres: effects on length range of active force production in rat muscle. European Journal of Applied Physiology and Occupational Physiology 68, 489-496.

Wohlfart, B., Grimm, A. F. and Edman, K. A., 1977. Relationship between sarcomere length and active force in rabbit papillary muscle. Acta Physiologica Scandinavica 101, 155-164.

Yucesoy, C. A., Koopman, H. J. F. M., Guus, C. B., Grootenboer, H. J. and Huijing, P. A., 2002a. Extramuscular myofascial force transmission: Experiments and finite element modeling. Archives of Physiology and Biochemistry, in revision.

Yucesoy, C. A., Koopman, H. J. F. M., Huijing, P. A. and Grootenboer, H. J. (2001). Finite element modeling of intermuscular interactions and myofascial force transmission. 23rd Annual International Conference of the IEEE Engineering in Medicine and Biology Society, Istanbul, Turkey.

Yucesoy, C. A., Koopman, H. J. F. M., Huijing, P. A. and Grootenboer, H. J., 2002b. Three-dimensional finite element modeling of skeletal muscle using a two-domain approach: Linked fiber-matrix mesh model. Journal of Biomechanics 35, 1253-1262.

Chapter 6

Finite element modeling of relative position of a muscle:
Effects of extramuscular myofascial force transmission

Abstract

In some recent studies it has been shown that inter- and extramuscular myofascial force transmission affects the length-force characteristics of rat extensor digitorium longus (EDL) muscle significantly after distal or proximal lengthening. This suggested that the relative position of a muscle with respect to its surrounding connective tissues is a co-determinant of muscle force in addition to muscle length. In the present work, the studied muscle is kept at constant length while its relative position is altered. This allowed assessment of the effects of extramuscular myofascial force transmission on muscular mechanics exclusively.

The modeled muscle kept at constant high as well as low length showed that forces exerted at distal and proximal tendons are not equal at almost all muscle relative positions. The proximo-distal force difference was enhanced as the muscle was repositioned away from its reference position. This confirmed the role of relative position of a muscle as a co-determinant of muscle force. At higher muscle lengths, our results showed that extramuscular myofascial force transmission leads to significant distributions of length sarcomeres arranged in series within muscle fibers. The force transmitted by extracellular matrix domain is a sizable part of muscle total force. At lower muscle lengths distributions of sarcomere lengths is relatively limited indicating that intramuscular connective tissues are bearing the extramuscular force. The interaction between the intra- and extramuscular connective tissues determines the proximo-distal muscle total force differences. It is concluded that extramuscular myofascial force transmission has substantial effects on muscular mechanics

Introduction

In addition to myotendinous force transmission, the multimolecular complexes (Berthier and Blaineau, 1997) connecting sarcomeres to elements of the subsarcolemmal cytoskeleton and from there to trans-sarcolemmal molecules provide a pathway of force transmission onto the extracellular matrix. This was shown to be a mechanism of force transmission intramuscularly (Street, 1983; Danowski et al., 1992; Trotter and Purslow, 1992; Hijikata et al., 1993; Huijing et al., 1998; Huijing, 1999a; Yucesoy et al., 2002b), and was referred to as myofascial force transmission (Huijing, 1999a). Moreover, recent studies on muscles of the anterior tibial compartment of the rat showed the significant role of myofascial force transmission also inter- and extramuscularly (Huijing and Baan, 2001a; Huijing and Baan, 2001b; Maas et al., 2001; Huijing et al., 2003; Yucesoy et al., 2002a). Those studies involved lengthening of extensor digitorium longus (EDL) muscle where as the surrounding non-muscular structures exclusively, or together with the other muscles of the compartment, were kept in their original positions. The results, which showed the effects of extramuscular myofascial force transmission on muscle length-force characteristics, indicated the role of muscle relative position. Therefore, we hypothesized that the relative position of a muscle with respect to its surrounding connective tissues is a co-determinant of muscle force in addition to muscle length. Due to the continuity of intramuscular connective tissues to extramuscular connective tissues, we also hypothesized that myofascial force transmission may significantly affect muscular mechanics. We aimed at investigating the role of the extracellular matrix as well.

The goal of the present study is to test these hypotheses using a finite element muscle model (Yucesoy et al., 2002b) that was designed for such analyses. The modeled muscle is kept at constant length while its relative position is altered. This allows studying the effects of extramuscular myofascial force transmission on muscular mechanics exclusively.

Methods

Description of the "linked fiber matrix mesh model"

A 3D-finite element muscle model (linked fiber-matrix mesh model: lfmm model) with a two-domain approach was developed (Yucesoy et al., 2002b). The lfmm model consists of two meshes occupying the same space that are linked elastically. The two meshes represent the extracellular matrix domain (matrix mesh) and intracellular domain (fiber mesh). The two meshes are built using the self-programmed "myofiber" or "extracellular matrix" elements (Yucesoy et al., 2002b) that are introduced as user defined elements into the finite element program ANSYS 5.7.1. The elements have eight nodes, linear interpolation functions and a large deformation analysis is employed. A 3D local coordinate system representing the fiber, cross-fiber (normal to the fiber direction), and thickness directions is used. For the myofiber element, the total stress that acts exclusively in the local fiber

direction is the sum of the active stress of the contractile elements and the stress due to intracellular passive tension. It is assumed that, at initial muscle length and in the passive state, the sarcomeres arranged in series within muscle fibers have identical lengths and material properties. The extracellular matrix element incorporates a strain energy density function that accounts for the non-linear and anisotropic material properties and the constancy of muscle volume.

Within the biological context, one muscle element is defined to represent a segment of a bundle of muscle fibers with identical material properties, its connective tissues and the links between them. This is realized as a linked system of extracellular matrix and myofiber elements. Both matrix and fiber meshes are connected rigidly to single layers of elements forming the muscles' proximal and distal aponeurosis. To represent the aponeuroses, a standard 3D, 8-node element HYPER58, from the element library of ANSYS 5.7.1 was used. This element is a hyperelastic element for which the strain energy density function is defined using the Mooney-Rivlin material law. For the elastic links between the two meshes, which represent the trans-sarcolemmal attachments of the cytoskeleton and extracellular matrix, another standard element, COMBIN39 was used. This is a 2-node spring element, which is set to be uniaxial and have linear stiffness characteristics.

The geometry of the model (Fig.1) is defined by the contour of a longitudinal slice at the middle of the isolated rat EDL muscle belly. Three muscle elements in series and six in parallel fill this slice. Therefore any collection of three muscle elements arranged in series represents a big muscle fascicle. All aponeurosis elements have identical mechanical properties but using a variable thickness in the fiber-cross fiber plane, the increasing cross-sectional area of the aponeurosis toward the tendon (Zuurbier et al., 1994) is accounted for.

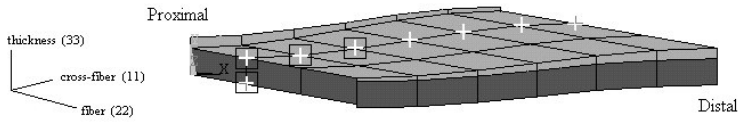

Fig.1. The geometry of the muscle model. The geometry is defined by the contour of a longitudinal slice of the rat extensor digitorum longus (EDL) muscle belly. The muscle model is composed of three in series and six in parallel muscle elements. A 3D local coordinate system is used for the analysis and presentation of the results. At the nodes indicated with a white "+", the extramuscular connections are made and the ones marked also with a black square are stiffer as they represent the connective tissues supporting the neurovascular tract to the EDL muscle.

Model of EDL with extramuscular connections

In the present study, the lfmm model was extended to include extramuscular connections of EDL muscle. An extramuscular sheet of connective tissue connects EDL all along the

muscle to the tibia, part of interosseal membrane and anterior intermuscular septum (for images see Huijing and Baan, 2001a; Maas et al., 2001). This sheet defines the anatomical path of the extramuscular myofascial force transmission. In our previous experimental study (Yucesoy et al., 2002a), the locations of the extramuscular connections of EDL muscle were determined to be at one-third of the fascicle length from the most proximal side of each muscle fascicle. In that study it was also shown that the extramuscular connective tissues supporting the neurovascular tract to the EDL muscle, which consists of less than the proximal half of the connective tissue structure, are much stiffer than the rest of the connective tissues. Using spring elements, these connections were modeled by linking a set of nodes of the matrix mesh (Fig. 1) to a set of fixed points, representing the "mechanical ground". The corresponding fixed points of the mechanical ground and the nodes of the model were at identical locations initially (i.e., muscle length = 28.7 mm, and before moving any of the tendon ends). The extramuscular links were defined to have linear stiffness. To represent these links, the spring element COMBIN39 was used which was set to be uniaxial. The higher stiffness of the connective tissues supporting the neurovascular tract to the EDL muscle is taken into account by making the three most proximal links stiffer than remainder. This model is referred to as model of EDL with extramuscular connections.

The effects of relative position of EDL muscle with respect to its surrounding tissues were tested at two muscle lengths. (1) At high length, which is 2.0 mm over muscle optimum length (lo+2.0 mm). (2) At low length, which is 5.0 mm below muscle optimum length (lo-5.0 mm). In both cases, muscle length was kept constant throughout the analysis. However, the relative position of the muscle with respect to the mechanical ground was altered. The most distal relative position of the muscle belly was referred to as "0 mm". The effects of changes of relative position were assessed by moving both distal and proximal tendon ends of the muscle model by 1 mm increments in the proximal direction at a time.

In order to identify the contributions of the fiber and matrix meshes of the modeled EDL muscle with extramuscular connections to muscle total force, the forces exerted onto the proximal and distal aponeuroses acting in the direction of the line of pull of the muscle were studied. The force exerted by the intracellular domain will be referred to as "fiber mesh force", the contribution of the extracellular matrix domain is referred to as "matrix mesh force" and the resultant force acting on the proximal and distal aponeuroses will be referred to as "aponeurosis force". Note that the aponeurosis force is the sum of fiber mesh and matrix mesh forces.

Model of isolated EDL

A model representing EDL muscle which is completely isolated from the surrounding connective tissues was used to identify effects on muscular mechanics ascribable to muscle geometry exclusively. This model was also studied at the same muscle lengths (i.e. lo+2.0

mm and lo-5.0 mm). Note that muscle optimum length (lo) used as reference length in the present study, represents the optimum length belonging to the model of isolated EDL (i.e., muscle length = 28.7 mm).

Results

Muscle kept at high length (lo+2.0 mm)

Total muscle force calculated using model of EDL with extramuscular connections is compared to experimental data (Maas et al., 2002b), as a function of muscles' relative position for EDL muscle kept at lo+2.0 mm in Fig.2. For most muscle relative positions, both experimental and modeled forces show that for EDL with intact extramuscular connections, forces exerted at distal and proximal tendons are not equal, except at one particular position. Experimental data shows that, at the most distal relative position studied (ΔEDL muscle relative position = 0 mm), distal total EDL force is significantly higher (approximately 46%) than proximal total force. As the muscle is repositioned in the proximal direction, the force exerted at the distal tendon decreases where as the force exerted proximally increases. At the most proximal relative position studied (ΔEDL muscle relative position = 9 mm), total proximal EDL force is higher than distal force by approximately 4%.

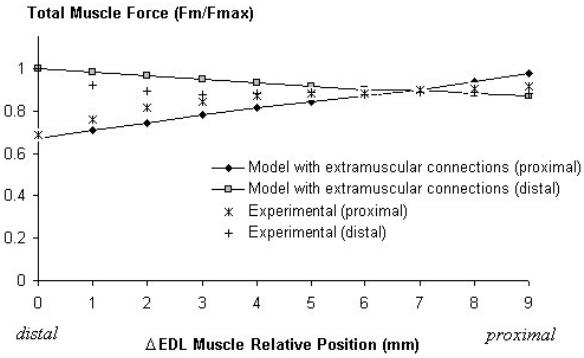

Fig.2. Effects of muscle relative position on muscle total force at high muscle length. The modeled forces of EDL muscle with intact extramuscular connections are compared to experimental data (Maas et al., 2002b). Both experimental and modeled forces are normalized for maximum value of muscle total force. The muscle length is kept constant at lo+2.0 mm. 0 mm represents the most distal and 9 mm represents the most proximal relative position of the muscle belly studied.

The modeled forces (using the model of EDL with extramuscular connections) agree reasonably well with the experimental data. However, in contrast to the experimental data, the modeled forces show a linear behavior as a function of muscle relative position. The linear stiffness of the extramuscular linking elements is likely to be the reason for this. In

addition, the modeled proximo-distal force difference at the most proximal relative position studied is higher than the experimentally measured force difference. We concluded that changes in the relative position of EDL muscle with respect to its surrounding connective tissues have significant effects on muscle force at higher muscle lengths and is therefore a co-determinant of muscle force.

The relative position effects on muscle force exerted at the proximal and distal tendons indicate a strong effect of extramuscular myofascial force transmission on intramuscular mechanics. We hypothesize that such effects can lead to distribution of lengths of sarcomeres arranged in series within muscle fibers. The results of our model are used to test this hypothesis. Local fiber direction strain, as a measure of change of length, reflects the lengthening (positive strain values) or shortening (negative strain values) of sarcomeres. Therefore, strain distributions within the fiber mesh of the lfmm model represent distribution of lengths of sarcomeres. Note that zero strain in the model represents the undeformed state of sarcomeres (i.e., sarcomere length ≅ 2.5 μm) in the passive condition.

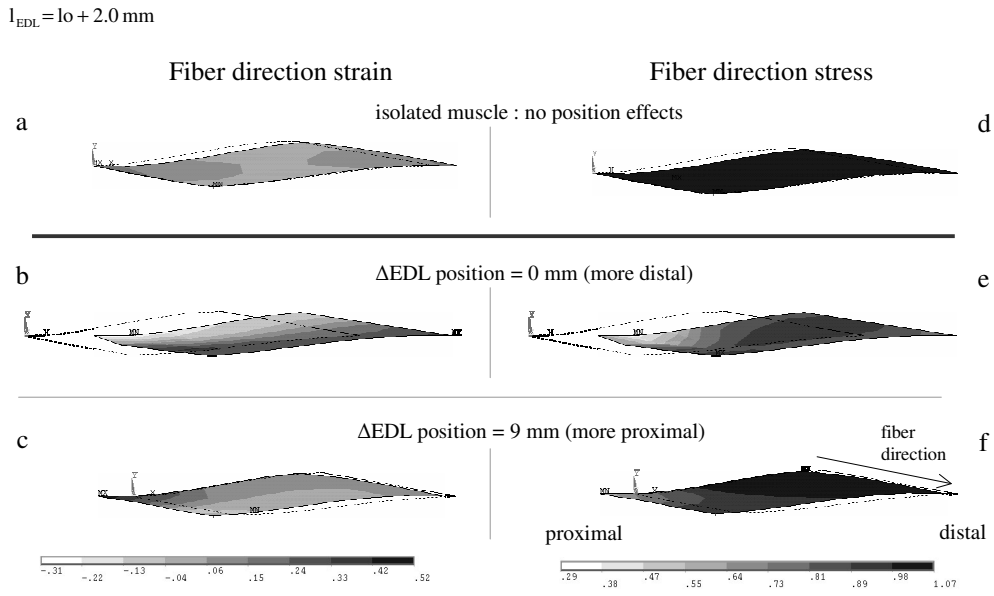

Fig.3. Effect of muscle relative position on strain and stress distributions for the fiber mesh at high muscle length. Strain distributions in the fiber (22) direction are shown for (a) the model of isolated EDL and, for the model of EDL with extramuscular connections at (b) the most distal (0 mm) and (c) the most proximal (9 mm) muscle relative positions studied. Stress distributions in the fiber (22) direction are shown for (d) the model of isolated EDL and, for the model of EDL with extramuscular connections at (e) the most distal (0 mm) and (f) the most proximal (9 mm) muscle relative positions studied. The muscle length is kept constant at lo+2.0 mm. The dotted line contour indicates muscle geometry at the initial length and muscle relative position. The fiber direction as well as the proximal and distal ends of the muscle is shown in (f).

The strain distribution within the fiber mesh of the model of the isolated EDL is highly uniform (Fig.3a). Small values of positive strain are found throughout the intracellular domain indicating lengthening of sarcomeres, which is a consequence of the higher length of the muscle belly. In contrast, for a muscle embedded in its natural surrounding of connective tissues, strain distributions for the most distal (0 mm) and proximal (9 mm) EDL relative positions are substantial. At the most distal relative position (Fig.3b) the sarcomeres located at the proximal ends of muscle fibers are shortened (up to 31%), whereas the ones located at the distal ends of muscle fibers are lengthened (maximally 51%). This effect is reversed for the most proximal relative position (Fig.3c) such that the proximally located sarcomeres are lengthened and the distally located ones are shortened. These results show that at high lengths, the altered relative position of a muscle, exclusively due to extramuscular myofascial force transmission leads to significant distribution of lengths of sarcomeres arranged in series within muscle fibers.

Reflecting the effects of sarcomere length distributions, stress in the fiber mesh is an important determinant of muscle force exerted at each tendon. At high muscle lengths, the stress approximates unity throughout the fiber mesh of the model of isolated EDL (Fig.3d). However, the relative position effects are highly dominant at the most distal relative position studied (Fig.3e). The stress values found at the proximal ends of muscle fibers are much lower than unity (especially for the most proximal fibers stress is as low as 0.29). For the distal ends of muscle fibers, the stress calculated approximates 0.80. For the most proximal relative position studied (Fig.3f), effects of extramuscular myofascial force transmission are seen mainly for the proximally located muscle fibers (i.e. where the stiffer extramuscular links, representing the connective tissues of the neuromuscular tract are). In this part of the muscle belly, the stress values are lower at the proximal ends of muscle fibers (minimally 0.47) and higher at the distal ends of muscle fibers (maximally 0.89). These results yield two major conclusions. (1) Extramuscular myofascial force transmission prevents muscle fibers to function as units exerting equal forces at both ends. (2) The contribution of the intracellular domain to muscle total force exerted at the tendons should be smaller for EDL with extramuscular connections compared to that of the isolated muscle. Therefore, we hypothesize that the extracellular matrix domain plays a significant role in force transmission.

In order to test this hypothesis, the contributions of the fiber and matrix meshes of the modeled muscles to muscle total force are analyzed. Fig.4 shows the aponeurosis, fiber mesh and matrix mesh forces found at the ends of groups of fascicles. The collections of nodes along the longitudinal sides of muscle elements represent different fascicle groups within the muscle belly (in Fig.4a they are numbered from 1 to 7). All forces shown in Fig.4 are acting in the direction of the line of pull of the muscle and are normalized for muscle total distal force at 0 mm. Note the sign convention: positive forces are acting in the

proximal, and negative forces are acting in the distal direction. Fig.4b, c and d show the distribution of the aponeurosis, fiber mesh and matrix mesh forces respectively as a function of fascicle position within the muscle belly. At higher muscle lengths, all aponeurosis and fiber mesh forces found at the proximal ends of muscle fibers are in the proximal direction (positive forces) and similarly, all aponeurosis and fiber mesh forces found at the distal ends of muscle fibers are in the distal direction (negative forces, Fig.4b and c). Fig.4c shows that the fiber mesh forces found at the proximal and distal ends of different fascicles are not the same, indicating that extramuscular myofascial force transmission leads to unequal forces to be exerted at both ends of muscle fibers. Unlike the fiber mesh forces, the matrix mesh forces are distributed rather non-uniformly (Fig.4c).

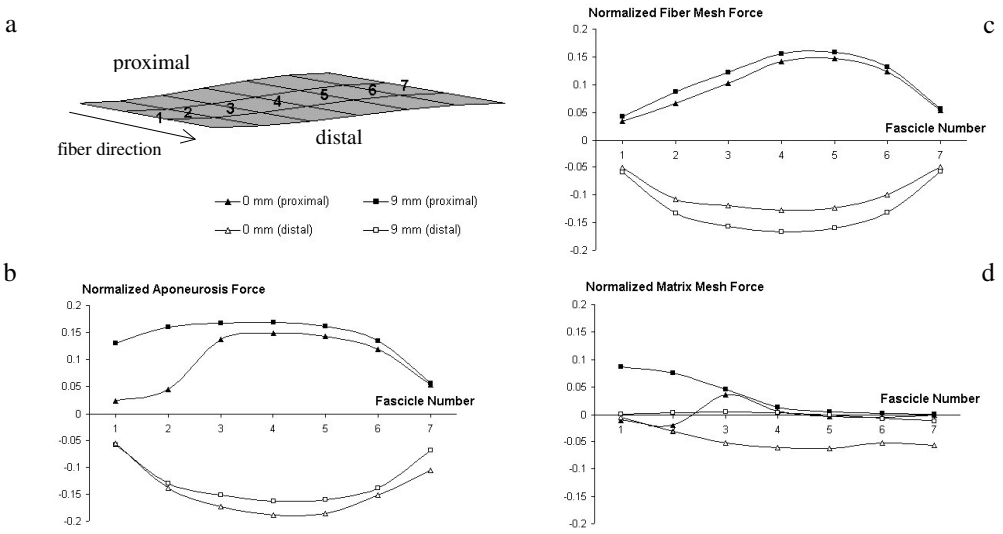

Fig.4. Forces at the fascicle ends for high muscle length. (a) The forces transmitted onto the proximal and distal aponeuroses were calculated for the nodes at which the fiber and matrix meshes are connected to the aponeurosis elements. The collections of nodes along the longitudinal sides of myofiber or extracellular matrix elements represent different fascicle groups within the muscle belly. Each fascicle is indicated by a number from 1 to 7. (b) The aponeurosis force which is the sum of the forces exerted onto the aponeuroses by the fiber and matrix meshes (c) the fiber mesh force and (d) the matrix mesh force are plotted as a function of fascicle number. All forces are normalized for the maximal muscle total force (i.e. muscle total distal force at the most distal muscle relative position, 0 mm).

Table.1 shows the absolute value of summed aponeurosis, fiber mesh and matrix mesh forces in the distal and proximal directions. At the most distal muscle relative position (0 mm), the summed fiber mesh distal force is very close to the summed fiber mesh proximal force (Table.1). However, comparing the summed matrix mesh distal force to summed matrix mesh proximal force shows a large difference (Table.1). It is concluded that the

proximo-distal muscle total force difference at this relative position is almost exclusively caused by the force transmitted by the matrix mesh. At the most proximal muscle relative position (9 mm), the proximo-distal muscle total force difference is in favor of the proximal force. In contrast, the difference between the summed fiber mesh distal force and summed fiber mesh proximal force favors the distal force (Table.1). However, the matrix mesh forces show a sizable difference (Table.1), which leads to the significantly higher muscle total proximal force shown in Fig.2 for this relative position. These results indicate the major role of the extracellular matrix domain in force transmission for a muscle with intact extramuscular connections at higher muscle lengths and confirm our earlier hypothesis.

Table.1

Muscle relative position	0 mm		9 mm	
lo+2.0 mm	Proximal	Distal	Proximal	Distal
Σ Normalized* fiber mesh force	0.66	-0.68	0.75	-0.86
Σ Normalized* matrix mesh force	0.01	-0.32	0.23	-0.01
Σ Normalized* aponeurosis force	0.67	-1.00	0.98	-0.87

* Normalized for muscle total distal force at the most distal muscle relative position, 0 mm

Muscle kept at low length (lo-5.0 mm)

Fig.5 shows a comparison of the total muscle force calculated using model of EDL with extramuscular connections to experimental data (Maas et al., 2002b), as a function of muscles' relative position for EDL muscle kept at lo-5.0 mm. Except at one particular position, both experimental and modeled forces show that, for EDL with intact extramuscular connections, forces exerted at distal and proximal tendons are not equal. Experimental data shows that, at the most distal relative position studied (ΔEDL muscle relative position = 0 mm), total EDL distal force is significantly higher (approximately 54%) than total proximal force. As the muscle is repositioned in the proximal direction, the force exerted at the distal tendon decreases where as the force exerted proximally increases. At the most proximal relative position studied (ΔEDL muscle relative position = 7 mm), EDL total proximal force is higher than distal force by nearly 31%. The modeled forces agree reasonably well with the experimental data. The linear stiffness of the extramuscular linking elements is likely to be the cause of the linear behavior of the modeled forces plotted as a faction of muscle relative position, which behavior is more nonlinear for the experimental data. We conclude that also at lower muscle lengths, the effects of changes in the relative position of EDL muscle with respect to its surrounding connective tissues on muscle force are substantial and even more pronounced than at high muscle lengths.

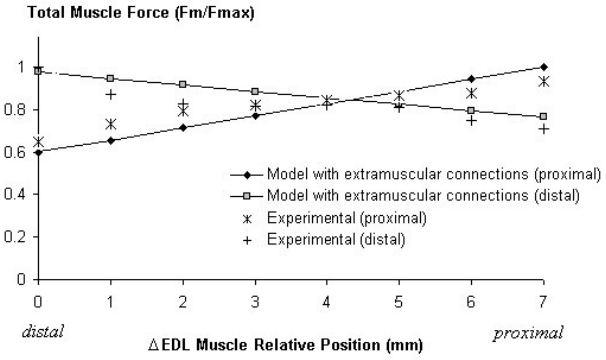

Fig.5. Effects of muscle relative position on muscle total force at low muscle length. The modeled forces of EDL muscle with intact extramuscular connections are compared to experimental data (Maas et al., 2002b). Both experimental and modeled forces are normalized for maximum value of muscle total force. The muscle length is kept constant at lo-5.0 mm. 0 mm represents the most distal and 7 mm represents the most proximal relative position of the muscle belly studied.

Despite the more pronounced relative position effects on muscle total force, the fiber direction strain and stress distributions are relatively limited for EDL with extramuscular connections and not very different from the isolated EDL (Fig.6). For the more proximal muscle fibers, the strain distribution within the fiber mesh of the model of isolated EDL (Fig.6a) shows more shortened sarcomeres at the proximal ends of fibers (maximally 45% shortened) than the ones located at the distal ends (minimally 28% shortened). In the middle part of the muscle belly a uniform shortening (mean 36%) is found, i.e. almost no distribution of length of sarcomeres in that part. The most distal part of the muscle belly also shows a certain distribution: sarcomeres at the proximal ends of muscle fibers are shortened less than the ones located at the distal ends. This becomes more pronounced toward the most distal muscle fiber. The most distal relative position (0 mm) studied leads to minor changes in strain distribution. The section, which shows no distribution, is shifted more to the distal part of the muscle belly (Fig.6b). The sarcomere length distribution in the more proximal part becomes slightly more pronounced. More effects of changing relative position are found for the most proximal EDL relative position (7 mm): the middle part of the muscle belly, which showed no sarcomere length distribution at the most distal relative position as well as for isolated EDL is reduced to a very small fascicle only (Fig.6c).

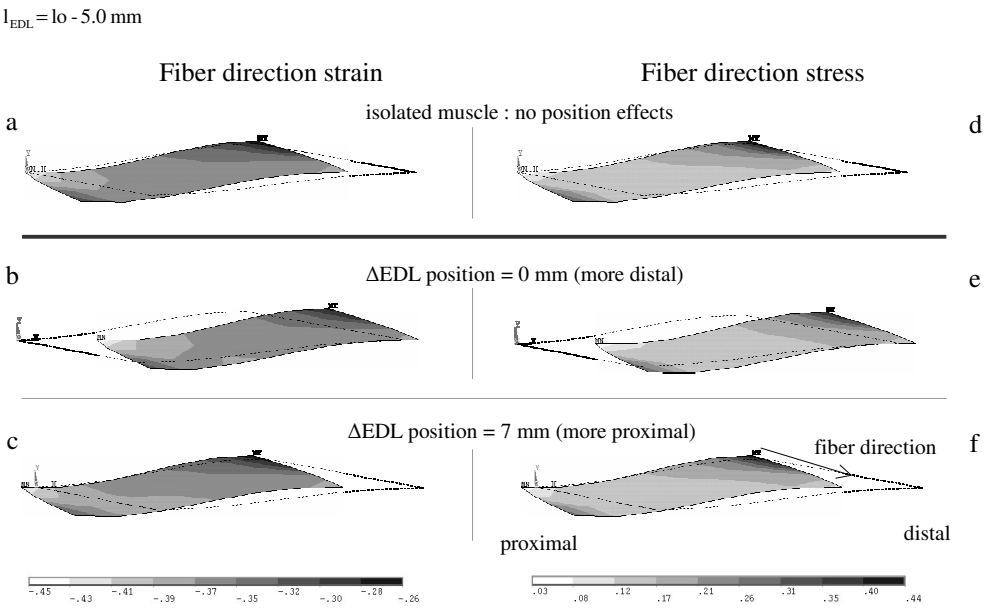

Fig.6. Effect of muscle relative position on strain and stress distributions for the fiber mesh at low muscle length. Strain distributions in the fiber (22) direction are shown for (a) the model of isolated EDL and, for the model of EDL with extramuscular connections at (b) the most distal (0 mm) and (c) the most proximal (7 mm) muscle relative positions studied. Stress distributions in the fiber (22) direction are shown for (d) the model of isolated EDL and, for the model of EDL with extramuscular connections at (e) the most distal (0 mm) and (f) the most proximal (7 mm) muscle relative positions studied. The muscle length is kept constant at lo-5.0 mm. The dotted line contour indicates muscle geometry at the initial length and muscle relative position. The fiber direction as well as the proximal and distal ends of the muscle is shown in (f).

The distribution of stress within the fiber mesh of the model of isolated EDL (Fig.6d) is similar to that of model of EDL with extramuscular connections studied at 0 mm (Fig.6e) and 7 mm (Fig.6f) relative positions except for minor differences. It is concluded that at lower muscle lengths after manipulation of the muscle relative position, the myofascial effects on sarcomere length distributions are less compared to the substantial effects shown for higher muscle lengths. This suggests that at lower muscle lengths, the deformation of the muscle, which is determined by the muscle length, is altered to a limited extend by the extramuscular force (which builds up as a function of the changing relative position) acting on the muscle. Such resistance is likely to be a result of sizable changes taking place in the muscle volume together with the introduced shear (in the local, fiber cross-fiber directions) as a consequence of the reduced muscle length. Both volume and shear effects are only ascribable to the extracellular matrix domain. Therefore, we hypothesize that at lower muscle lengths, the matrix mesh should have a major role in bearing the extramuscular load.

Fig.7 shows the aponeurosis, fiber mesh and matrix mesh forces found at the ends of groups of fascicles within the muscle belly (numbered from 1 to 7, Fig.7a). Note that all forces are normalized for muscle total proximal force at 7 mm. In contrast to the aponeurosis forces shown in Fig.4b for higher muscle lengths, for lower muscle lengths all aponeurosis forces found at the proximal and distal ends of fascicles are not acting in the same direction (Fig.7b). For the proximal aponeurosis, the forces exerted by fascicles 1 to 3 are in distal direction (negative forces) while the remaining fascicles exert forces in the proximal direction (positive forces). For the distal aponeurosis, fascicles 1 to 4 exert forces directed distally and 5 to 7 exert forces directed proximally at the most proximal muscle relative position studied. At the most distal muscle relative position, nearly all fascicle forces are directed distally except for fascicle 7, which exerts a force in the proximal direction. The reason for this heterogeneity in the direction of the fascicle forces is not the force generated in the fiber mesh (as in general fiber mesh proximal forces are in the proximal and fiber mesh distal forces are in the distal direction, Fig.7c) but the matrix mesh forces (Fig.7d).

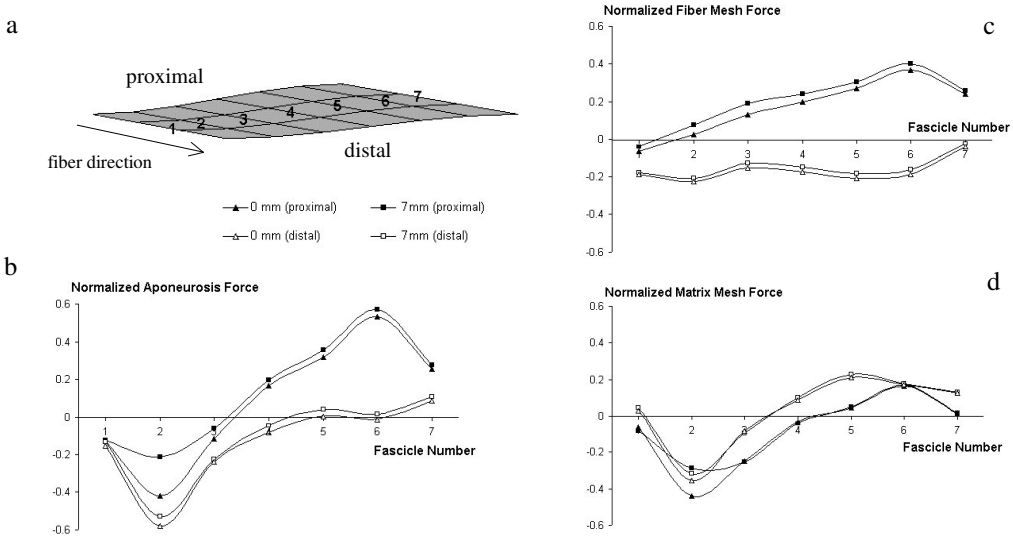

Fig.7. Forces at the fascicle ends for low muscle length. (a) The forces transmitted onto the proximal and distal aponeuroses were calculated for the nodes at which the fiber and matrix meshes are connected to the aponeurosis elements. The collections of nodes along the longitudinal sides of myofiber or extracellular matrix elements represent different fascicle groups within the muscle belly. Each fascicle is indicated by a number from 1 to 7. (b) The aponeurosis force which is the sum of the forces exerted onto the aponeuroses by the fiber and matrix meshes (c) the fiber mesh force and (d) the matrix mesh force are plotted as a function of fascicle number. All forces are normalized for the maximal muscle total force (i.e. muscle total proximal force at the most proximal muscle relative position, 7 mm).

Comparing the proximal aponeurosis forces for the two muscle relative positions (0 mm and 7 mm), in general two types of differences in are found: (1) Relatively small but almost constant differences, valid for the fascicles 3 to 7, as well as fascicle 1. (2) More pronounced but local differences, valid mainly for fascicle 2 (Fig.7b). This is also generally true for the comparison of distal aponeurosis forces for the two muscle relative positions. The first type of difference is ascribable to the intracellular domain since the curves showing the fiber mesh force are approximately equidistant to each other (Fig.7c). On the other hand, for the two muscle relative positions, the matrix mesh forces are similar for all fascicles except for fascicle 2, which shows a sizable force difference at both proximal and distal ends (Fig.7d). Therefore, the second type of difference is caused by the extracellular matrix domain.

Table.2 shows the summed distal and proximal aponeurosis, fiber mesh and matrix mesh forces. Comparing the summed fiber mesh proximal forces at the two muscle relative positions shows that the summed proximal force at 7 mm is higher. Comparing the summed fiber mesh distal forces shows that the summed distal force at 0 mm is higher. We concluded that, for the intracellular domain, minor changes in the distribution of length of sarcomeres lead to an accumulated difference of force exerted on the proximal and distal tendons. Similar to the higher length condition, also at lower muscle lengths, the matrix mesh force plays a significant role in the proximo-distal muscle total force difference. However, in contrast to the higher length condition, at lower muscle lengths, the force exerted by the extracellular matrix is in the opposite direction to the force exerted by the myofibers. At the most distal muscle relative position (0 mm), the absolute value of summed fiber mesh distal force is very close the summed fiber mesh proximal force (Table.2). Our present results show that, changing the relative position of the muscle manipulates the absolute value of the summed force exerted by the extracellular matrix. The absolute value of summed matrix mesh distal force is much lower than the summed matrix mesh proximal force (Table.2). This leads to the differences in muscle total force exerted at the distal and proximal tendons. At the most proximal relative position, 7 mm (for which more pronounced fiber direction strain and stress distributions were shown in Fig.6c and f respectively), the summed fiber mesh proximal force is higher than the summed fiber mesh distal force (Table.2). The difference between the absolute values of the matrix mesh forces is also very high (Table.2). We concluded that the interaction of intramuscular and extramuscular connective tissues leads to altered extracellular matrix forces exerted at the proximal and distal tendons, which play a significant role in proximo-distal muscle total force difference.

Table.2

Muscle relative position	0 mm		7 mm	
lo-5.0 mm	Proximal	Distal	Proximal	Distal
Σ Normalized* fiber mesh force	1.17	-1.18	1.43	-1.04
Σ Normalized* matrix mesh force	-0.57	0.20	-0.43	0.27
Σ Normalized* aponeurosis force	0.60	-0.98	1.00	-0.77

* Normalized for muscle total proximal force at the most proximal muscle relative position, 7 mm

In summary, major effects of the relative position of a muscle with respect to its surrounding connective tissues on muscular mechanics are shown. It was found that at both higher and lower muscle lengths, changing the muscle relative position in distal direction increases the muscle total force exerted at the distal tendon and decreases the total force exerted at the proximal tendon. Repositioning the muscle in the proximal direction lead to opposite effects. At higher muscle lengths, the model shows that extramuscular myofascial force transmission causes a substantial distribution of lengths of sarcomeres arranged in series within muscle fibers, which leads to unequal forces exerted at proximal and distal ends of muscle fibers. Such distribution of force within the intracellular domain indicates that a smaller force is generated within the myofibers in an active muscle with intact extramuscular connections compared to a muscle, which is truly isolated from the surroundings. However, the model results show that at higher muscle lengths, the force transmitted by the extracellular matrix is substantial. This force plays a major role, which leads to the proximo-distal muscle total force differences. At lower muscle lengths, a limited distribution of lengths of sarcomeres arranged in series within muscle fibers is found. It was shown that the proximo-distal muscle total force differences are explained by relatively small but accumulated force differences ascribable to the intracellular space, as well as local but sizable force differences ascribable to the extracellular matrix. Due to the high stiffness of the extracellular matrix at lower muscle lengths, the extramuscular force acting on the muscle leads to only limited deformation thus distribution of lengths of sarcomeres, but it is supported by the extracellular matrix. However, the extramuscular load manipulates the force exerted by the extracellular matrix, which acts as a major determinant of muscle total force.

Discussion

Effects of relative position as a co-determinant of muscle force

In some recent studies, significant effects of inter- and extramuscular myofascial force transmission on isometric muscle force have been shown. Large differences were found

between the simultaneously measured forces exerted at the proximal and distal tendons of EDL muscle within the intact anterior tibial compartment (Huijing, 1999b; Huijing, 2000). A study investigating the effects of blunt dissection and compartmental fasciotomy (Huijing and Baan, 2001b) showed that a systematic manipulation of the extra and inter-muscular connective tissue structures altered the muscle length-force characteristics. A decrease in muscle optimum force and changes in the muscle optimum and active slack lengths were found, as a result of reduced inter and extra-muscular interactions. Huijing and Baan (2001a) found significant proximo-distal differences of active and passive EDL isometric force measured after proximal EDL lengthening, while tibialis anterior (TA) and extensor hallucis longus (EHL) muscles, as well as EDL were simultaneously and maximally activated. Experiments focused on intermuscular myofascial force transmission also showed unequal proximal and distal EDL forces (Maas et al., 2001). These results identified the role of myofascial force transmission as a determinant of muscle length-force characteristics together with the altered muscle length. The present work on EDL kept at a constant length, studied the isolated effects of extramuscular myofascial force transmission on muscle force. Our results showed that at both higher and lower muscle lengths, effects of extramuscular myofascial force transmission introduced by the changes in muscle relative position on muscle force are significant. Therefore, we concluded that relative position of a muscle with respect to its surrounding connective tissue structures is a co-determinant of isometric muscle force.

For in vivo muscle functioning myofascial effects challenge the classical concepts

Skeletal muscle can be represented as an extensive 3D set of endomysial tunnels within which the myofibers operate (Trotter and Purslow, 1992). The multimolecular complexes (Berthier and Blaineau, 1997) provide a connection between the sarcomeres and the extracellular matrix. Although a certain general knowledge about such connections has existed for a long time (e.g. Pond, 1982), this knowledge has not generally been used in physiological experiments on muscle to consider their role in force transmission explicitly (e.g. Heslinga and Huijing, 1993; Hawkins and Bey, 1997). Not accounting for intramuscular myofascial force transmission (i.e. ascribing the transmission of force from the muscle fibers completely to the myotendinous junction) lead to consideration of muscle fibers as units exerting equal forces at both ends. However our present results showed that at higher muscle lengths due to extramuscular myofascial force transmission and at lower muscle lengths essentially due to intramuscular myofascial force transmission, this is not the case. The mechanical interaction between the linked intracellular and extracellular matrix domains was shown in some specific work (e.g. Street, 1983; Trotter and Purslow, 1992) and force transmission from the full perimeter surface of myofibrils onto the extracellular matrix was evident in a number of experiments (e.g. Huijing et al., 1998; Huijing, 1999a; Huijing,

1999b).

There is a large body of earlier experimental work on muscle. However, evidence on extramuscular myofascial effects has been shown in only a few recent studies. The majority of earlier experiments were performed on muscles in situ, with measurement of muscle force only at one of the tendons. In such approach, it was implicitly assumed that the force exerted at the other tendon is the same. Therefore, in the classical point of view, the length-force characteristics of a certain muscle are unique and are identical for both tendons. This can only be true for a muscle, which is completely isolated from its surrounding connective tissues. However, for a muscle in situ, the tissues of the major neurovascular tract to the muscle studied are always left intact in order to keep it in physiological conditions. Our previous results (Yucesoy et al., 2002a) showed that for the rat EDL muscle, such tissues are stiffer than the remaining connective tissues and therefore, transmit a large amount of force extramuscularly. It was found that the connective tissues of the major neurovascular tract exclusively lead to a sizable proximo-distal difference in muscle total force. For a muscle in vivo, myofascial force transmission takes place inter-and extramuscularly involving a more complex structure of connective tissue organization. The results of experiments, which took into account the intact pathways of myofascial force transmission (Huijing and Baan, 2001a; Huijing and Baan, 2001b; Maas et al., 2001; Yucesoy et al., 2002a) indicate that, for in vivo muscle functioning, at most muscle lengths, the isometric muscle force measured at proximal and distal tendons will be different.

Commonly each muscle is considered to have specific length-force characteristics, which includes a particular muscle length at which the muscle force is maximal (muscle optimal length) or a muscle length at which the muscle force is zero (muscle active slack length). In our present work the high and low muscle lengths studied were selected with reference to optimum length of isolated EDL. Our results showed that at both high and low muscle lengths, proximal and distal muscle total forces vary as a function of muscle relative position. Explorative modeling of the effects of muscle relative position for EDL kept at muscle optimum length (not presented here) yields similar results: changing the muscle relative position from the most distal to the most proximal position leads to an increase of approximately 50 % in the proximal muscle force and a decrease of approximately 12 % in the distal muscle force, for identical positions studied at high muscle length in the present study. Recent experimental testing of relative position effects on EDL length-force characteristics revealed substantial differences between the length-force curves obtained at several different muscle relative positions (Maas et al., 2002c). EDL muscle was lengthened distally after placing the proximal tendon at different positions relative to a reference position. Repositioning the proximal tendon in the proximal direction increased the active slack length as well as muscle optimum length. Moreover, the magnitude of muscle optimum force for different muscle relative positions was different. Experimental

investigation of the effects of blunt dissection and compartmental fasciotomy for the anterior tibial compartment of the rat (Huijing and Baan, 2001b) showed that systematically reduced inter and extra-muscular interactions of EDL muscle decreased muscle optimum force and changed active slack length. We concluded that the determinants of muscle length range of active force production, are not specific properties of muscle related only to filament overlap in sarcomeres, but are a function of the muscle relative position and the conditions in which the muscle is operating.

Limitations and implications of this study

The results of our present study show that extramuscular myofascial force transmission exclusively has significant effects on muscular mechanics imposed by the changing muscle relative position with respect to its surrounding connective tissues. However, in vivo, relative position effects are more complex since myofascial force transmission takes place also intermuscularly. Combined effects of inter- and extramuscular myofascial force transmission on isometric force of EDL muscle kept at constant length were studied recently (Maas et al., 2002a). The connective tissues at the muscle bellies of EDL, tibialis anterior and extensor hallucis longus muscles were left intact. Altered relative position of EDL muscle within the anterior tibial compartment lead to significant effects on EDL force. In vivo, relative position effects may also originate from length changes of the muscle studied as well as the surrounding muscles with joint motion. Differences in moment arm will contribute to relative movement. For bi- or polyarticular muscle, relative movement of muscles will be much larger. Therefore, for given tasks, studies aiming at identification of the relative positions of in vivo muscles with respect to their surroundings are indicated. Using cine phase-contrast magnetic resonance imaging, changes in the relative position of muscle bellies has been measured in vivo, for human rectus femoris and vastus intermedius muscles (Asakawa et al., 2002). Their results show that joint rotations alter the relative positions of adjacent muscles.

In the present study, EDL muscle was modeled maximally activated which was also the condition for the experimental data (Maas et al., 2002b) used in comparison to the modeled forces. For a muscle in vivo, this is hardly the case. The mechanical interaction between the muscle studied and the surrounding connective tissues (or between adjacent muscles) strongly depends on the stiffness of the muscular tissues. Maximal activation leads to a higher stiffness than sub-maximal activation. Therefore the effects of muscle relative position and myofascial force transmission is expected to depend strongly on the level of activation, which needs to be studied in the future.

Using linearly stiff spring elements to represent the inter- and extramuscular connections must be considered as a significant simplification. Such connective tissues feature non-linear length-force characteristics. It should be noted that in order to achieve a reasonable

agreement between the modeled and experimental muscle forces, the stiffness values selected for the modeled extramuscular links used for EDL at high length were greater than that of the links used for EDL at low length. At high length, the muscle force is much higher and calculation of the proximo-distal force differences as a function of muscle relative position requires stiffer links to be used. This suggests that the morphology of the neurovascular tract at higher or lower muscle lengths may be different possibly due to differences in the orientation of collagen fibers that comprise the tract which will conceivably lead to a higher total extramuscular force at higher muscle lengths. New experimental studies to investigate the mechanical and morphological properties of extramuscular connective tissues are indicated.

Finite element modeling, featuring mechanical equilibrium of a continuum that represents the muscle tissue, shows that intra- and extramuscular myofascial force transmission leads to distribution of lengths of sarcomeres arranged in series within muscle fibers. However, such distributions have not been validated experimentally. It should be noted that doing this for a whole muscle surrounded by compartmental connective tissues and other muscles is very difficult. Using ultrasound techniques could be a possibility to show length distributions within muscle fascicles.

At higher muscle lengths, our present model results show that extramuscular myofascial force transmission leads to distribution of lengths of sarcomeres arranged in series within muscle fibers. At both distal and proximal muscle relative positions, such distributions are shown to result in a certain decrease in the total force exerted by the intracellular domain compared to a muscle which is modeled completely isolated from the surrounding connective tissues. However, our results also show that at higher muscle lengths, such a decrease is compensated by the force exerted by the extracellular matrix domain. Moreover the intermuscular myofascial force transmission between adjacent muscles (Huijing and Baan, 2001a; Maas et al., 2001; Yucesoy et al., 2001) is also likely to contribute to that. On the other hand, distribution of lengths of sarcomeres as the determinant of heterogeneity of mean sarcomere length in different muscle fibers was shown to affect the length range of active force production (Willems and Huijing, 1994; Huijing, 1996). At lower muscle lengths, our present results show that the contribution of the force exerted by the extracellular matrix domain is manipulated by the extramuscular myofascial effects which leads to the differences between the proximal and distal muscle total forces. These results suggest that extramuscular myofascial force transmission may have a significant role in neuromuscular coordination.

Conclusions

Relative position of a muscle with respect to its surrounding connective tissues has major effects on skeletal muscle functioning and it is a co-determinant of muscle force besides

muscle length. At higher muscle lengths extramuscular myofascial force transmission leads to substantial distributions of sarcomere lengths for sarcomeres arranged in series within myofibers. Extracellular matrix domain transmits a significant amount of force, which constitutes a sizable proportion of muscle total force. At lower muscle lengths the effect of extramuscular myofascial force transmission on distributions of sarcomere lengths is relatively limited. This indicates that the intramuscular connective tissues are bearing the extramuscular force. However, the extramuscular force manipulates the force exerted by the extracellular matrix domain, which leads to the proximo-distal muscle total force differences. Therefore, continuity of intra- and extramuscular connective tissues allows myofascial force transmission and affects muscular mechanics significantly.

References

Asakawa, D. S., Blemker, S. S., Gold, G. E. and Delp, S. L., 2002. In vivo motion of the rectus femoris muscle after tendon transfer surgery. Journal of Biomecanics 35, 1029-1037.

Berthier, C. and Blaineau, S., 1997. Supramolecular organization of the subsarcolemmal cytoskeleton of adult skeletal muscle fibers. A review. Biology of the Cell 89, 413-434.

Danowski, B. A., Imanaka-Yoshida, K., Sanger, J. M. and Sanger, J. W., 1992. Costameres are sites of force transmission to the substratum in adult rat cardiomyocytes. The Journal of Cell Biology 118, 1411-1420.

Hawkins, D. and Bey, M., 1997. Muscle and tendon force-length properties and their interactions in vivo. Journal of Biomechanics 30, 63-70.

Heslinga, J. W. and Huijing, P. A., 1993. Muscle length-force characteristics in relation to muscle architecture: a bilateral study of gastrocnemius medialis muscles of unilaterally immobilized rats. European Journal of Applied Physiology and Occupational Physiology 66, 289-298.

Hijikata, T., Wakisaka, H. and Niida, S., 1993. Functional combination of tapering profiles and overlapping arrangements in nonspanning skeletal muscle fibers terminating intrafascicularly. Anatomical Record 236, 602-610.

Huijing, P. A., 1996. Important experimental factors for skeletal muscle modeling: non-linear changes of muscle length force characteristics as a function of degree of activity. European Journal of Morphology 34, 47-54.

Huijing, P. A., 1999a. Muscle as a collagen fiber reinforced composite material: Force transmission in muscle and whole limbs. Journal of Biomechanics 32, 329-345.

Huijing, P. A., 1999b. Muscular force transmission: A unified, dual or multiple sytem? A review and some explorative experimental results. Archives of Physiology and Biochemistry 170, 292-311.

Huijing, P. A. 2000. In vivo, force is transmitted from muscle also at other locations than the tendons: Extramuscular myofascial force transmisison. 5th Annual Congress of the European College of Sports Science, Jyvaskyla, Finland, University of Jyvaskyla.

Huijing, P. A. and Baan, G. C., 2001a. Extramuscular myofascial force transmission within the rat anterior tibial compartment: Proximo-distal differences in muscle force. Acta Physiologica Scandinavica 173, 1-15.

Huijing, P. A. and Baan, G. C., 2001b. Myofascial force transmission causes interaction between adjacent muscles and connective tissue: Effects of blunt dissection and compartmental fasciotomy on length force characteristics of rat extensor digitorum longus muscle. Archives of Physiology and Biochemistry 109, 97-109.

Huijing, P. A., Baan, G. C. and Rebel, G., 1998. Non myo-tendinous force transmission in rat extensor digitorum longus muscle. Journal of Experimental Biology 201, 682-691.

Huijing, P. A., Maas, H. and Baan, G. C., 2003. Compartmental fasciotomy and isolating a muscle from neighboring muscles interfere with extramuscular myofascial force transmission within the rat anterior tibial compartment. Journal of Morphology 256, 306-321.

Maas, H., Baan, G. C. and Huijing, P. A., 2001. Intermuscular interaction via myofascial force transmission: effects of tibialis anterior and extensor hallucis longus length on force transmission from rat extensor digitorum longus muscle. Journal of Biomechanics 34, 927-940.

Maas, H., Baan, G. C. and Huijing, P. A. 2002a. The position of EDL muscle relative to surrounding tissues is a major determinant of isometric EDL force: combined effects of inter- and extramuscular myofascial force transmission. 12 th International Conference on Mechanics in Medicine and Biology, Lemnos, Greece.

Maas, H., Baan, G. C. and Huijing, P. A. 2002b. The relative position of extensor digitorum longus muscle, kept at constant length, affects isometric force exerted at its proximal and distal tendons: effects of extramuscular myofascial force transmission. 12 th International Conference on Mechanics in Medicine and Biology, Lemnos, Greece.

Maas, H., Yucesoy, C. A. and Huijing, P. A., 2002c. Implications of muscle relative position as a co-determinant of isometric muscle force: a review and some experimental results. International Journal of Mechanics in Medicine and Biology, in press.

Pond, C. M., 1982. The importance of connective tissue within and in between muscles. The Behavioral and Brain Sciences 5, 562.

Street, S. F., 1983. Lateral transmission of tension in frog myofibers: a myofibrillar network and transverse cytoskeletal connections are possible transmitters. Journal of Cellular Physiology 114, 346-364.

Trotter, J. A. and Purslow, P. P., 1992. Functional morphology of the endomysium in series fibered muscles. Journal of Morphology 212, 109-122.

Willems, M. E. and Huijing, P. A., 1994. Heterogeneity of mean sarcomere length in different fibres: effects on length range of active force production in rat muscle. European Journal of Applied Physiology and Occupational Physiology 68, 489-496.

Yucesoy, C. A., Koopman, H. J. F. M., Guus, C. B., Grootenboer, H. J. and Huijing, P. A., 2002a. Extramuscular myofascial force transmission: Experiments and finite element modeling. Archives of Physiology and Biochemistry, in revision.

Yucesoy, C. A., Koopman, H. J. F. M., Huijing, P. A. and Grootenboer, H. J. 2001. Finite element modeling of intermuscular interactions and myofascial force transmission. 23rd Annual International Conference of the IEEE Engineering in Medicine and Biology Society, Istanbul, Turkey.

Yucesoy, C. A., Koopman, H. J. F. M., Huijing, P. A. and Grootenboer, H. J., 2002b. Three-dimensional finite element modeling of skeletal muscle using a two-domain approach: Linked fiber-matrix mesh model. Journal of Biomechanics 35, 1253-1262.

Zuurbier, C. J., Everard, A. J., van der Wees, P. and Huijing, P. A., 1994. Length-force characteristics of the aponeurosis in the passive and active muscle condition and in the isolated condition. Journal of Biomechanics 27, 445-453.

Chapter 7

General Discussion

Goals and Principles

Finite element modeling approach

Building any model involves simplification of reality. Such simplifications have to be made in accordance with the goals of modeling and the related limitations should be accounted for while interpreting the model results. On the other hand, a model designed with a careful strategy can make contribution to the understanding of the problem studied by supporting the experimental findings, and help generation of new ideas for designing of different experiments. In modeling of mechanics of muscle, the finite element method (FEM) has been shown to be valuable (e.g. Huyghe et al., 1991; Vankan et al., 1996; Gielen, 1998; van der Linden, 1998). The advantage that FEM modeling provides is consideration of muscle tissue as a continuum that accounts for material and geometric nonlinearities, and its capability of studying mechanics of skeletal muscle for various conditions and muscle lengths. Moreover, modeling of muscle tissue makes it possible to manipulate specific properties and conditions, and allows extrapolation of the experimental results, in order to address questions for which no direct measurements were made. This allows testing of hypotheses, which can be expensive or difficult to perform in animal experiments and perhaps, impossible to do in human.

The FEM model developed in this thesis was designed specifically to study the principles of myofascial force transmission. Certain studies propose a role of transsarcolemmal connections (e.g. Berthier and Blaineau, 1997) as mechanical coupling between the intracellular space and the extracellular matrix (e.g. Danowski et al., 1992). As a consequence of such coupling, transmission of force from the full perimeter of myofibers to the extracellular matrix occurs (Street and Ramsey, 1965; Street, 1983; Trotter, 1993; Huijing et al., 1998; Huijing, 1999; Jaspers et al., 1999). In the linked fiber matrix mesh model, this concept has been represented by modeling skeletal muscle tissue as two separate, but elastically linked domains, representing the intracellular space and the extracellular matrix. In earlier applications of FEM in modeling of mechanics of skeletal muscle, both active and passive properties of muscle tissue were lumped in one finite element (e.g. van der Linden, 1998; Johansson et al., 2000; Jenkyn et al., 2002). This is equivalent to the linked fiber matrix mesh model with rigid links between the two domains. Due to the assumption of continuity, also in such approach myofascial force transmission mechanism is active but only, implicitly. In the linked fiber matrix mesh model this mechanism is accounted for explicitly. This allows addressing specific questions regarding the effects of the two domains in muscle functioning and the links between them.

Limited goals of this thesis in relation to future research goals

The research conducted in the field of mechanics of skeletal muscle aims at generating an appropriate understanding of in vivo muscle functioning in association to motor control and

muscular coordination. Recent findings as well as the results of this thesis indicate the likelihood of a significant contribution of myofascial force transmission on in vivo muscle functioning. In order to study this adequately, besides in vivo experiments, the ultimate goal of modeling has to be building models in the level of a whole limb including antagonists as well as synergistic muscles and related extramuscular tissues. In this thesis, the major pathways of myofascial force transmission were investigated in a systematical manner. From a single isolated muscle to consideration of the synergistic muscles within a compartment, intra-, inter- and extramuscular myofascial force transmission was studied. The goal was to show the principles of the potential functional significance of myofascial force transmission at a fundamental level, and therefore, to take a first step towards identifying its effects in vivo.

Relevance of the Study

How realistic are the conditions studied compared to the situation in vivo?

Conditions in the experiments

In the studies presented, the experiments involved certain extreme conditions, which are not likely to occur in vivo.

(1) The muscles studied in both experimental and modeling work presented in this thesis were activated maximally. Activation of both the target muscle and the adjacent muscles sub-maximally, or activation of each muscle (even parts of muscles) at a different level is expected to change the relative stiffness of the muscular tissues significantly. These conditions are highly likely to influence the effects of myofascial force transmission. Yet, as sizable effects of myofascial force transmission on muscle force were shown even in the passive condition (Maas et al., 2001; Yucesoy et al., 2002b; Yucesoy et al., 2002a; Huijing and Baan, 2003) significant effects for in vivo muscle functioning are expectable, even though the level of activation may be much lower.

(2) In the experiments, the femur was secured at a knee angle of 90° whereas the ankle was in extreme plantar flexion. This allows a standardized fixation of the target leg of the experimented animal onto the setup as well as making room for the passage of the distal tendon complexes and their attached Kevlar threads. However, such an ankle joint angle is not a realistic condition to be encountered in vivo. Due to the fact that joint ligaments are continuous with muscles and other connective tissue structures within a limb (e.g. van Mameren and Drukker, 1984; van der Wal, 1988), the extreme ankle joint angle is likely to alter the relative stiffness of connective tissues, which constitute the myofascial pathways. If this leads to stiffer myofascial pathways, more pronounced effects of myofascial force transmission on muscle force is conceivable compared to more commonly encountered ankle joint angles in vivo.

(3) Only one of the experimented muscles was moved with respect to its neighboring muscles as well as surrounding connective tissues. This is not likely to occur in vivo, as more muscles will change length with joint motion. This issue is discussed in detail in a later section.

Modeling the actual 3D muscle geometry

The real geometry and architecture of most muscles and associated connective tissues are highly complex. However, the muscles studied in this thesis were modeled only as a longitudinal slice as can be obtained at the middle of the muscle belly. This represents a considerable simplification of the real situation as, although the developed elements representing the muscle tissue were in 3D, the models in its present form make only limited use of the third dimension. In order to improve the relevance of modeling for muscle function in vivo, and to perform studies in the level of a whole limb it will be necessary to account for a more realistic 3D geometry. Above all this will allow a better representation of muscle architecture as well as changes of morphology during muscle functioning and of the effects of these aspects on muscular mechanics. If the actual 3D geometry of neighboring muscles is modeled, the representation of inter- and extramuscular connections as interfaces for myofascial force transmission will be more realistic. The distance of inter- and extramuscular connections to muscle fibers located at different parts of muscle belly will be accounted for. It is conceivable that such factors will lead to a more realistic calculation of serial and parallel distributions of lengths of sarcomeres. Nevertheless, the present model results yielded fairly good qualitative agreement with the experimental results suggesting that with the models used, the principles of myofascial force transmission were taken into account adequately. Besides, the present modeling study provided an important contribution to our understanding of the effects of myofascial force transmission on muscle properties.

Simplified representation of the intra-, inter- and extramuscular connections

In the models studied, spring elements were used to represent muscles' intra-, inter- and extramuscular connections. This approach includes an over-simplification of reality. Therefore, certain features of these connections were not characterized adequately:

(1) Muscular connective tissues feature non-linear length-force characteristics (e.g. Zuurbier et al., 1994). Therefore modeling of the intra-, inter- and extramuscular connections with linear length-force characteristics is not realistic. Moreover, the experimental results presented in Chapter 6 show that for a certain range of deformations, the extramuscular connections of muscle may be slack: the total extramuscular force was close to zero at a number of EDL relative positions. This indicates that there are neutral positions of muscle (i.e., positions at which the total extramuscular force is zero), which depends also on muscle

length. In the muscles modeled, the neutral position was selected to be at a particular muscle length at which all extramuscular linking elements were set to have a length of zero.
(2) The multimolecular complexes (Berthier and Blaineau, 1997) that connect sarcomeres to the extracellular matrix consist of several different proteins and form different cytoskeletal systems. This complex system is modeled as lumped in intramuscular linking elements that are identical at all locations. Inter- and extramuscular connections are modeled similarly assuming that these connections have homogeneous mechanical properties. This is unlikely to be realistic. For example, experiments on EDL with fully intact and with minimal extramuscular connections showed that the mechanical properties of the neurovascular tract are not homogeneous (Yucesoy et al., 2002b). Moreover, the connective tissues comprising muscles' inter- and extramuscular connections are continuous structures of collagen fiber reinforced composites presumably with a certain fiber orientation rather than their modeled representations as a discrete set of spring elements. Borg and Caulfield (1980) examined the arrangement and distribution of connective tissue in different muscles by scanning electron microscopy. They pointed out the morphological differences between the endomysial and perimysial tissues and indicated the contribution of the differences in the arrangement of collagen to mechanical properties of muscular connective tissues.

Nevertheless, not much is known about the mechanical properties as well as structural morphology of such connective tissue. Therefore, in modeling of different experimented muscles, suitable stiffness values were selected for inter- and extramuscular linking elements, which provide a reasonable agreement between the modeled and experimental muscle forces. It should be noted that in Chapter 6, for the same purpose, the stiffness values selected for the extramuscular links used for the modeled EDL at high length were greater than that of the modeled EDL at low length. This is because at high length, the muscle force is much higher and calculation of the proximo-distal force differences as a function of muscle relative position at this length requires the stiffness values selected for the modeled extramuscular links to be greater. This suggests that the differences in the calculated fiber direction strain distributions at the two muscle lengths can partially be attributed to the differences in stiffness of the modeled extramuscular links. On the other hand, it is also likely that the morphology of the neurovascular tract at higher or lower muscle lengths is different which conceivably will alter the total extramuscular force. The differences in the structure of the tract at the two different muscle lengths can be characterized by differences in the orientation of collagen fibers that comprise the tract. Fig.1 shows an exaggerated illustration of this. In Fig.1a, muscle is shown at an assumed neutral position and the tract is represented by an oblique set of collagen fibers for which the angle with the horizontal is selected arbitrarily. In Fig.1b and c the muscle is shown at a distal relative position at a low and a high length respectively. Comparison of the extent the collagen fibers are stretched at each length indicates that the total extramuscular force at higher muscle lengths is higher.

Therefore, in Chapter 6, due to the simplified representation of the modeled extramuscular connections i.e., as the altered structure was not represented, it was only possible to use stiffer linking elements to account for this higher extramuscular force. It should be noted that the example shown in Fig.1 is valid also for proximal relative positions of the muscle as well as for different angles of the collagen fibers with the horizontal.

Yet, along with the other simplifications of the model, such linear links served well for the study of the major principles of myofascial force transmission. However, for the models to provide a better description of the in vivo situation, an adequate representation of the mechanical and morphological properties of connective tissues that constitute the myofascial pathways is necessary. To accomplish that, new experimental studies to investigate these properties are indicated.

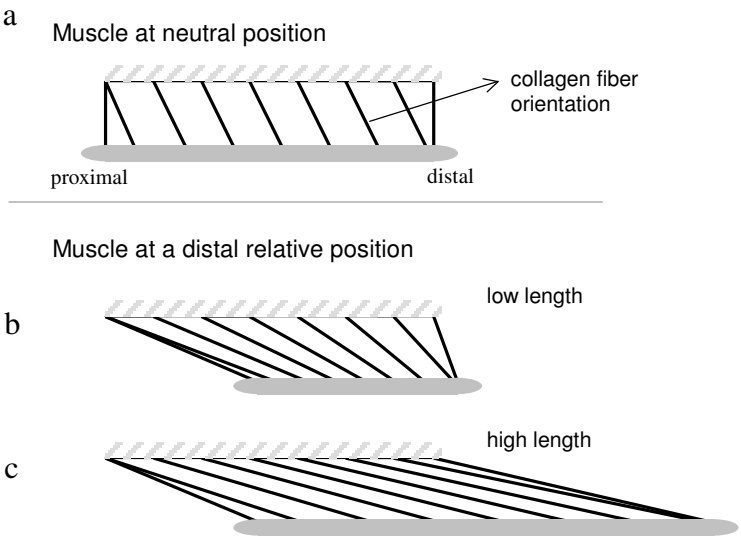

Fig.1. Illustration of the changes in the orientation of collagen fibers that comprise the neurovascular tract at different muscle lengths. (a) The muscle is shown at an assumed neutral position i.e., the extramuscular force is equal to zero. The collagen fibers are shown at an arbitrarily selected angle with the horizontal. The muscle is at a distal relative position (b) at a low length and (c) at a high length.

Experimental Verification is necessary for sarcomere length distributions

The results of this thesis, which indicate that myofascial force transmission is capable of causing significant distributions of lengths of sarcomeres, are supported by the model results only. These results have to be verified experimentally. The difficulty in doing that for a whole muscle surrounded by compartmental connective tissues and other muscles is the obscured view. Gradual isolation of EDL as a result of systematic manipulation of its inter- and extramuscular connections resulted in sizable differences in muscle length force

characteristics (Huijing and Baan, 2001b). Therefore, greater access to target muscles by dissection will alter mechanical connections of such muscles. The difficulty due to the obscured view becomes even more pronounced for verification of sarcomere length distributions in vivo. To overcome this problem, techniques such as magnetic resonance imaging may be used.

In earlier studies on rat muscle isolated in situ, strains within the muscle were measured using fluorescent spheres on the muscle (van Bavel et al., 1996; Savelberg et al., 2001). Similar measurements were also performed for human muscles in vivo (Pappas et al., 2002), using magnetic resonance imaging. Lieber and coworkers applied laser diffraction methods to directly measure sarcomere length intraoperatively for human extensor carpi radialis brevis (Lieber et al., 1994) and flexor carpi ulnaris (Lieber and Friden, 1997) muscles. However, in those studies dissection of connective tissues was performed. Moreover, the primary goal was not determining possible effects of myofascial force transmission on distribution of lengths of sarcomeres. For example in the work of Lieber and coworkers sarcomere length was measured at only one location suggesting that this will be representative of the whole muscle (Lieber and Friden, 1997). Therefore, new in vivo experimental studies designed specifically for the purpose of measurement of sarcomere length distribution in association to the effects of myofascial force transmission are indicated.

<u>To what extent do changes in muscle relative position occur in vivo?</u>

The changes in muscle length will alter the relative position of a muscle with respect to the neighboring muscles and other nonmuscular structures. This seems to be a key parameter, which determines the extent of the effects of myofascial force transmission on muscle length force characteristics. In this thesis, both in experimental and modeling work, conditions were manipulated to emphasize the role of relative position of a muscle. Such conditions included lengthening of only one muscle at a time while all surrounding muscles and connective tissues were prevented from any position changes. However, in vivo, not only the muscle studied, but also the surrounding muscles will change length and relative position with joint motion. The effects of in vivo joint motion on relative position of a muscle can be characterized by two factors.

(1) Number of joints a muscle spans i.e., if it is mono-articular or, bi- or polyarticular. For a polyarticular muscle, the length and position changes of the muscle are determined by more joints: movement of a proximal joint or a distal joint not crossed by adjacent mono-articular muscles will cause potentially important change of muscle length and relative position. Consequently, for a bi- or polyarticular muscle, effects of muscle relative position can be larger than for a mono-articular muscle.

(2) Differences in moment arms between synergists. Such differences have been shown to exist (e.g. van der Helm et al., 1992; Wretenberg et al., 1996; Murray et al., 2002). Besides, the moment arm of a muscle changes as the joint angle changes. It should be noted that any difference in moment arm length between synergists is conceivable to alter the relative position of the muscles. Therefore, although the conditions studied in this thesis are not truly realistic, it is expected that effective changes in relative position of a muscle are likely to occur in vivo. For human rectus femoris and vastus intermedius muscles joint movement was shown to change the relative position of muscle bellies in vivo, using cine phase-contrast magnetic resonance imaging (Asakawa et al., 2002). Further studies employing in vivo imaging techniques are indicated for identification of such changes.

Is it realistic to ascribe the measured proximo-distal force differences only to myofascial force transmission?

A consistent result of the studies in which inter- and extramuscular myofascial force transmission is accounted for, is differences between muscle force exerted at proximal and distal tendons (Huijing and Baan, 2001a; Maas et al., 2001; Yucesoy et al., 2002b; Yucesoy et al., 2002a; Huijing and Baan, 2003). If a muscle is truly isolated from its surrounding connective tissues, than the proximo-distal force difference will be equal to zero. Therefore, the measured force differences can only be explained by transmission of the force generated by the muscle to locations other than the tendons. For this to occur, there has to be a mechanical medium. For example, friction or in dynamic conditions viscous resistance to movement could provide such medium and lead to proximo-distal force differences even for a muscle, which has no direct connections to its surroundings except for its tendons. The possible contribution of such factors needs to be studied. However, even when the muscles' intermuscular connections are not considered, for a muscle to maintain its physiological condition, the neurovascular tract to it has to be intact as well. This suggests that there will always be a direct mechanical medium present to transmit force via non-myotendinous pathways. Therefore, myofascial force transmission is likely to be the major factor that is responsible with the proximo-distal force differences.

On the other hand, the possibility of other factors to affect the proximo-distal force differences also has to be considered. For example, effects of previous activity at high length and hysteresis effects of experimental order of changes in muscle length (increasing or decreasing) were shown to alter such force difference for EDL (Huijing and Baan, 2001a). Besides, in addition to the studied isometric conditions, it is necessary to confirm the occurrence of myofascial effects also in dynamic conditions. In the experiments presented in this thesis, the lower leg of the animal was positioned parallel to the horizontal. Due to that, the role of gravity will conceivably be different in vivo since in many cases the lower leg is oriented at a certain angle with respect to the horizontal.

Are the effects shown for the anterior crural compartment of the rat also valid for other parts in the rat and also for the human?

In this thesis, the experimental work was performed in the anterior crural compartment of the rat. This is because this compartment provides significant advantages for the specific purposes of the studying myofascial force transmission: (1) Distally EDL muscle in the rat is a multi tendoned muscle. These tendons span a long distance before they attach to the four digits of the foot (e.g. Balice-Gordon and Thompson, 1988; Chleboun et al., 1997). This makes EDL a very interesting muscle for the study of intramuscular myofascial force transmission (Huijing et al., 1998; Huijing, 1999). (2) In rat the proximal EDL tendon also spans the knee joint which allows simultaneous measurement of proximal and distal muscle forces without opening the anterior crural compartment. This makes the anterior crural compartment a good choice for studying the effects of inter- and extramuscular myofascial force transmission. However, it is necessary to investigate the likelihood of such effects on muscle length-force characteristics to occur in other compartments in the rat as well as in other species including the human. Some points associated with that are briefly discussed below.

Due to the high contribution of the tibia and the fibula to its walls, the anterior crural compartment is a relatively stiff compartment. As stiffness of muscular and nonmuscular tissues is a major determinant of effects of myofascial force transmission on muscle length-force characteristics, it is likely that these effects may be more pronounced in such stiffer compartments. The anterior crural compartment of humans is also a stiffer compartment, which is apparent from a relatively high incidence of compartment syndrome for this compartment.

In contrast to the biarticular EDL muscle in the anterior crural compartment of the rat, in human, EDL is a monoarticular muscle. The significance of the number of joints a muscle spans as an important determinant of effects of in vivo joint motion on relative position of a muscle was discussed in an earlier section. As the changes in relative position of a muscle with respect to its neighboring muscles and nonmuscular structures is the major determinant of myofascial effects, these effects may conceivably be less pronounced in the anterior crural compartment of the human compared to the effects shown presently for the rat. Similarly, in the rat and in other species, the differences in the number of joints spanned by the muscles within different compartments, is expected to alter the effects of myofascial force transmission.

The size of animals varies largely. Obviously, such size differences are reflected in the sizes of muscles. Assuming that the dimensions of a muscle change by a certain factor, the change in the surface area of the muscle will be in the order of the square of that factor. Note that muscles' surface can be idealized to represent the interface for inter-, and extramuscular myofascial force transmission. On the other hand, the change in the muscles'

volume will be in the order of the cube of the same factor. Therefore, due to a more pronounced increase in muscle physiological cross-sectional area, the ratio of muscle force to inter- and extramuscular force is likely to be smaller in larger species compared to a smaller animal such as the rat. Consequently, the effects of myofascial force transmission on muscle length-force characteristics as well as on properties of muscle tissue may be relatively less pronounced in larger species.

Such points and possibly others suggest that the mechanical basis for myofascial force transmission will be different in different parts of animals. To quantify such differences, new studies are indicated. However, in any case it is conceivable that a certain organization of inter- and extramuscular connective tissues, continuous with intramuscular connective tissues will be found: always neurovascular tracts are present near the muscles and adjacent muscles may have direct connections. Therefore, even though the degree of the effects of myofascial force transmission might vary, it is likely to play a role in different parts of the locomotor apparatus of mammals, including human.

Implications of the Effects of Myofascial Force Transmission on Muscle Function

The results of this dissertation indicate that in vivo, muscle is not a fully independent functional unit exerting equal force at both tendons. Moreover, it is suggested that muscles are not comprised of muscle fibers, which function independent of their neighboring muscle fibers and exert equal force at both ends. The major feature proposed to play the key role in this novel point of view is the relative position of a muscle with respect to its surrounding muscles and non-muscular connective tissue structures. This feature is shaped by the integrated effects of intra- inter- and extramuscular myofascial force transmission. It is likely that these effects may have important implications for muscle function. Below some selected potential effects of myofascial force transmission on some of such fields will be discussed.

Motor control

The results presented in this thesis show that myofascial force transmission affects muscle force and length range of force exertion significantly. This indicates a sizeable role of myofascial force transmission in determining joint moment as well as joint range of movement. Therefore a significant effect of myofascial force transmission on body movement is conceivable.

Any effect of muscular activation on body movement is controlled by the nervous system. The neural control of muscle force involves controlling of: (1) the degree of activation of each motor unit, and (2) the number of motor units recruited at a time. Therefore, both the firing frequency of individual motor units (to vary the tension generated in that unit) and the recruitment of motor units (to vary the number of active fibers) are

controlled. Yet, the primary means of varying muscle force is provided by the recruitment of motor units according to the size principle (e.g. Henneman et al., 1965; Henneman, 1985). This allows for a fine control of muscle force depending on the number and size of the motor units, which comprises the muscle. However, this is already a highly complex mechanism. The question necessary to address is how is the effect of myofascial force transmission on body movement incorporated into this mechanism? It is making it more complex and therefore, difficult to control? Obviously to understand this adequately, more work is necessary. However, with a more involved point of view than the well established, reconsidering the elements of the local control mechanism of motor neurons may provide a perspective. This will be discussed in two subsections (1) sensory information and (2) coordination of different muscles.

Sensory information

The relative position of a muscle with respect to its neighboring muscles and non-muscular connective tissue structures, which includes the changes in muscle length, plays the key role in the effects of myofascial force transmission on muscle length-force characteristics. Therefore, in order to incorporate the effects of myofascial force transmission in neural control, reception of information associated with muscle relative position is necessary. Muscle-related receptors conceivably function to generate such information.

Joint sensors: Joint range of movement is restricted by the joint capsule as well as capsular ligaments and it is controlled by the sensors located in these structures. Often the role ascribed to the joint sensors is limited to sensing of the extreme joint positions only, owing to the argument that such sensors are not triggered because the ligaments are not stretched at the mid range of joint movement (e.g. Janwantanakul et al., 2001). However, it was shown earlier that joint capsule and capsular ligaments are not separate elements but are continuous with muscles and other connective tissue structures within a limb (van Mameren and Drukker, 1984; van der Wal, 1988). Therefore, it is conceivable that due to myofascial force transmission force is exerted at the joint capsule and capsular ligaments also at the mid range of joint movement. This suggests that joint sensors are likely to be actually involved in the control of body movement and therefore, information regarding joint angle can be incorporated. It also suggests that myofascial force transmission may be helping to improve joint stability.

Golgi tendon organs: Located very close to the junction between the tendon and muscle fibers, the Golgi tendon organs function as force transducers. In a point of view that considers muscle as a fully independent functional unit, these sensors are expected to generate information of an identical muscle force exerted at both tendons. However, taking into account myofascial force transmission, one can expect that the Golgi tendon organs can be providing information regarding the proximo-distal muscle force differences.

Muscle spindles: These complex sensory units are scattered deep within the muscles and are responsible with the function of length monitoring. They are considered as attached at both ends to the extrafusal muscle fibers and hence, experience the same relative length changes as the whole muscle. However, it is likely that the intrafusal fibers comprising the muscle spindles are connected to their neighboring extrafusal muscle fibers also along their peripheral surface similar to such connections between adjacent extrafusal muscle fibers which constitute the main muscle mass. Therefore, muscle spindles may be providing information regarding not only the overall length changes of the muscle fibers and of the whole muscle but also regarding more local strains. This suggests that information representing serial and parallel distribution of lengths of sarcomeres may be available.
Receptors located within the compartment walls: Several receptors of different kinds and nerve endings are reported to be located at specialized locations within the connective tissues such as general fascia, intermuscular septum and interosseal membrane (van der Wal, 1988). Such connective tissues constitute the walls of the compartments and these receptors can monitor relative positions of muscles and connective tissue structures.

Coordination of different muscles

In accordance with morphological knowledge, individual muscles have been distinguished anatomically. Conceivably due to that, each muscle is commonly considered to have unique length-force characteristics. In other words, individual muscles are considered as independent functional units. However, the results of this thesis suggest that muscle length-force characteristics are not unique to individual muscles. In contrast, the determinants of muscle length range of active force exertion are a function of the relative position of muscle and the conditions in which the muscle is operating. Therefore, the present results suggest that rather than individual muscles, groups of neighboring synergistic muscles may form functional units. With the same line of thought, the concept of motor unit pool could be extended to include motor units of synergistic muscles (Huijing and Baan, 2003). If control of motor units for coordination of muscle activity is based exclusively on individual muscles, then the neural control system has to organize the recruitment of motor units of different muscles separately. Consequently, optimization of the relative activities of motor units necessary for coordinated muscle activity is a substantial task for the neural control system. This is analogous to an optimization problem described by a function of several "independent" variables. However, if the level of organization is higher than the muscle, then it can be conceptualized that the neural control process will be simplified down to recruitment of all motor units according to the size principle. Such advantages of extension of the concept of motor unit pool were argued by Cope and Sokoloff (1999). Assuming that the motor unit pool consists of the motor units of all active synergists within a limb, the optimization task for coordinated muscle activity is analogous to an optimization problem

described by a function of several "dependent" variables. In this perspective, the aspect, which makes the relative activities of different motor units mechanically dependent on each other, is myofascial force transmission. This can be characterized as a game of relative stiffness of muscular and nonmuscular structures. Controlling of this game is likely to be the major function of motor control, which is conceivably assisted by (1) the integrated information provided by several receptors to generate a perception of muscle relative position and (2) by an everlasting process of learning how to deal with different tasks of body movement. Nevertheless, it should be noted that the size principle may not be applicable to the pool of motor units of "all" active synergists within a limb. Although they showed experimental results that are in favor of an extended concept of motor unit pool, Sokoloff and coworkers (1999) were not consistently able to show that this is true for certain synergistic muscles of the cat. Therefore, new studies focused on identification of motor unit pools within a limb will conceivably help generating a better understanding of how myofascial force transmission is incorporated in motor control.

Muscle diseases

Diseases associated with over-use

The continuous connective tissue associated with the four separate EDL heads was shown to allow for myofascial force transmission between them (Huijing et al., 1998). Therefore, force exertion by a muscle head to the target digit of the foot is likely to be also dependent on the activity of the other muscle heads. This point of view can be extrapolated to the muscles of the human hand. For example studies on unintended force exertion showed that production of isometric force with one, two, or three fingers caused the other fingers of the hand also to exert a certain force (Li et al., 2000; Zatsiorsky et al., 2002). In a precision task like clicking the mouse button, there is force exertion and movement performed by only one finger whereas the other fingers are restrained. This can be characterized as an intermuscular myofascial force transmission problem with a strong analogy to the work presented in Chapter 5: the three intermuscularly connected synergists are analogous to the four interconnected muscle heads of EDL. In Chapter 5, such force transmission was shown to affect deformation of muscular tissue significantly. This suggests that the concept of myofascial force transmission may be involved in the principles of pathologies associated with over use such as repetitive strain injury and musicians arm. Deformations due to length changes of only one muscle, or even only a part of a muscle while all the surrounding muscles are restrained may play a role in such conditions. In recent experiments in which connective tissues of the compartment at the muscle bellies of TA, EHL and EDL as well as the retinaculae at the ankle were left intact, intermittent concentric contractions of the distal tendon of only head III of EDL muscle was performed (Maas, 2003). After 3 hours of intermittent concentric contractions damage within EDL muscle as well as within TA and

EHL muscles was found: several swollen muscle fibers were observed in which discontinuous fragmented dystrophin staining was found at the sarcolemma. Such damage was explained by intramuscular as well as intermuscular myofascial force transmission.

Genetic muscular diseases

The multimolecular cytoskeletal complexes based on several proteins including dystrophin (Berthier and Blaineau, 1997) are assumed to play a key role in intramuscular myofascial force transmission, as they actually may provide the pathway between the intracellular space and the extracellular matrix. Therefore any missing link in this pathway is expected to hamper the full functioning of the intramuscular myofascial force transmission mechanism. Muscular dystrophies are genetically determined disorders, patients of which show progressive degeneration of muscle fibers (Mokhtarian et al., 1999) followed by fibrosis. For example in Duchenne's muscular dystrophy, the problem is associated with the absence of the protein dystrophin (e.g. Hoffman et al., 1987; Bonilla et al., 1988) or its presence in a non-functional form. The mechanics of a dystrophin deficient muscle as well as the mechanism of myofiber degeneration remains unclear. However, it is likely that that the cause of the problem is related to myofascial force transmission. The study presented in Chapter 2 theoretically indicates that at the presence of local compliant links between the intracellular domain and the extracellular matrix domain, the muscle fibers become deformed beyond physiological limits. Besides, in association to the altered sarcomere length distributions, the work presented in the remainder of the thesis suggests that different effects are likely to occur due to inter- and extramuscular myofascial force transmission. This needs to be studied in future work. It should be noted that also in less severe pathology of eccentric contractions in genetically healthy muscle, dystrophin may be absent (e.g. Komulainen et al., 1998). This suggests that the damage seen in muscle after eccentric contraction may be similar in nature to that of Duchenne's muscular dystrophy. In a recent study, dystrophin, negative muscle fibers were indicated also after concentric contraction (Maas, 2003).

References

Asakawa, D. S., Blemker, S. S., Gold, G. E. and Delp, S. L., 2002. In vivo motion of the rectus femoris muscle after tendon transfer surgery. Journal of Biomecanics 35, 1029-1037.

Balice-Gordon, R. J. and Thompson, W. J., 1988. The organization and development of compartmentalized innervation in rat extensor digitorum longus muscle. Journal of Physiology 398, 211-231.

Berthier, C. and Blaineau, S., 1997. Supramolecular organization of the subsarcolemmal cytoskeleton of adult skeletal muscle fibers. A review. Biology of the Cell 89, 413-434.

Bonilla, E., Samitt, C. E., Miranda, A. F., Hays, A. P., Salviati, G., DiMauro, S., Kunkel, L. M., Hoffman, E. P. and Rowland, L. P., 1988. Duchenne muscular dystrophy: deficiency of dystrophin at the muscle cell surface. Cell 54, 447-452.

Borg, T. K. and Caulfield, J. B., 1980. Morphology of connective tissue in skeletal muscle. Tissue Cell 12, 197-207.

Chleboun, G. S., Patel, T. J. and Lieber, R. L., 1997. Skeletal muscle architecture and fiber-type distribution with the multiple bellies of the mouse extensor digitorum longus muscle. Acta Anatomica 159, 147-155.

Cope, T. C. and Sokoloff, A. J., 1999. Orderly recruitment among motoneurons supplying different muscles. Journal of Physiology, Paris 93, 81-85.

Danowski, B. A., Imanaka-Yoshida, K., Sanger, J. M. and Sanger, J. W., 1992. Costameres are sites of force transmission to the substratum in adult rat cardiomyocytes. The Journal of Cell Biology 118, 1411-1420.

Gielen, S., A continuum approach to the mechanics of contracting skeletal muscle (PhD thesis). Eindhoven, The Netherlands: Eindhoven University of Technology, 1998.

Henneman, E., 1985. The size-principle: a deterministic output emerges from a set of probabilistic connections. Journal of Experimental Biology 115, 105-112.

Henneman, E., Somjen, G. and Carpenter, D. O., 1965. Excitability and inhibitability of motoneurons of different sizes. Journal of Neurophysiology 28, 599-620.

Hoffman, E. P., Brown, R. H. and Kunkel, L. M., 1987. Dystrophin: the protein product of the Duchenne muscular dystrophy locus. Cell 51, 919-928.

Huijing, P. A., 1999. Muscle as a collagen fiber reinforced composite material: Force transmission in muscle and whole limbs. Journal of Biomechanics 32, 329-345.

Huijing, P. A. and Baan, G. C., 2001a. Extramuscular myofascial force transmission within the rat anterior tibial compartment: Proximo-distal differences in muscle force. Acta Physiologica Scandinavica 173, 1-15.

Huijing, P. A. and Baan, G. C., 2001b. Myofascial force transmission causes interaction between adjacent muscles and connective tissue: Effects of blunt dissection and compartmental fasciotomy on length force characteristics of rat extensor digitorum longus muscle. Archives of Physiology and Biochemistry 109, 97-109.

Huijing, P. A. and Baan, G. C., 2003. Myofascial force transmission: muscle relative position and length determine agonist and synergist muscle force. Journal of Applied Physiology 94, 1092-1107.

Huijing, P. A., Baan, G. C. and Rebel, G., 1998. Non myo-tendinous force transmission in rat extensor digitorum longus muscle. Journal of Experimental Biology 201, 682-691.

Huyghe, J. M., van Campen, D. H., Arts, T. and Heethaar, R. M., 1991. A two-phase finite element model of the diastolic left ventricle. Journal of Biomechanics 24, 527-538.

Janwantanakul, P., Magarey, M. E., Jones, M. A. and Dansie, B. R., 2001. Variation in shoulder position sense at mid and extreme range of motion. Archives of Physical Medicine and Rehabilitation 82, 840-844.

Jaspers, R. T., Brunner, R., Pel, J. J. M. and Huijing, P. A., 1999. Acute effects of intramuscular aponeurotomy on rat GM: Force transmission, muscle force and sarcomere length. Journal of Biomechanics 32, 71-79.

Jenkyn, T. R., Koopman, B., Huijing, P., Lieber, R. L. and Kaufman, K. R., 2002. Finite element model of intramuscular pressure during isometric contraction of skeletal muscle. Physics in Medicine and Biology 47, 4043-4061.

Johansson, T., Meier, P. and Blickhan, R., 2000. A finite-element model for the mechanical analysis of skeletal muscles. Journal of Theoretical Biology 206, 131-149.

Komulainen, J., Takala, T. E., Kuipers, H. and Hesselink, M. K., 1998. The disruption of myofibre structures in rat skeletal muscle after forced lengthening contractions. Pflugers Archiv : European Journal of Physiology 436, 735-741.

Li, Z. M., Zatsiorsky, V. M. and Latash, M. L., 2000. Contribution of the extrinsic and intrinsic hand muscles to the moments in finger joints. Clinical Biomechanics 15, 203-211.

Lieber, R. L. and Friden, J., 1997. Intraoperative measurement and biomechanical modeling of the flexor carpi ulnaris-to-extensor carpi radialis longus tendon transfer. Journal of Biomechanical Engineering 119, 386-391.

Lieber, R. L., Loren, G. J. and Friden, J., 1994. In vivo measurement of human wrist extensor muscle sarcomere length changes. Journal of Neurophysiology 71, 874-881.

Maas, H., (PhD thesis). Amsterdam, The Netherlands: Vrije Universiteit, 2003.

Maas, H., Baan, G. C. and Huijing, P. A., 2001. Intermuscular interaction via myofascial force transmission: effects of tibialis anterior and extensor hallucis longus length on force transmission from rat extensor digitorum longus muscle. Journal of Biomechanics 34, 927-940.

Mokhtarian, A., Lefaucheur, J. P., Even, P. C. and Sebille, A., 1999. Hindlimb immobilization applied to 21-day-old mdx mice prevents the occurrence of muscle degeneration. Journal of Applied Physiology 86, 924-931.

Murray, W. M., Buchanan, T. S. and Delp, S. L., 2002. Scaling of peak moment arms of elbow muscles with upper extremity bone dimensions. Journal of Biomechanics 35, 19-26.

Pappas, G. P., Asakawa, D. S., Delp, S. L., Zajac, F. E. and Drace, J. E., 2002. Nonuniform shortening in the biceps brachii during elbow flexion. Journal of Applied Physiology 92, 2381-2389.

Savelberg, H. H., Willems, P. J., Baan, G. C. and Huijing, P. A., 2001. Deformation and three-dimensional displacement of fibers in isometrically contracting rat plantaris muscles. Journal of Morphology 250, 89-99.

Sokoloff, A. J., Siegel, S. G. and Cope, T. C., 1999. Recruitment order among motoneurons from different motor nuclei. Journal of Neurophysiology 81, 2485-2492.

Street, S. F., 1983. Lateral transmission of tension in frog myofibers: a myofibrillar network and transverse cytoskeletal connections are possible transmitters. Journal of Cellular Physiology 114, 346-364.

Street, S. F. and Ramsey, R. W., 1965. Sarcolemma: transmitter of active tension in frog skeletal muscle. Science 149, 1379-1380.

Trotter, J. A., 1993. Functional morphology of force transmission in skeletal muscle. A brief review. Acta Anatomica (Basel) 146, 205-222.

van Bavel, H., Drost, M. R., Wielders, J. D., Huyghe, J. M., Huson, A. and Janssen, J. D., 1996. Strain distribution on rat medial gastrocnemius (MG) during passive stretch. Journal of Biomechanics 29, 1069-1074.

van der Helm, F. C., Veeger, H. E., Pronk, G. M., Van der Woude, L. H. and Rozendal, R. H., 1992. Geometry parameters for musculoskeletal modelling of the shoulder system. Journal of Biomechanics 25, 129-144.

van der Linden, B. J. J. J., Mechanical modeling of muscle functioning (PhD thesis). Enschede, The Netherlands: University of Twente, 1998.

van der Wal, J. C., The Organization of the Substrate of Proprioceptation in the Elbow Region of the Rat (PhD thesis). Maastricht, The Netherlands: University of Limburg, 1988.

van Mameren, H. and Drukker, J. A., 1984. Functional anatomical basis of injuries to the ligamentum and other soft tissues around the elbow joint: transmission of tensile and compressive loads. International Journal Sports Medicine 5, 88-92.

Vankan, W. J., Huyghe, J. M., Janssen, J. D. and Huson, A., 1996. A 3-D finite element model of blood perfused rat gastrocnemius medialis muscle. European Journal of Morphology 34, 19-24.

Wretenberg, P., Nemeth, G., Lamontagne, M. and Lundin, B., 1996. Passive knee muscle moment arms measured in vivo with MRI. Clinical Biomechanics 11, 439-446.

Yucesoy, C. A., Koopman, H. J. F. M., Guus, C. B., Grootenboer, H. J. and Huijing, P. A., 2002a. Effects of inter- and extramuscular myofascial force transmission on adjacent synergistic muscles: assessment by experiments and finite element modeling. Journal of Biomechanics, in press.

Yucesoy, C. A., Koopman, H. J. F. M., Guus, C. B., Grootenboer, H. J. and Huijing, P. A., 2002b. Extramuscular myofascial force transmission: Experiments and finite element modeling. Archives of Physiology and Biochemistry, in revision.

Zatsiorsky, V. M., Gregory, R. W. and Latash, M. L., 2002. Force and torque production in static multifinger prehension: biomechanics and control. I. Biomechanics. Biological Cybernetics 87, 50-57.

Zuurbier, C. J., Everard, A. J., van der Wees, P. and Huijing, P. A., 1994. Length-force characteristics of the aponeurosis in the passive and active muscle condition and in the isolated condition. Journal of Biomechanics 27, 445-53.

Appendix A

Large deformation analysis of solid continuum with material and geometric nonlinearities

In this thesis, skeletal muscle tissue is considered as a continuum that accounts for material and geometric nonlinearities. Mechanics of skeletal muscle tissue involves large deformations for which the linear elasticity theory is not applicable because the following two major assumptions of linear elasticity theory are not valid anymore:
(1) The displacements remain infinitesimal: There is no difference between the deformed state and the undeformed state.
(2) The strains are infinitesimal: The relationship between strain and displacement is linear.
Theory of large deformations that is employed in the development of the elements that represent the skeletal muscle tissue is outlined in this Appendix.

Geometric Relations

In a large deformation analysis a distinction has to be made between the coordinate systems that can be chosen to describe the behavior of the deformable body whose motion is under consideration. Descriptions of relevant quantities can be made in terms of where the body was before deformation (material description) or where it is during deformation (spatial description). Alternatively these are referred to as Lagrangian and Eulerian descriptions respectively.

Lagrangian description

$\underset{\sim}{x}^{G}$: position vector in undeformed state (material coordinates of a material point)

$\underset{\sim}{u} = \underset{\sim}{u}(\underset{\sim}{x}^{G})$: displacement vector as a function of material coordinates

Eulerian description

$\underset{\sim}{x}$: position vector in deformed state (space coordinates of a material point)

$\underset{\sim}{u} = \underset{\sim}{u}(\underset{\sim}{x})$: displacement vector as a function of space coordinates

The formulation used for the developed elements is based on the Lagrangian description. Therefore, the position of a point in the deformed state can be expressed as a function of the position of the point in the undeformed state as follows:

$$\underset{\sim}{x} = \underset{\sim}{x}^{G} + \underset{\sim}{u}(\underset{\sim}{x}^{G}) \qquad \text{(A.1)}$$

Deformation Tensors

A key quantity in large deformation analysis is the deformation tensor, which is involved in all equations relating quantities before deformation to corresponding quantities after (or

during) deformation. The deformation tensor allows the relative spatial position of two neighboring particles after deformation to be described in terms of their relative material position before deformation therefore it is fundamental to the description of deformation and hence strain.

$$\underset{\sim}{x}\overleftarrow{\underset{\sim}{\nabla}}^{G} = \underline{F}^{G} \text{ : Green deformation tensor} \tag{A.2}$$

or alternatively,

$$\underset{\sim}{x}^{G}\overleftarrow{\underset{\sim}{\nabla}} = \underline{F}^{E} \text{ : Euler deformation tensor} \tag{A.3}$$

where

$$\underset{\sim}{\nabla}^{G} = \frac{d}{d\,\underset{\sim}{x}^{G}} \tag{A.4}$$

and

$$\underset{\sim}{\nabla} = \frac{d}{d\,\underset{\sim}{x}} \tag{A.5}$$

are the gradient operators

The position of a point in the deformed state as a function of its position in the undeformed state can be written as:

$$\underset{\sim}{dx} = \underline{F}^{G}.\underset{\sim}{d\,x}^{G} \tag{A.6}$$

Or alternatively the position of a point in the undeformed state as a function of its position in the deformed state can be written as:

$$\underset{\sim}{d\,x}^{G} = \underline{F}^{E}.\underset{\sim}{dx} \tag{A.7}$$

Constancy of volume

For an infinitesimal parallelepiped element described by the vectors $\underset{\sim}{da}$, $\underset{\sim}{db}$ and $\underset{\sim}{dc}$, the volume of the element in the deformed state can be written as:

$$\Delta\Omega = \underset{\sim}{da}.(\underset{\sim}{db}\times\underset{\sim}{dc}) \tag{A.8}$$

Making use of Green's deformation tensor

$$\underset{\sim}{da} = \underline{F}^{G}.\underset{\sim}{da}^{G} \tag{A.9}$$

$$\underset{\sim}{db} = \underline{F}^{G}.\underset{\sim}{db}^{G} \tag{A.10}$$

$$\underset{\sim}{dc} = \underline{F}^{G}.\underset{\sim}{dc}^{G} \tag{A.11}$$

the volume of the element can also be written in terms of the vectors in the undeformed state

$$\Delta\Omega = (\underline{F}^{G}.\underset{\sim}{da}^{G}).[(\underline{F}^{G}.\underset{\sim}{db}^{G})\times(\underline{F}^{G}.\underset{\sim}{dc}^{G})] \tag{A.12}$$

or

$$\begin{aligned}\Delta\Omega &= (\underline{F}^{G}.\underset{\sim}{da}^{G}).(\underline{F}^{G})^{-T}.(\underset{\sim}{db}^{G}\times\underset{\sim}{dc}^{G})\det(\underline{F}^{G})\\ &= \underset{\sim}{da}^{G}.(\underline{F}^{G})^{T}.(\underline{F}^{G})^{-T}.(\underset{\sim}{db}^{G}\times\underset{\sim}{dc}^{G})\det(\underline{F}^{G})\\ &= \det(\underline{F}^{G})\,[\underset{\sim}{da}^{G}.(\underset{\sim}{db}^{G}\times\underset{\sim}{dc}^{G})]\end{aligned} \tag{A.13}$$

where

$[\underset{\sim}{da}^{G}.(\underset{\sim}{db}^{G}\times\underset{\sim}{dc}^{G})] = \Delta\Omega^{G}$, i.e., the volume of the element in the undeformed state

then

$$\Delta\Omega = \det(\underline{F}^{G})\,\Delta\Omega^{G} = J\,\Delta\Omega^{G} \tag{A.14}$$

where J is the Jacobian of the deformation tensor (constancy of volume requires $J = 1$).

Strain

Consider two neighboring material points in the undeformed state and the vector $\underset{\sim}{dx}^{G}$ representing the position differences of these points. The length ds^{G} of this vector is:

$$ds^G = \sqrt{d\underset{\sim}{x}^G . d\underset{\sim}{x}^G} \tag{A.15}$$

In the deformed state the length ds of this vector $\underset{\sim}{dx}$ is

$$ds = \sqrt{\underset{\sim}{dx}.\underset{\sim}{dx}} \tag{A.16}$$

Then the change in length can be written as:

$$\frac{ds - ds^G}{ds^G} \tag{A.17}$$

The Green-Lagrange strain tensor is defined as follows:

$$\underline{L}^G = \frac{1}{2}\frac{(ds)^2 - (ds^G)^2}{(ds^G)^2} \tag{A.18}$$

in which definition the square roots are avoided for convenience. Note that:

$$\begin{aligned}(ds)^2 - (ds^G)^2 &= (\underset{\sim}{dx}.\underset{\sim}{dx}) - (\underset{\sim}{dx}^G . \underset{\sim}{dx}^G) \quad \text{or} \\ &= \underset{\sim}{dx}^G .(\underline{F}^G)^T \cdot \underline{F}^G \cdot \underset{\sim}{dx}^G - \underset{\sim}{dx}^G . \underset{\sim}{dx}^G \\ &= \underset{\sim}{dx}^G .[(\underline{F}^G)^T \cdot \underline{F}^G - \underline{I}] \cdot \underset{\sim}{dx}^G \end{aligned} \tag{A.19}$$

therefore the Green-Lagrange strain tensor in terms of Green deformation tensor is

$$\underline{L}^G = \frac{1}{2}[(\underline{F}^G)^T . \underline{F}^G - \underline{I}] \tag{A.20}$$

note that the tensor $(\underline{F}^G)^T \cdot \underline{F}^G$ is referred to as Cauchy-Green strain tensor.

Equation A.20 can be rewritten in terms of displacements making use of equation A.1 such that as $\underset{\sim}{x} = \underset{\sim}{x}^G + \underset{\sim}{u}(\underset{\sim}{x}^G)$ and $\underset{\sim}{dx} = \underline{F}^G . \underset{\sim}{dx}^G$, the Green deformation tensor becomes

$$\underset{\sim}{\underline{F}}^{G} = \underline{I} + \underset{\sim}{u}^{G} \overleftarrow{\underset{\sim}{\nabla}}^{G} \tag{A.21}$$

Substituting (A.21) into (A.20)

$$\underline{L}^{G} = \frac{1}{2}\left[\underset{\sim}{u}^{G} \overleftarrow{\underset{\sim}{\nabla}}^{G} + \overrightarrow{\underset{\sim}{\nabla}}^{G} \underset{\sim}{u}^{G} + [\overrightarrow{\underset{\sim}{\nabla}}^{G} \underset{\sim}{u}^{G}].[\underset{\sim}{u}^{G} \overleftarrow{\underset{\sim}{\nabla}}^{G}] \right] \tag{A.22}$$

Stress and Equilibrium

For a deformable body defined by a volume Ω with boundaries Γ, assuming that the body is under the action of body forces f per unit volume and traction forces t per unit area acting on the boundary (in the deformed state), the equilibrium equations can be written as:

$$\overrightarrow{\underset{\sim}{\nabla}}.\underline{\sigma} + \underset{\sim}{f} = 0 \qquad \text{in } \Omega \tag{A.23}$$

$$\underset{\sim}{n}.\underline{\sigma} - \underset{\sim}{t} = 0 \qquad \text{on } \Gamma \tag{A.24}$$

where, $\underline{\sigma}$ is the Cauchy stress tensor that represents the current force per unit deformed area. The equilibrium equations can be rewritten in the Lagrangian description in an attempt to relate the forces in the deformed state to unit area in the undeformed state. As the first step for this transformation the forces acting on the body have to be represented as forces per unit volume and per unit area in the undeformed state. As derived above, the volume of an infinitesimal element in the deformed state is related to its volume in the undeformed state as:

$$\Delta\Omega = J\ \Delta\Omega^{G} \tag{A.25}$$

similarly for an area element :

$$\Delta\Gamma = J_a\ \Delta\Gamma^{G} \tag{A.26}$$

where

$J_a = J\left\| (\underline{F}^{G})^{-T}.\underset{\sim}{n}^{G} \right\|$ and $\underset{\sim}{n}^{G}$ is the unit normal to the surface

Transformation of the forces yield:

$$J \underset{\sim}{f} = \underset{\sim}{f}^{G} \tag{A.27}$$

$$J_a \underset{\sim}{t} = \underset{\sim}{t}^{G} \tag{A.28}$$

Therefore the equilibrium equations become

$$J \underset{\sim}{\vec{\nabla}}.\underline{\sigma} + \underset{\sim}{f}^{G} = \underset{\sim}{0} \qquad \text{in } \Omega \tag{A.29}$$

$$J_a \underset{\sim}{n}.\underline{\sigma} - \underset{\sim}{t}^{G} = \underset{\sim}{0} \qquad \text{on } \Gamma \tag{A.30}$$

Further:

$$\underset{\sim}{\vec{\nabla}} = \underset{\sim}{\vec{\nabla}}^{G}.(\underline{F}^{G})^{-1} \tag{A.31}$$

and

$$J_a \underset{\sim}{n} = J \underset{\sim}{n}^{G}.(\underline{F}^{G})^{-1} \tag{A.32}$$

Substituting these relations and after rearranging, the equilibrium equations become

$$\underset{\sim}{\vec{\nabla}}^{G}.[J\ (\underline{F}^{G})^{-1}.\underline{\sigma}\ ] + \underset{\sim}{f}^{G} = \underset{\sim}{0} \qquad \text{in } \Omega \tag{A.33}$$

$$\underset{\sim}{n}^{G}.[J\ (\underline{F}^{G})^{-1}.\underline{\sigma}\ ] - \underset{\sim}{t}^{G} = \underset{\sim}{0} \qquad \text{on } \Gamma \tag{A.34}$$

The stress tensor referred to as first Piola-Kirchhoff stress tensor is defined as:

$$\underline{T} = J\ (\underline{F}^{G})^{-1}.\underline{\sigma} \tag{A.35}$$

In terms of first Piola-Kirchhoff stress tensor, the equilibrium equations become

$$\vec{\nabla}^{G}_{\sim}.\underline{T} + \underset{\sim}{f}^{G} = \underset{\sim}{0} \quad \text{in } \Omega \tag{A.36}$$

$$\underset{\sim}{n}^{G}.\underline{T} - \underset{\sim}{t}^{G} = \underset{\sim}{0} \quad \text{on } \Gamma \tag{A.37}$$

In is possible to make the unsymmetrical first Piola-Kirchhoff stress tensor symmetric by multiplying with $(\underline{F}^{G})^{-T}$. The resulting symmetric tensor is known as second Piola-Kirchhoff stress tensor:

$$\underline{S} = J\,(\underline{F}^{G})^{-1}.\underline{\sigma}.(\underline{F}^{G})^{-T} \tag{A.38}$$

The first Piola-Kirchhoff stress tensor in terms of second Piola-Kirchhoff stress tensor is:

$$\underline{T} = \underline{S}.(\underline{F}^{G})^{T} \tag{A.39}$$

Therefore, the equilibrium equations in terms of second Piola-Kirchhoff stress tensor become:

$$\vec{\nabla}^{G}_{\sim}.[\underline{S}.(\underline{F}^{G})^{T}] + \underset{\sim}{f}^{G} = \underset{\sim}{0} \quad \text{in } \Omega \tag{A.40}$$

$$\underset{\sim}{n}^{G}.[\underline{S}.(\underline{F}^{G})^{T}] - \underset{\sim}{t}^{G} = \underset{\sim}{0} \quad \text{on } \Gamma \tag{A.41}$$

Equations A.40 and A.41 describe the equilibrium to be satisfied for the extracellular matrix element and the myofiber element developed in this study. The solution of these equilibrium equations is done by using the finite element method, implementation of which is outlined in Appendix B.

Constitutive Equations

The equilibrium equations are written in terms of stresses inside the body. These stresses result from the deformation and it is necessary to express them in terms of some measure of this deformation such as strain. As a first step consider the internal work done by the Cauchy stresses per unit time which is expressed as

$$\delta W = \int_{\Omega} \underline{\sigma} : \underline{D} d\Omega \delta\lambda \tag{A.42}$$

where

$$\underset{\sim}{\underline{D}} = \frac{1}{2}[\underset{\sim}{\vec{\nabla}}\,\underset{\sim}{\dot{u}}^{G} + \underset{\sim}{\dot{u}}^{G}\,\underset{\sim}{\overleftarrow{\nabla}}] \tag{A.43}$$

is the rate of deformation tensor and the superscript "." represents the time derivative. Therefore, the Cauchy stresses tensor and the rate of deformation tensor are work conjugates. The rate of change of Green-Lagrange strain tensor can be written as

$$\dot{\underline{L}}^{G} = \frac{1}{2}[(\dot{\underline{F}}^{G})^{T}.\underline{F}^{G} + (\underline{F}^{G})^{T}.\dot{\underline{F}}^{G}] \quad \text{or} \tag{A.44}$$

$$\dot{\underline{L}}^{G} = \frac{1}{2}[(\underset{\sim}{\vec{\nabla}}\,\underset{\sim}{\dot{u}}^{G})^{T}.\underline{F}^{G} + (\underline{F}^{G})^{T}.(\underset{\sim}{\dot{u}}^{G}\,\underset{\sim}{\overleftarrow{\nabla}})]$$

$$= (\underline{F}^{G})^{T}.[\frac{1}{2}(\underset{\sim}{\vec{\nabla}}\,\underset{\sim}{\dot{u}}^{G} + \underset{\sim}{\dot{u}}^{G}\,\underset{\sim}{\overleftarrow{\nabla}})].\underline{F}^{G} \tag{A.45}$$

therefore,

$$\underline{D} = (\underline{F}^{G})^{-T}.\dot{\underline{L}}^{G}.(\underline{F}^{G})^{-1} \tag{A.46}$$

Rewriting equation A.42 in the Lagrangian description yields

$$\delta W^{G} = \int_{\Omega} \underline{\sigma} : [(\underline{F}^{G})^{-T}.\dot{\underline{L}}^{G}.(\underline{F}^{G})^{-1}] J \, d\Omega^{G} \, \delta\lambda \tag{A.47}$$

rearranging the integrand

$$\delta W^{G} = \int_{\Omega} J\underline{\sigma} : [(\underline{F}^{G})^{-T}.\dot{\underline{L}}^{G}.(\underline{F}^{G})^{-1}] \, d\Omega^{G} \, \delta\lambda$$

$$= \int_{\Omega} [J(\underline{F}^{G})^{-1}.\underline{\sigma}.(\underline{F}^{G})^{-T}] : \dot{\underline{L}}^{G} d\Omega^{G} \, \delta\lambda \quad \text{therefore,}$$

$$= \int_{\Omega} \underline{S} : \dot{\underline{L}}^{G} \, d\Omega^{G} \, \delta\lambda \tag{A.48}$$

Therefore, the second Piola-Kirchhoff stress tensor and Green-Lagrange strain tensor are work conjugates.

In this study the passive material properties of muscle tissue are described by hyperelasticity (i.e., as a material that can experience a finite elastic deformation that is completely recoverable). For a hyperelastic material there exists a strain energy function that relates the stresses to strains such that

$$\underline{S} = \frac{d\dot{W}^G}{d\dot{\underline{L}}^G} \tag{A.49}$$

Note that the viscoelastic behavior of the muscle tissue is not studied here assuming that the conditions studied are quasi-static. For equation A.49 as the right hand side expression includes time derivative of both the term in the numerator and the one in the denominator, it can also be written that

$$\underline{S} = \frac{dW^G}{d\underline{L}^G} \tag{A.50}$$

The relationship between the second Piola-Kirchhoff stress tensor and Green-Lagrange strain tensor can also be written as

$$\underline{S} = \underline{\underline{C}} : \underline{L} \tag{A.51}$$

where $\underline{\underline{C}}$ is known as the Lagrangian or material elasticity tensor.

References

Bonet, J. and Wood, R. D. (1997). Nonlinear Continuum Mechanics for Finite Element Analysis. Cambridge, United Kingdom, Cambridge University Press.

Reddy, J. N. (1993). An Introduction to The Finite Element Method. Singapore, McGraw-Hill Book Co.

Spiering, R. M. E. J. and Grootenboer, H. J. (1991). Eindige Elementen Methode in de Werktuigbouwkunde. Enschede, The Netherlands, University of Twente.

Zienkiewicz, O. C. and Taylor, R. L. (2000). The Finite Element Method. Oxford, Butterworth-Heinemann.

Appendix B

Implementation of the finite element method

General scheme

Posing the problem to be solved in general, it is aimed at finding an unknown function, which satisfies a set of certain differential equations that describe the problem such as:

$$\{A(\underset{\sim}{u})\} = \underset{\sim}{0} \tag{B.1}$$

in a domain (volume, area, etc.) Ω together with its boundary conditions

$$\{B(\underset{\sim}{u})\} = \underset{\sim}{0} \tag{B.2}$$

on the boundaries Γ of the domain where, $\underset{\sim}{u}$ is the unknown function

Integral or "weak" statements equivalent to the differential equations

As the set of differential equations has to be zero at each point of the domain, it follows that

$$\int_{\Omega} v^T \{A(\underset{\sim}{u})\}\, d\Omega = 0 \tag{B.3}$$

$$\int_{\Gamma} \overline{v}^T \{B(\underset{\sim}{u})\}\, d\Gamma = 0 \tag{B.4}$$

where v and $\overline{v}$ are sets of arbitrary equations

Satisfaction of the integral statement for all v and $\overline{v}$ that can be rewritten as

$$\int_{\Omega} v^T \{A(\underset{\sim}{u})\}\, d\Omega + \int_{\Gamma} \overline{v}^T \{B(\underset{\sim}{u})\}\, d\Gamma = 0 \tag{B.5}$$

is equivalent to satisfaction of the original set of differential equations and their boundary conditions. If the unknown function $\underset{\sim}{u}$ is approximated by the following expansion:

$$\underset{\sim}{u} = \{\underline{N}\}^T \{u\} \tag{B.6}$$

then it is necessary to put a finite set of approximate functions in place of v and $\overline{v}$ in the integral statement such that:

$$v^T = \sum_{j=1}^{n} w_j \delta u_j \quad \text{and} \quad \overline{v}^T = \sum_{j=1}^{n} \overline{w}_j \delta u_j \tag{B.7}$$

in which δu_j are arbitrary parameters and n is the number of unknowns. Substituting these functions into the integral statement yields:

$$\delta u_j{}^T \left[\int_\Omega w_j{}^T \{A(Nu)\}\, d\Omega + \int_\Gamma \overline{w}_j{}^T \{B(Nu)\}\, d\Gamma \right] = 0 \tag{B.8}$$

Since δu_j are arbitrary the following statement provides sufficient number of equations to determine the unknowns, u_j

$$\int_\Omega w_j{}^T \{A(Nu)\}\, d\Omega + \int_\Gamma \overline{w}_j{}^T \{B(Nu)\}\, d\Gamma = 0 \tag{B.9}$$

Note that $A(Nu)$ and $B(Nu)$ represent the residual or error obtained by substitution of the approximation into the differential equations and the above expression is a weighted integral of such residuals. Therefore, the approximation is called method of weighted residues. Note also that in the Galerkin Method, simply the shape functions are used as weighting.

Application of the Galerkin Method to solve the equilibrium equations

The equilibrium equations that were derived in Appendix A represent the differential equations to be solved in order to analyze the deformation of an elastic body.

$$\underset{\sim}{\vec{\nabla}}^G . [\underline{S} . (\underline{F}^G)^T] + \underset{\sim}{f}^G = \underset{\sim}{0} \qquad \text{in } \Omega \tag{B.10}$$

$$\underset{\sim}{n}^G . [\underline{S} . (\underline{F}^G)^T] - \underset{\sim}{t}^G = \underset{\sim}{0} \qquad \text{on } \Gamma \tag{B.11}$$

These equations can be rewritten in the weak form as:

$$\int_{\Omega^G} \{\underset{\sim}{w}\} . [\underset{\sim}{\vec{\nabla}}^G . [\underline{S} . (\underline{F}^G)^T]]\, d\Omega^G + \int_{\Omega^G} \{\underset{\sim}{w}\} . \underset{\sim}{f}^G\, d\Omega^G = \underset{\sim}{0} \tag{B.12}$$

$$\int_{\Gamma^G} \{\underset{\sim}{w}\} . [\underset{\sim}{n}^G . [\underline{S} . (\underline{F}^G)^T]]\, d\Gamma^G - \int_{\Gamma^G} \{\underset{\sim}{w}\} . \underset{\sim}{t}^G\, d\Gamma^G = \underset{\sim}{0} \tag{B.13}$$

where, $\{\underset{\sim}{w}\}$ are weighting functions. Combining the two equations B.12 and B.13 will finally yield:

$$\int_{\Omega^G} \{\underset{\sim}{w}\} \overleftarrow{\underset{\sim}{\nabla}}^G .. [\underline{S} . (\underline{F}^G)^T] \, d\Omega^G = \int_{\Gamma^G} \{\underset{\sim}{w}\} . \underset{\sim}{t}^G \, d\Gamma^G + \int_{\Omega^G} \{\underset{\sim}{w}\} . \underset{\sim}{f}^G \, d\Omega^G \qquad \text{(B.14)}$$

Recall the approximation

$$\underset{\sim}{u} = \{\underset{\sim}{N}\}^T \{u\} \qquad \text{(B.15)}$$

where,

$\{u\}$ are the displacements of the nodal points and

$\{\underset{\sim}{N}\}$ are the shape functions (i.e., functions that relate the deformation of the nodal points to the deformation at an arbitrary point of an element)

As a function of $\{u\}$ and $\{\underset{\sim}{N}\}$, the deformation tensor becomes

$$\begin{aligned} \underline{F}^G &= \underline{I} + \underset{\sim}{u}^G \overleftarrow{\underset{\sim}{\nabla}}^G \\ &= \underline{I} + \{u\}^T \{\underset{\sim}{N}\} \overleftarrow{\underset{\sim}{\nabla}}^G \end{aligned} \qquad \text{(B.16)}$$

The Green-Lagrange strain tensor becomes

$$\underline{L}^G = \frac{1}{2} [\{u\}^T \{\underset{\sim}{N}\} \overleftarrow{\underset{\sim}{\nabla}}^G + \overrightarrow{\underset{\sim}{\nabla}}^G \{\underset{\sim}{N}\}^T \{u\} + [\overrightarrow{\underset{\sim}{\nabla}}^G \{\underset{\sim}{N}\}^T \{u\}] . [\{u\}^T \{\underset{\sim}{N}\} \overleftarrow{\underset{\sim}{\nabla}}^G]] \qquad \text{(B.17)}$$

Recall the stress-strain relationship from equation A.49

$$\underline{S} = \underline{\underline{C}} : \underline{L} \qquad \text{(B.18)}$$

also that in the Galerkin Method

$$\{\underset{\sim}{w}\} = \{\underset{\sim}{N}\} \qquad \text{(B.19)}$$

Substituting equations B.16 to B.19 into equation B.14 gives the equilibrium equation as a function of the unknown displacements of the nodal points

$$\int_{\Omega^G} \underset{\sim}{\{N\}} \overleftarrow{\underset{\sim}{\nabla}}^G \,..\underline{\underline{C}} : \frac{1}{2}\Big[\{u\}^T \underset{\sim}{\{N\}} \overleftarrow{\underset{\sim}{\nabla}}^G + \overrightarrow{\underset{\sim}{\nabla}}^G \underset{\sim}{\{N\}}^T \{u\} + [\overrightarrow{\underset{\sim}{\nabla}}^G \underset{\sim}{\{N\}}^T \{u\}].[\{u\}^T \underset{\sim}{\{N\}} \overleftarrow{\underset{\sim}{\nabla}}^G \Big].$$

$$[\underline{I} + \{u\}^T \underset{\sim}{\{N\}} \overleftarrow{\underset{\sim}{\nabla}}^G]^T \, d\Omega^G = \int_{\Gamma^G} \underset{\sim}{\{N\}}.\underset{\sim}{t}^G \, d\Gamma^G + \int_{\Omega^G} \underset{\sim}{\{N\}}.\underset{\sim}{f}^G \, d\Omega^G \qquad \text{(B.20)}$$

Solution of the equilibrium equations using Newton-Raphson method

Note that the solution of the problem has to be carried out using an iterative procedure. The most commonly used iterative procedure is the Newton-Raphson method. In general terms to find the solution for a function $\{F\}$ i.e., to find the roots of the equation $\{F\} = 0$, let

$$\{G(\{u\})\} = \{F\} \qquad \text{(B.21)}$$

the solution is calculated with the following scheme

$$\frac{d\{G(\{u\}^i)\}}{d\{u\}} \Delta\{u\}^i = \{F\} - \{G(\{u\}^i)\} \qquad \text{(B.22)}$$

and

$$\{u\}^{i+1} = \{u\}^i + \Delta\{u\}^i \qquad \text{(B.23)}$$

where the index *i* represents the iteration number. The iteration is repeated until the right hand side of equation B.22 approaches zero.

If this scheme is applied to solve for the unknown displacements then let $\{G(\{u\}^i)\}$ be equal to the left hand side of equation B.14 with $\underset{\sim}{\{w\}} = \underset{\sim}{\{N\}}$

$$\{G(\{u\}^i)\} = \int_{\Omega^G} \underset{\sim}{\{N\}} \overleftarrow{\underset{\sim}{\nabla}}^G \,..[\underline{S} \,.\, (\underline{F}^G)^T]^i \, d\Omega^G \qquad \text{(B.24)}$$

then finally the iterative scheme reduces down to

$$[K_t(S^i, \{u\}^i)]\Delta\{u\}^i = \{T\} + \{Q\} - \{G(\{u\}^i)\} \qquad \text{(B.25)}$$

$$\{u\}^{i+1} = \{u\}^i + \Delta\{u\}^i \tag{B.26}$$

where $[K_t(S^i, \{u\}^i)]$ is referred to as the tangent stiffness matrix and $\{T\} + \{Q\}$ represents the load calculated from the right hand side of equation B.14. Defining

$$\{T\} + \{Q\} - \{G(\{u\}^i) = \{R\} \tag{B.27}$$

convergence for the solution is achieved when the residual vector $\{R\}$ is small enough depending on the tolerance for the convergence criteria.

References

Bonet, J. and Wood, R. D. (1997). Nonlinear Continuum Mechanics for Finite Element Analysis. Cambridge, United Kingdom, Cambridge University Press.

Reddy, J. N. (1993). An Introduction to The Finite Element Method. Singapore, McGraw-Hill Book Co.

Spiering, R. M. E. J. and Grootenboer, H. J. (1991). Eindige Elementen Methode in de Werktuigbouwkunde. Enschede, The Netherlands, University of Twente.

Zienkiewicz, O. C. and Taylor, R. L. (2000). The Finite Element Method. Oxford, Butterworth-Heinemann.

Appendix C

Anatomical and physiological terms

Selected anatomical terms

Proximal: Nearer to a point of reference such as an origin, or a point of attachment

Distal: Located far from a point of reference, such as an origin or a point of attachment

Anterior: Toward the front, or in front of

Posterior: Situated in the back

Medial: The side of the body or body part that is nearer to the middle or center of the body

Lateral: Denoting a position farther from the medial plane of the body

Dorsal: Of, toward, on, in, or near the back or upper surface of an organ

Plantar: Of, relating to, or occurring on the sole of the foot

Crural: Of or relating to the leg

Peroneal: Of or pertaining to the fibula; in the region of the fibula

Extension: The act of straightening or a limb

Flexion: The act of bending a joint or limb

Synergistic muscles: Muscles having a similar and mutually helpful function or action

Antagonist muscles: Muscles having an opposite function. The contraction of one has the potential to neutralize that of the other.

Levels of organization within a skeletal muscle

Fascicle: Bundles of muscle fibers and surrounding connective tissues

Muscle fiber: The activatable single cells of skeletal muscle

Myofibril: Thread like fibrils that make up the contractile part of a muscle fiber

Sarcomere: One of the segments into which a myofibril of striated muscle is divided

Myofilament: Any of the ultramicroscopic filaments, made up of actin and myosin that are the structural units of a myofibril which function in muscle contraction

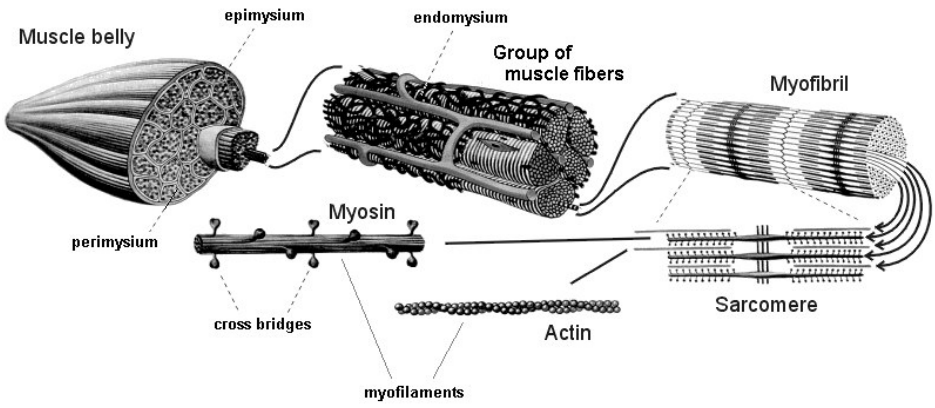

Fig.1 Successive levels of organization within a skeletal muscle, from whole muscle to myofilaments. Modified from Gray's Anatomy (1980)

Connective tissue organizations

Fascia: A sheet or band of fibrous connective tissue enveloping, separating, or binding together muscles, and other soft structures of the body

Collagen: The fibrous protein constituent of connective tissues

Aponeurosis: A sheet like fibrous membrane, resembling a flattened tendon, that serves as a fascia to bind muscles together or as a means of connecting muscle to bone

Epimysium: The external sheath of connective tissue surrounding a whole muscle

Perimysium: The sheath of connective tissue enveloping bundles of muscle fibers

Endomysium: The sheet of connective tissue that surrounds muscle fibers

Basal Lamina: A specialized component of extracellular matrix that surrounds individual muscle fibers and separates the muscle fibers from the underlying or surrounding connective tissue

Sarcolemma: A thin membrane enclosing a striated muscle fiber

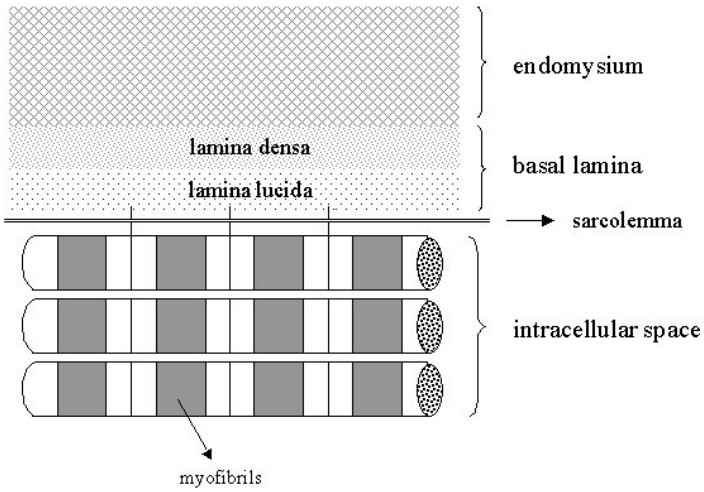

Fig.2 Schematic representation of the connective tissue organizations that surround muscle fibers. Note that the scale of the elements shown in this figure is exaggerated individually for clarity. Modified from Huijing (1999).

Extracellular matrix: Macromolecules (proteins) that form a complex meshwork in which cells are embedded to construct tissues. Variations in the relative types of macromolecules and their organization determine the type of extracellular matrix, each adapted to the functional requirements of the tissue. In broad terms there are three major components: fibrous elements (particularly collagen, elastin or reticulin), link proteins (e.g. laminin) and space filling molecules (usually glycosaminoglycans).

Intermuscular septum: A term applied to aponeurotic sheets separating various muscles of the limbs.

Ligament: A band of fibrous tissue that connects bones or cartilages, serving to support and strengthen joints.

Collateral ligament: One of a number of ligaments found on either side of a joint that has a hinge like movement (e.g. knee joint). It serves as a radius of movement of the joint.

Interosseal: Situated between bones.

Neurovascular tract: Connective tissue components formed by structures that encapsulate extramuscular main nerves and blood vessels.

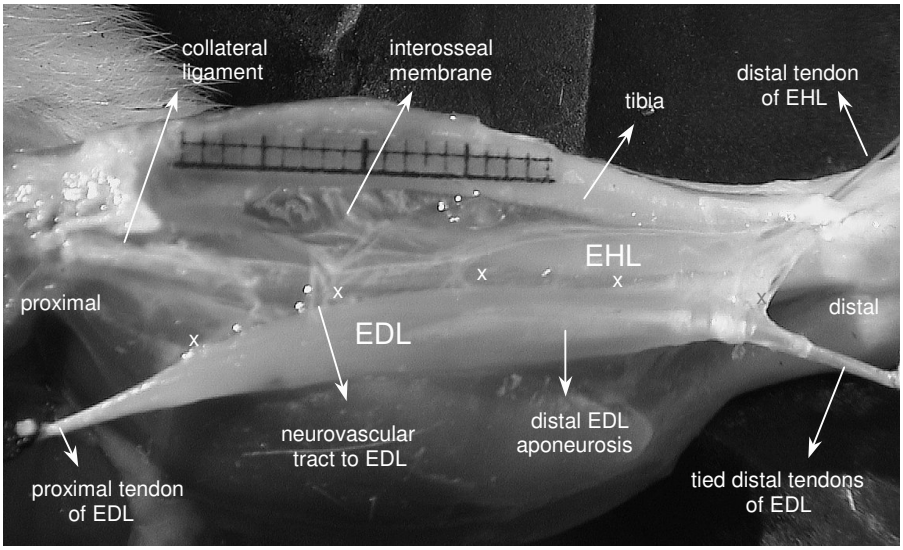

Fig.3 Picture showing the extensor digitorum longus (EDL) and the extensor hallucis longus (EHL) muscles as well as the nonmuscular elements of the anterior crural compartment of the rat (see for more pictures and illustrations of the muscular and nonmuscular elements of the anterior crural compartment, Huijing and Baan, 2001; Maas et al., 2001; Huijing and Baan, 2003; Huijing et al., 2003). Note that m. tibialis anterior (TA) which is also enclosed within the anterior crural compartment is dissected completely. A downward force is exerted on both proximal and distal tendons of EDL to illustrate the connections between EDL and EHL muscles as well as the connective tissue elements such as the neurovascular tract. Note that several "x" signs mark the neurovascular tract to EDL muscle. The picture shows part of the interosseal membrane, which is connected both to the tibia (the large bone between the knee and the ankle that supports most of the weight) and to the fibula (the long bone in the lower leg that is adjacent to the tibia). The anterior intermuscular septum is continuous with the interosseal membrane and with the collateral ligament (see Fig.4 for a clear representation of the relationship between these connective tissue elements). All muscle fibers of EHL originate from the anterior intermuscular septum and insert on a distal aponeurosis.

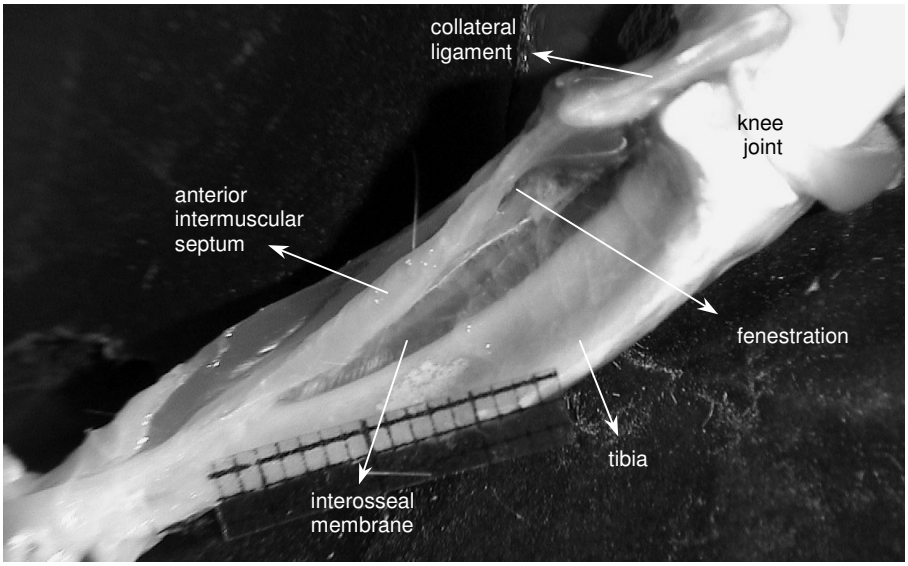

Fig.4 Picture showing the boundaries of the anterior crural compartment of the rat (the muscles contained in the compartment i.e., EDL, TA and EHL are removed). Note that the anterior crural compartment is delimited by the anterior intermuscular septum, the interosseal membrane, the tibia and the crural fascia that covers the surface of TA (not shown). The fenestration within the anterior intermuscular septum through which the neurovascular tract to the muscles of the anterior crural compartment passes is shown.

References

Huijing, P. A., 1999. Muscle as a collagen fiber reinforced composite material: Force transmission in muscle and whole limbs. Journal of Biomechanics 32, 329-345.

Huijing, P. A. and Baan, G. C., 2001. Extramuscular myofascial force transmission within the rat anterior tibial compartment: Proximo-distal differences in muscle force. Acta Physiologica Scandinavica 173, 1-15.

Huijing, P. A. and Baan, G. C., 2003. Myofascial force transmission: muscle relative position and length determine agonist and synergist muscle force. Journal of Applied Physiology 94, 1092-1107.

Huijing, P. A., Maas, H. and Baan, G. C., 2003. Compartmental fasciotomy and isolating a muscle from neighboring muscles interfere with extramuscular myofascial force transmission within the rat anterior crural compartment. Journal of Morphology 256, 306-321.

Maas, H., Baan, G. C. and Huijing, P. A., 2001. Intermuscular interaction via myofascial force transmission: effects of tibialis anterior and extensor hallucis longus length on force transmission from rat extensor digitorum longus muscle. Journal of Biomechanics 34, 927-940.

Williams, P. L. and Warwick, R. (1980). Gray's Anatomy. Edinburgh, Longman Group Limited.